

Final Report on Effects of Irradiation on Material G347A

- Prepared for Tokai Carbon Co., Ltd.



Anne A. Campbell
Yutai Katoh
Mary A. Snead

December 2015

DOCUMENT AVAILABILITY

Reports produced after January 1, 1996, are generally available free via US Department of Energy (DOE) SciTech Connect.

Website <http://www.osti.gov/scitech/>

Reports produced before January 1, 1996, may be purchased by members of the public from the following source:

National Technical Information Service
5285 Port Royal Road
Springfield, VA 22161
Telephone 703-605-6000 (1-800-553-6847)
TDD 703-487-4639
Fax 703-605-6900
E-mail info@ntis.gov
Website <http://www.ntis.gov/help/ordermethods.aspx>

Reports are available to DOE employees, DOE contractors, Energy Technology Data Exchange representatives, and International Nuclear Information System representatives from the following source:

Office of Scientific and Technical Information
PO Box 62
Oak Ridge, TN 37831
Telephone 865-576-8401
Fax 865-576-5728
E-mail reports@osti.gov
Website <http://www.osti.gov/contact.html>

This report was prepared as an account of work sponsored by an agency of the United States Government. Neither the United States Government nor any agency thereof, nor any of their employees, makes any warranty, express or implied, or assumes any legal liability or responsibility for the accuracy, completeness, or usefulness of any information, apparatus, product, or process disclosed, or represents that its use would not infringe privately owned rights. Reference herein to any specific commercial product, process, or service by trade name, trademark, manufacturer, or otherwise, does not necessarily constitute or imply its endorsement, recommendation, or favoring by the United States Government or any agency thereof. The views and opinions of authors expressed herein do not necessarily state or reflect those of the United States Government or any agency thereof.

Irradiation Performance of Tokai Carbon Graphite Materials
DOE Project No. NFE-09-02345

**FINAL REPORT ON EFFECTS OF IRRADIATION ON MATERIAL G347A
TOKAI CARBON CO., LTD**

Anne A. Campbell
Yutai Katoh
Mary A. Snead

Date Published: December 2015

Prepared by
OAK RIDGE NATIONAL LABORATORY
Oak Ridge, Tennessee 37831-6283
managed by
UT-BATTELLE, LLC
for the
US DEPARTMENT OF ENERGY
under contract DE-AC05-00OR22725

CONTENTS

	Page
LIST OF FIGURES	v
LIST OF TABLES	ix
ACRONYMS	xi
EXECUTIVE SUMMARY	1
ACKNOWLEDGEMENT	3
1. INTRODUCTION	5
2. MATERIALS	6
2.1 MATERIALS USED IN THIS PROGRAM	6
2.2 SPECIMEN INFORMATION	6
3. EXPERIMENTAL PROGRAM	9
3.1 IRRADIATION VEHICLES	9
3.2 HFIR INFORMATION	11
3.3 TEST PROCEDURES	13
4. RESULTS AND DISCUSSION	14
4.1 DETERMINING FINAL IRRADIATION CONDITIONS	14
4.2 IRRADIATION-INDUCED CHANGES TO PROPERTIES	16
4.2.1 362°C±43°C	17
4.2.2 462°C±22°C	21
4.2.3 546°C±23°C	25
4.2.4 659°C±27°C	29
4.2.5 738°C±27°C	33
4.3 GRADE COMPARISON	36
4.4 HISTORICAL BEHAVIOR COMPARISON	39
5. QUALITY ASSURANCE DOCUMENTATION	45
6. SUMMARY	46
7. REFERENCES	47
APPENDIX A. RABBIT INFORMATION	A-1
A.1 IRRADIATION RESULTS SUMMARY	A-1
A.2 TEMPERATURE MONITOR ANALYSIS RESULTS	A-2
APPENDIX B. SPECIMEN RESULTS	B-1
B.1 MB-W6	B-1
B.1.1 Pre-Irradiation (G347A only)	B-1
B.1.2 Post-Irradiation (G347A only)	B-2
B.2 SB-W3	B-3
B.2.1 Pre-Irradiation Dimensions	B-3
B.2.2 Pre-irradiation CTE	B-5
B.2.3 Post-Irradiation Dimensions	B-6
B.2.4 Post-Irradiation CTE	B-7
B.3 SB-W4	B-8
B.3.1 Pre-irradiation Dimensions (G347A only)	B-8
B.3.2 Pre-Irradiation CTE (G347A only)	B-10
B.3.3 Post-Irradiation Dimensions (G347A only)	B-11
B.3.4 Post-Irradiation CTE (G347A only)	B-13
B.4 TD-D6	B-15
B.4.1 Pre-Irradiation Dimensions	B-15

B.4.2	Pre-Irradiation Thermal Conductivity.....	B-18
B.4.3	Post-Irradiation Dimensions	B-19
B.4.4	Post-Irradiation Thermal Conductivity	B-22
B.5	SQ6 Strength Coupons.....	B-28
B.5.1	Pre-Irradiation (G347A only, AG only).....	B-28
B.5.2	Post-Irradiation (G347A only).....	B-29

LIST OF FIGURES

Figure	Page
Figure 2.1. Orientation of orthogonal directions, relative to billet molding directions.	6
Figure 2.2. Specimen orientations relative to billet orthogonal directions.	7
Figure 3.1. Example schematic cross section of a GRIC-1 rabbit.	9
Figure 3.2. 3-dimensions heat-transfer design of the (a) GRIC-1 and (b) GRIC-2 rabbits.	10
Figure 3.3. Planned irradiation envelope, showing the planned irradiation temperatures and total neutron fluences.....	11
Figure 3.4. Drawing of the HFIR core, where the rabbits were irradiated in the central yellow and white region.	12
Figure 3.5. Plot of the fast and thermal neutron fluxes versus the rabbit position along the core height (rabbit 1 located at the bottom and rabbit 9 is located at the top). The rabbits in this program were irradiated in positions that correspond to the “Peripheral Target Rabbit” fluxes.	12
Figure 4.1. Example analysis of passive temperature monitor for rabbit TOK-01.....	15
Figure 4.2. Plot of temperature monitor measured temperature and total fluence of each rabbit, where the data points are sorted by shape and color according to the design temperature.	16
Figure 4.3. Length change of G347A, versus neutron fluence, irradiated at $362^{\circ}\text{C}\pm 43^{\circ}\text{C}$	17
Figure 4.4. Volume change of G347A, versus neutron fluence, irradiated at $362^{\circ}\text{C}\pm 43^{\circ}\text{C}$	17
Figure 4.5. Young’s modulus change of G347A, versus neutron fluence, irradiated at $362^{\circ}\text{C}\pm 43^{\circ}\text{C}$	18
Figure 4.6. Shear modulus change of G347A, versus neutron fluence, irradiated at $362^{\circ}\text{C}\pm 43^{\circ}\text{C}$	18
Figure 4.7. Electrical resistivity change of G347A, versus neutron fluence, irradiated at $362^{\circ}\text{C}\pm 43^{\circ}\text{C}$	19
Figure 4.8. Strength changes of G347A, versus neutron fluence, irradiated at $362^{\circ}\text{C}\pm 43^{\circ}\text{C}$	19
Figure 4.9. (a) Mean CTE versus measurement temperature of G347A, and (b) mean CTE changes versus neutron fluence, irradiated at $362^{\circ}\text{C}\pm 43^{\circ}\text{C}$	20
Figure 4.10. (a) Thermal conductivity versus measurement temperature of G347A, and (b) thermal conductivity change versus neutron fluence, irradiated at $362^{\circ}\text{C}\pm 43^{\circ}\text{C}$	20
Figure 4.11. Length change of G347A, versus neutron fluence, irradiated at $462^{\circ}\text{C}\pm 22^{\circ}\text{C}$	21
Figure 4.12. Volume change of G347A, versus neutron fluence, irradiated at $462^{\circ}\text{C}\pm 22^{\circ}\text{C}$	21
Figure 4.13. Young’s modulus change of G347A, versus neutron fluence, irradiated at $462^{\circ}\text{C}\pm 22^{\circ}\text{C}$	22
Figure 4.14. Shear modulus change of G347A, versus neutron fluence, irradiated at $462^{\circ}\text{C}\pm 22^{\circ}\text{C}$	22
Figure 4.15. Electrical resistivity change of G347A, versus neutron fluence, irradiated at $462^{\circ}\text{C}\pm 22^{\circ}\text{C}$	23
Figure 4.16. Strength changes of G347A, versus neutron fluence, irradiated at $462^{\circ}\text{C}\pm 22^{\circ}\text{C}$	23
Figure 4.17. (a) Mean CTE versus measurement temperature of G347A, and (b) mean CTE changes versus neutron fluence, irradiated at $462^{\circ}\text{C}\pm 22^{\circ}\text{C}$	24
Figure 4.18. (a) Thermal conductivity versus measurement temperature of G347A, and (b) thermal conductivity change versus neutron fluence, irradiated at $462^{\circ}\text{C}\pm 22^{\circ}\text{C}$	24
Figure 4.19. Length change of G347A, versus neutron fluence, irradiated at $546^{\circ}\text{C}\pm 23^{\circ}\text{C}$	25
Figure 4.20. Volume change of G347A, versus neutron fluence, irradiated at $546^{\circ}\text{C}\pm 23^{\circ}\text{C}$	25
Figure 4.21. Young’s modulus change of G347A, versus neutron fluence, irradiated at $546^{\circ}\text{C}\pm 23^{\circ}\text{C}$	26
Figure 4.22. Shear modulus change of G347A, versus neutron fluence, irradiated at $546^{\circ}\text{C}\pm 23^{\circ}\text{C}$	26

Figure 4.23. Electrical resistivity change of G347A, versus neutron fluence, irradiated at 546°C±23°C.	27
Figure 4.24. Strength changes of G347A, versus neutron fluence, irradiated at 546°C±23°C.....	27
Figure 4.25. (a) Mean CTE versus measurement temperature of G347A, and (b) mean CTE changes versus neutron fluence, irradiated at 546°C±23°C.	28
Figure 4.26. (a) Thermal conductivity versus measurement temperature of G347A, and (b) thermal conductivity change versus neutron fluence, irradiated at 546°C±23°C.....	28
Figure 4.27. Length change of G347A, versus neutron fluence, irradiated at 659°C±27°C.	29
Figure 4.28. Volume change of G347A, versus neutron fluence, irradiated at 659°C±27°C.....	29
Figure 4.29. Young's modulus change of G347A, versus neutron fluence, irradiated at 659°C±27°C.	30
Figure 4.30. Shear modulus change of G347A, versus neutron fluence, irradiated at 659°C±27°C.....	30
Figure 4.31. Electrical resistivity change of G347A, versus neutron fluence, irradiated at 659°C±27°C.	31
Figure 4.32. Strength changes of G347A, versus neutron fluence, irradiated at 659°C±27°C.....	31
Figure 4.33. (a) Mean CTE versus measurement temperature of G347A, and (b) mean CTE changes versus neutron fluence, irradiated at 659°C±27°C.	32
Figure 4.34. (a) Thermal conductivity versus measurement temperature of G347A, and (b) thermal conductivity change versus neutron fluence, irradiated at 659°C±27°C.....	32
Figure 4.35. Length change of G347A, versus neutron fluence, irradiated at 738°C±27°C.	33
Figure 4.36. Volume change of G347A, versus neutron fluence, irradiated at 738°C±27°C.....	33
Figure 4.37. Young's modulus change of G347A, versus neutron fluence, irradiated at 738°C±27°C.	34
Figure 4.38. Shear modulus change of G347A, versus neutron fluence, irradiated at 738°C±27°C.....	34
Figure 4.39. Electrical resistivity change of G347A, versus neutron fluence, irradiated at 738°C±27°C.	35
Figure 4.40. Strength changes of G347A, versus neutron fluence, irradiated at 738°C±27°C.....	35
Figure 4.41. (a) Mean CTE versus measurement temperature of G347A, and (b) mean CTE changes versus neutron fluence, irradiated at 738°C±27°C.	36
Figure 4.42. (a) Thermal conductivity versus measurement temperature of G347A, and (b) thermal conductivity change versus neutron fluence, irradiated at 738°C±27°C.....	36
Figure 4.43. Comparison of physical, mechanical, and thermal property changes of the three grades irradiated around 462°C±22°C.	37
Figure 4.44. Comparison of physical, mechanical, and thermal property changes of the three grades irradiated around 659°C±27°C.....	38
Figure 4.45. Combined trend lines showing temperature effects on length change versus total fluence.	40
Figure 4.46. Combined trend lines showing temperature effects on volume change versus total fluence.	40
Figure 4.47. Combined trend lines showing temperature effects on Young's modulus change versus total fluence.	41
Figure 4.48. Combined trend lines showing temperature effects on shear modulus change versus total fluence.	41
Figure 4.49. Combined trend lines showing temperature effects on electrical resistivity change versus total fluence.	42
Figure 4.50. Combined trend lines showing temperature effects on strength change versus total fluence.	42
Figure 4.51. Combined trend lines showing temperature effects on the change of mean CTE versus total fluence.	43
Figure 4.52. Combined trend lines showing temperature effects on the change of thermal conductivity, measured at irradiation temperature, versus total fluence.	43

Figure A.1. Temperature monitor analysis from rabbit TOK-01.	A-2
Figure A.2. Temperature monitor analysis from rabbit TOK-02.	A-2
Figure A.3. Temperature monitor analysis from rabbit TOK-03.	A-3
Figure A.4. Temperature monitor analysis from rabbit TOK-04.	A-3
Figure A.5. Temperature monitor analysis from rabbit TOK-05.	A-4
Figure A.6. Temperature monitor analysis from rabbit TOK-06.	A-4
Figure A.7. Temperature monitor analysis from rabbit TOK-07.	A-5
Figure A.8. Temperature monitor analysis from rabbit TOK-08.	A-5
Figure A.9. Temperature monitor analysis from rabbit TOK-09.	A-6
Figure A.10. Temperature monitor analysis from rabbit TOK-10.	A-6
Figure A.11. Temperature monitor analysis from rabbit TOK-11.	A-7
Figure A.12. Temperature monitor analysis from rabbit TOK-12.	A-7
Figure A.13. Temperature monitor analysis from rabbit TOK-13.	A-8
Figure A.14. Temperature monitor analysis from rabbit TOK-14.	A-8
Figure A.15. Temperature monitor analysis from rabbit TOK-15.	A-9
Figure A.16. Temperature monitor analysis from rabbit TOK-16.	A-9
Figure A.17. Temperature monitor analysis from rabbit TOK-17.	A-10
Figure A.18. Temperature monitor analysis from rabbit TOK-18.	A-10
Figure A.19. Temperature monitor analysis from rabbit TOK-19.	A-11
Figure A.20. Temperature monitor analysis from rabbit TOK-20.	A-11
Figure A.21. Temperature monitor analysis from rabbit TOK-21.	A-12
Figure A.22. Temperature monitor analysis from rabbit TOK-22.	A-12
Figure A.23. Temperature monitor analysis from rabbit TOK-23.	A-13
Figure A.24. Temperature monitor analysis from rabbit TOK-24.	A-13
Figure A.25. Temperature monitor analysis from rabbit TOK-25.	A-14
Figure A.26. Temperature monitor analysis from rabbit TOK-26.	A-14
Figure A.27. Temperature monitor analysis from rabbit TOK-27.	A-15
Figure A.28. Temperature monitor analysis from rabbit TOK-28.	A-15
Figure A.29. Temperature monitor analysis from rabbit TOK-29.	A-16
Figure A.30. Temperature monitor analysis from rabbit TOK-30.	A-16
Figure A.31. Temperature monitor analysis from rabbit TOK-31.	A-17

LIST OF TABLES

Table	Page
Table 2.1. Summary of specimen types, dimensions, which rabbit and the quantity the specimen was included, and measurement performed before and after irradiation.	7
Table 2.2. Physical, mechanical, and thermal properties measured by ORNL on the pre-irradiation specimens.	8

ACRONYMS

AG	Against Gravity
ASME	American Society of Mechanical Engineers
ASTM	American Society for Testing and Materials
AX	Axial
CTE	Coefficient of Thermal Expansion
DOE	Department of Energy
HFIR	High Flux Isotope Reactor
HTGR	High Temperature Gas-cooled nuclear Reactor
LAMDA	Low Activation Materials Design and Analysis
ORNL	Oak Ridge National Laboratory
PSSV	Pre-Irradiation Specimen Size Validation
RSS	Research Safety Summary
SBMS	Standard Based Management System
SiC	Silicon Carbide
TR	Transverse
WG	With Gravity

EXECUTIVE SUMMARY

This joint program between Oak Ridge National Laboratory (ORNL) and Tokai Carbon Co., Ltd., began in 2009 with the final objective being the preliminary qualification of graphite grade G347A as a candidate material for use in the Generation-IV high temperature gas-cooled nuclear reactor (HTGR). The first segment of this program involved the planning and design of the irradiation program, and the investigation of the feasibility of using specimens smaller than recommended in the pertinent American Society for Testing and Materials (ASTM) International test standards. The results from the first segment were provided to the program sponsor in the document titled “Graphite Pre-Irradiation Specimen Size Validation and Testing Program – Results – Tokai Carbon Japan” [1]. The second segment of this program included the irradiation of the graphite and the measurement of the changes to a set of pre-defined physical, mechanical, and thermal properties.

This report contains the information regarding the planning, implementation of, and the results from the second segment of this program. The irradiation program was designed to cover a range of temperature and fluences that are relevant to the conditions expected to occur over the lifetime of the HTGR. The specimens were irradiated in irradiation capsules (called rabbits) in the High Flux Isotope Reactor (HFIR) at ORNL. The post-irradiation property measurements were performed in the Low Activation Materials Design and Analysis (LAMDA) laboratory. The changes in the various properties will be summarized, followed by a discussion on the comparison of the observed changes and similarity to changes in other nuclear graphite grades.

The properties measured, before and after neutron irradiation, include: mass, dimension, Young’s modulus, shear modulus, electrical resistivity, equibiaxial flexural strength, coefficient of thermal expansion (CTE), and thermal diffusivity/conductivity. The trends for the effects of increasing neutron fluence on the normalized change of specimen volume, Young’s modulus, mean CTE, equibiaxial strength, and thermal conductivity, of G347A irradiated at temperature of $362^{\circ}\text{C}\pm 43^{\circ}\text{C}$ and $738^{\circ}\text{C}\pm 27^{\circ}\text{C}$ are shown in the figure below. The trends observed in these property changes agree well with those reported in the literature for other graphite grades.

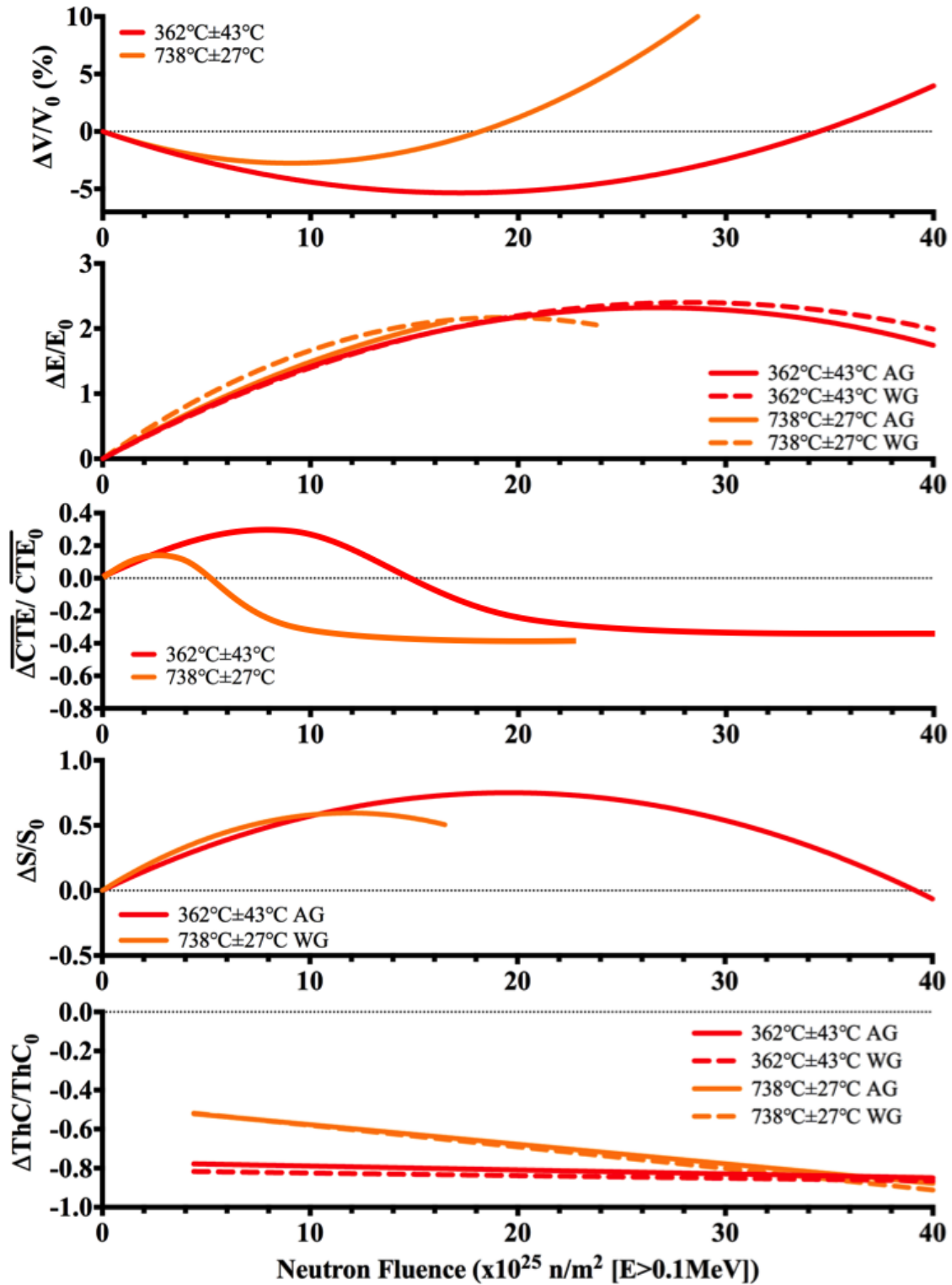


Figure. Change of volume, Young's modulus, coefficient of thermal expansion, equibiaxial strength, and thermal conductivity (top to bottom respectively) of G347A irradiated at 362°C±43°C and 738°C±27°C, versus accumulated fast neutron fluence. AG and WG denote specimen orientations against gravity and with gravity, respectively.

ACKNOWLEDGEMENT

This program would not have been completed without the expertise and input from numerous persons throughout the laboratory. Authors would like to acknowledge Kentaro Takizawa, Timothy Burchell, and Lance Snead for many useful discussions and scientific guidance. Special notice needs to be given to the staff of the LAMDA laboratory: Marie Williams, Patricia Tedder, Stephanie Curlin, Daniel Lewis, Michael McAllister, Bill Comings, Brian Eckhart, Ashli Clark, and Wallace Porter.

This work was sponsored by Tokai Carbon Co., Ltd., under contract NFE-09-02345 with UT-Battelle, LLC.

1. INTRODUCTION

This report summarizes the results from the joint research venture, between ORNL and Tokai Carbon Co., Ltd., to study the effect of neutron irradiation on a newer grade of nuclear graphite. The irradiations were performed in the flux trap of the ORNL HFIR. This report will cover the basics of the program (material, properties, and irradiation) and the results of the property changes due to different irradiation conditions (temperature and total fluence).

2. MATERIALS

2.1 MATERIALS USED IN THIS PROGRAM

The material of primary interest was Tokai Carbon Co., Ltd. Grade G347A, with a smaller emphasis placed on grade G458A. Additionally, extra experimental space allowed the addition of a small number of specimens of commercially available Toyo Tanso grade IG-110. The program sponsor provided bulk material of G347A and G458A, and IG-110 was purchased from the manufacturer. In extruded and pressed graphite, two orientations indications were used to distinguish the directions of preferred orientation. These directions were usually labeled With Grain and Against Grain. But, in near-isotropic graphite this distinction is difficult to make, and instead the two labels that were used are With Gravity (WG) and Against Gravity (AG), where the WG direction is parallel to the direction of gravity during the isostatic pressing portion of the manufacture process. These distinctions can easily be confused so another way of labeling these directions in isostatically pressed graphite is the use of Axial (AX) and Transverse (TR) indicators, where axial and with gravity indicate the same direction. A schematic representation of the different directions is given in Figure 2.1.

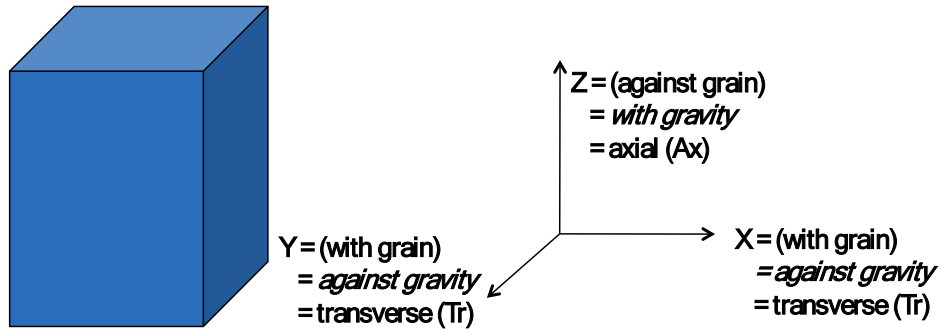


Figure 2.1. Orientation of orthogonal directions, relative to billet molding directions.

2.2 SPECIMEN INFORMATION

Specimens were cut from the larger material blocks. Various specimen sizes and shapes were employed to investigate different physical, thermal, and mechanical properties. Additionally some specimens were cut with multiple orientations relative to the bulk material to investigate pre-irradiation anisotropy and if there are any effects of orientation on the irradiation behavior. Figure 2.2 shows the different specimen shapes, sizes, and orientations, relative to the orthogonal directions of the bulk material. A summary of these specimen types, dimensions, and uses are in Table 2.1.

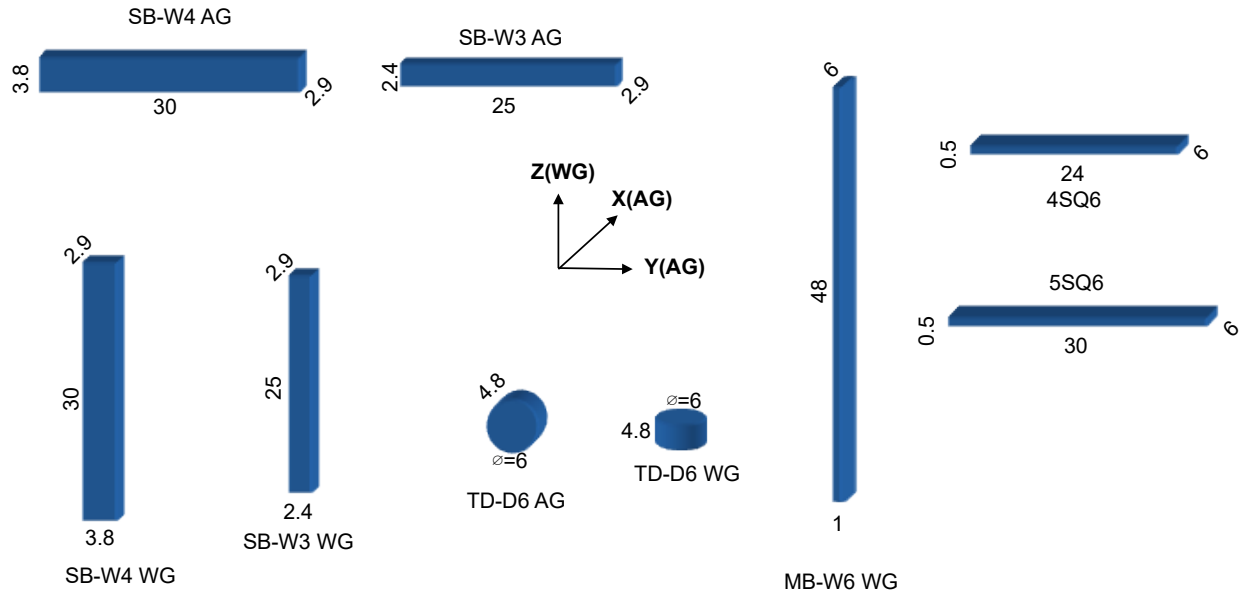


Figure 2.2. Specimen orientations relative to billet orthogonal directions.

Table 2.1. Summary of specimen types, dimensions, which rabbit and the quantity the specimen was included, and measurement performed before and after irradiation.

Specimen Type	Dimensions (mm)	Rabbit Usage	Number in Rabbit	Measurements
SB-W3	25 x 2.9 x 2.4	GRIC-2	4	Dimensions, mass, Young's modulus, CTE
SB-W4	30 x 3.8 x 2.9	GRIC-1	2	Dimensions, mass, Young's modulus, electrical resistivity, CTE
MB-W6	48 x 6 x 1	GRIC-1	1	Dimensions, mass, Young's modulus, shear modulus
TD-D6	Ø6 x 4.8	GRIC-1	3	Dimensions, mass, thermal conductivity
		GRIC-2	4	
5SQ6	30 x 6 x 0.5	GRIC-1	2	Dimensions, mass
4SQ6	24 x 6 x 0.5	GRIC-2	2	Dimensions, mass
SQ6 (individual coupons)	6 x 6 x 0.5	GRIC-1	10	Equibiaxial strength
		GRIC-2	8	

Before irradiation all the non-destructive tests were performed on each specimen for base-line values. The properties considered destructive were the CTE, thermal conductivity, and equibiaxial strength. The CTE and thermal conductivity are potentially destructive if there is a small amount of oxygen in the system resulting in possible oxidation or mass loss. Therefore only a few specimens were tested for these thermal properties and the ones tested were not used for irradiation. Likewise, the strength testing was also destructive so a small subset of the specimens was used for the baseline measurement. The results of the ORNL-measured as-received physical, mechanical, and thermal properties are summarized in Table 2.2. The results for G458A and IG-110 are limited to properties that were measured on the reduced specimen types.

Table 2.2. Physical, mechanical, and thermal properties measured by ORNL on the pre-irradiation specimens.

	Orientation	G347A	G458A	IG-110
Density (g/cm ³)	All	1.84 ± 0.01	1.84 ± 0.02	1.76 ± 0.01
Young's Modulus (GPa)	AG	11.13 ± 0.49		
	WG	10.72 ± 0.46	11.29 ± 1.24	9.71 ± 1.67
Shear Modulus (GPa)	AG	4.23 ± 0.03		
	WG	4.15 ± 0.06		
Poisson's Ratio	AG	0.27 ± 0.01		
	WG	0.24 ± 0.01		
Electrical Resistivity (μΩm ²)	AG	9.1 ± 0.03		
	WG	9.53 ± 0.11		
Equibiaxial Strength (MPa)	AG	87.15 ± 18.06		
4-point Flexural Strength (MPa)	AG	49.92 ± 2.20 ^a		
	WG	51.58 ± 2.04 ^a		
Mean CTE at 500°C (10 ⁻⁶ K ⁻¹)	AG	4.18 ± 0.05		
	WG	4.48 ± 0.02	3.81 ± 0.02	4.56 ± 0.1
Isotropy Ratio		1.07		
Thermal Conductivity at 500°C (W/m/K)	AG	85.55 ± 0.14		
	WG	86.48 ± 1.02	78.91 ± 2.4	

^a Note specimens for 4-point flexural testing were not used for irradiation.

3. EXPERIMENTAL PROGRAM

3.1 IRRADIATION VEHICLES

The specimens were irradiated in small capsules, called rabbits. Each rabbit consisted of multiple components (Figure 3.1) including the housing, specimen holder, specimens, and silicon carbide (SiC). This program utilized two different specimen configurations (GRIC-1 and GRIC-2). The small size of these rabbits (nominal 10 mm diameter and 60 mm in length) limited the ability to use on-line measurement techniques, such as thermocouples, and instead SiC was used as a passive temperature monitor. The outer diameter of the specimen holder was varied to get different gas gaps, which were then filled with different inert gasses to achieve the desired specimen temperatures. The necessary gas gap and fill gas was determined by modeling the rabbits in a two-dimensional finite element heat transfer software, and iteratively determining the gap and gas that gave the desired specimen temperature. The ANSYS software was acquired mid-way into this program, which provided the ability to model the rabbits in three-dimensions. At that time the rabbits were re-modeled in 3D with the parameters from the 2D design. The 3D thermal models for the two rabbit configurations are shown in Figure 3.2.

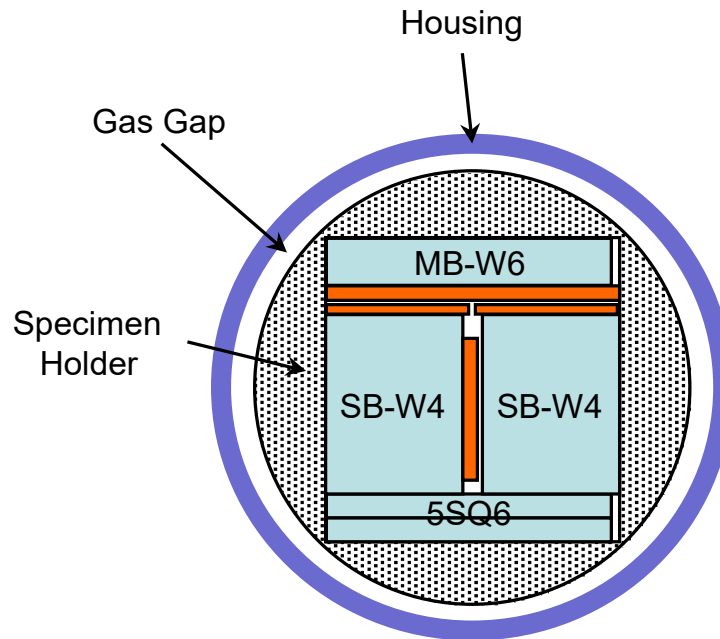


Figure 3.1. Example schematic cross section of a GRIC-1 rabbit.

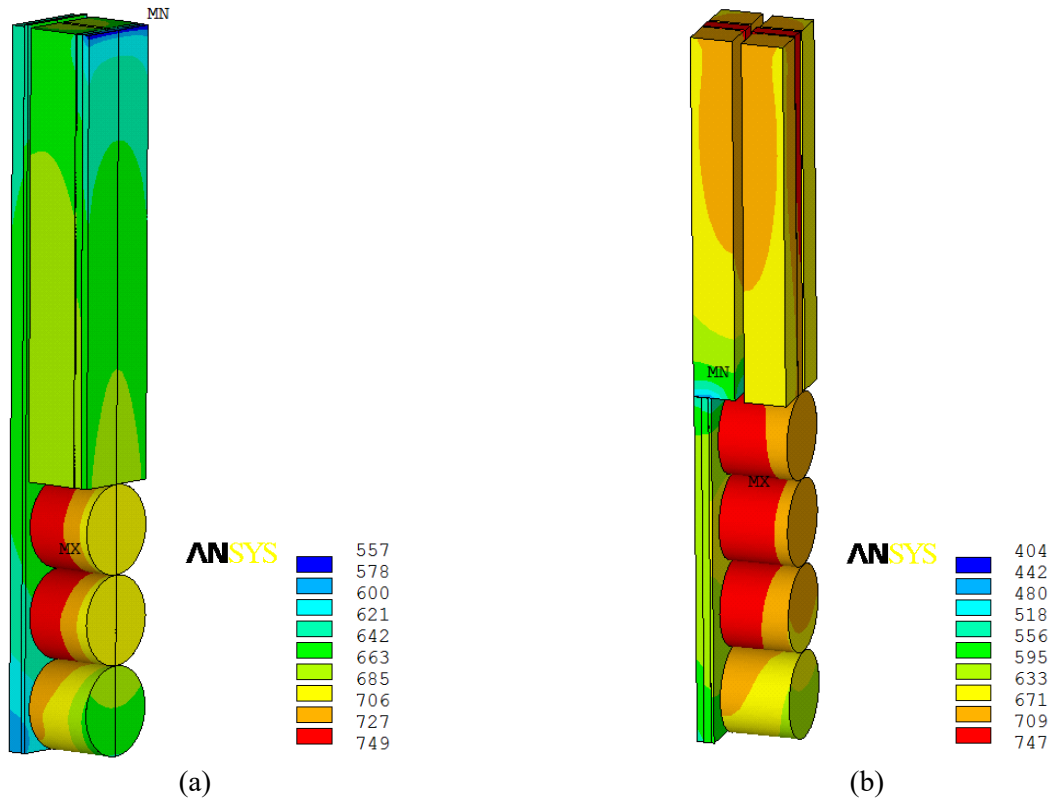


Figure 3.2. 3-dimensions heat-transfer design of the (a) GRIC-1 and (b) GRIC-2 rabbits.

The objective in planning the irradiation conditions was to achieve temperature and fluence combinations that were relevant to the two high-temperature gas reactor configurations: prismatic core and pebble bed core. The prismatic design has the fuel located within graphite blocks so the graphite will experience higher temperatures, whereas the pebble bed uses graphite for the reflector only so the temperature will be lower. The irradiation behavior of graphite is such that the property changes happen over a much shorter time when the temperature is higher. Therefore, the higher the irradiation temperature, the lower the final fluence that was necessary, which is shown in the planned irradiation envelope in Figure 3.3. The additional G458A and IG-110 specimens were only used in the GRIC-2 rabbits, which were interspersed with the primary rabbits on the irradiation envelope.

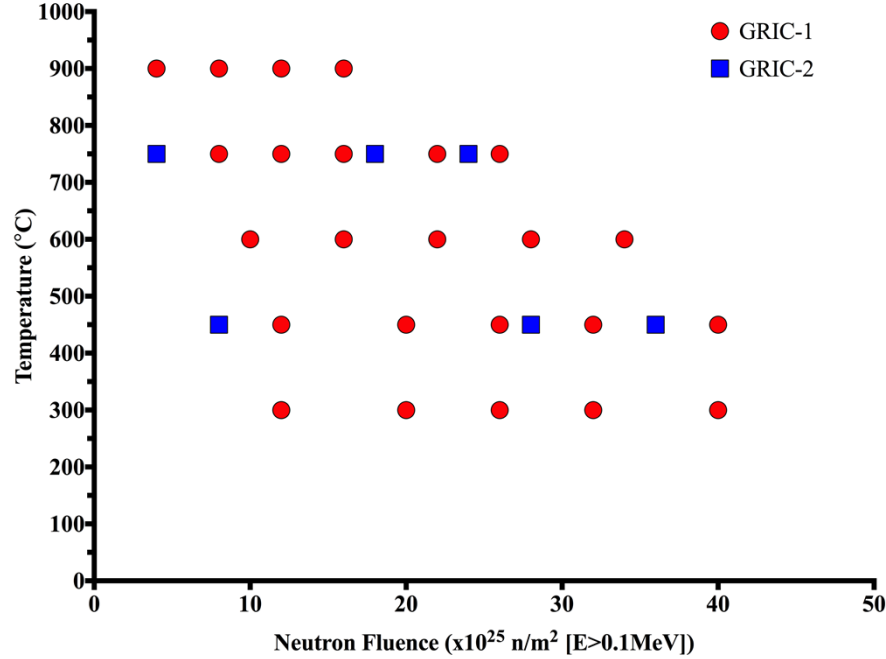


Figure 3.3. Planned irradiation envelope, showing the planned irradiation temperatures and total neutron fluences.

3.2 HFIR INFORMATION

The HFIR at ORNL has one of the highest flux levels available at any materials test reactor in the world. It is an 85MW pressurized-water reactor, which traditionally operates on approximately a 25-day fuel cycle. The world-leading flux is achieved because the reactor has an annular configuration, schematically shown in Figure 3.4. The central region is the flux trap, which where the flux levels are highest and where all of this program's specimens were irradiated. The grey region is the fuel, which is then surrounded by the beryllium reflector (purple), control rods (teal), and finally the outer beryllium (green). The rabbits were irradiated in either the peripheral target positions (orange circles in Figure 3.4) or in the outer-most target positions (white hexagons in Figure 3.4 such as B1, C1, A2, or A3). The thermal and fast flux profiles of HFIR, measured in the peripheral target positions and the hydraulic tubes, are plotted in Figure 3.5 versus axial rabbit position (equivalent to location along the height of the core). Along the length of the HFIR core there is room to stack up to 9 rabbits, but traditionally only positions 2-8 are used, with the central positions of 4-6 being preferred because the flux gradient within a rabbit is minimized.

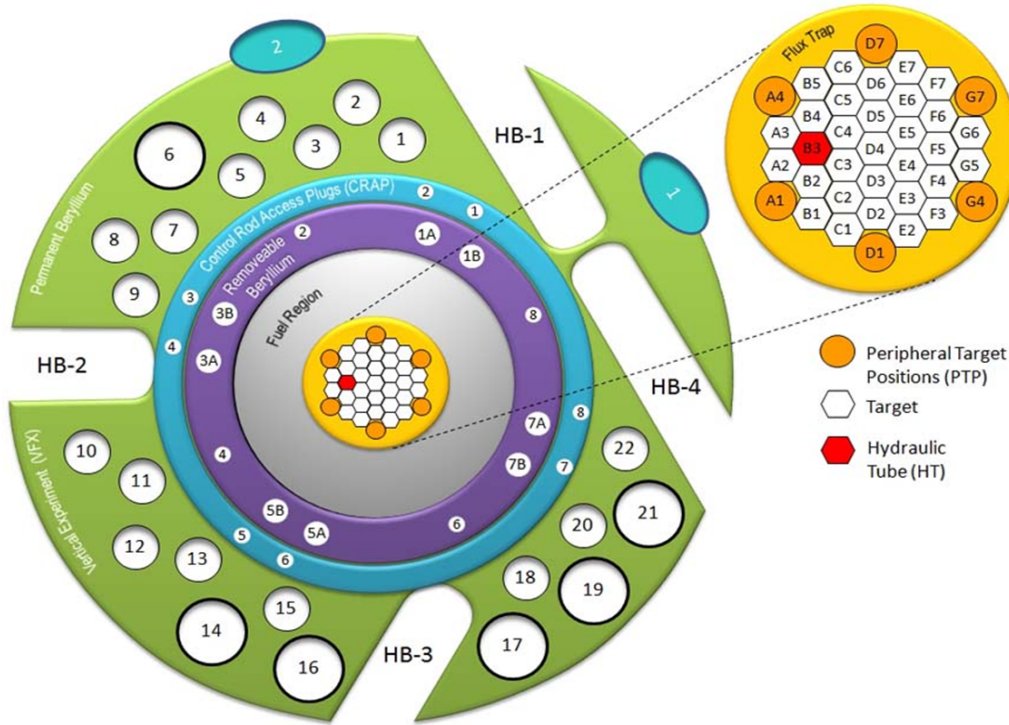


Figure 3.4. Drawing of the HFIR core, where the rabbits were irradiated in the central yellow and white region.

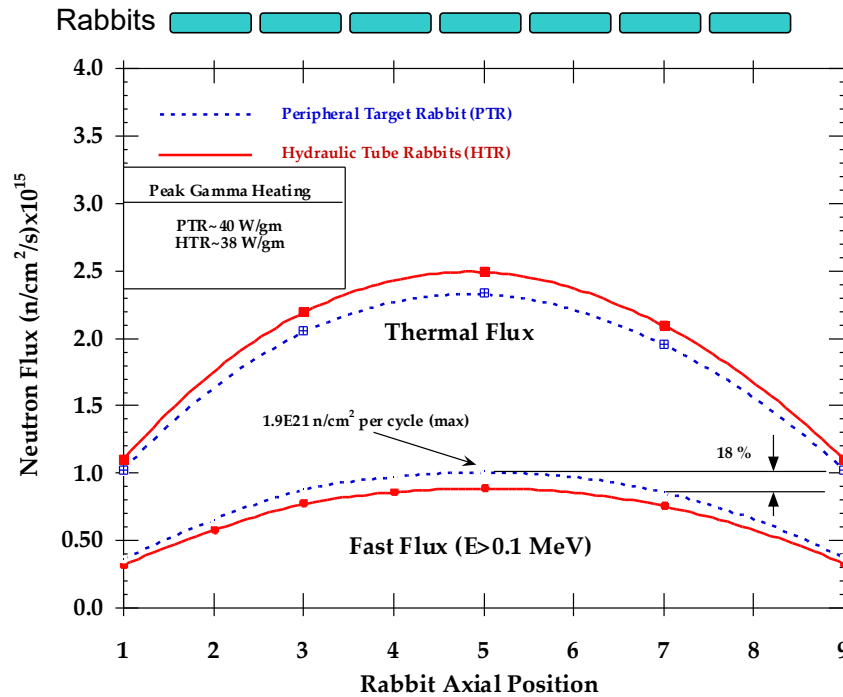


Figure 3.5. Plot of the fast and thermal neutron fluxes versus the rabbit position along the core height (rabbit 1 located at the bottom and rabbit 9 is located at the top). The rabbits in this program were irradiated in positions that correspond to the “Peripheral Target Rabbit” fluxes.

3.3 TEST PROCEDURES

All the pre- and post-irradiation measurements were performed in the LAMDA laboratory. The pre-irradiation measurements were performed in the clean laboratory space in LAMDA according to the Graphite Pre-Irradiation Sample Size Validation and Testing Program [2]. The post-irradiation measurements were performed in the radiation laboratory portion of LAMDA according to the Graphite Post-Irradiation Testing Program – Test Specification [3].

4. RESULTS AND DISCUSSION

4.1 DETERMINING FINAL IRRADIATION CONDITIONS

As was mentioned in Section 3.1, the total fluence and temperature were not measured during irradiation. Instead these values were determined via calculations and passive measurement techniques. The flux profiles of HFIR have been measured and modeled numerous times, so the calculation of the total fluence was straightforward. The HFIR is operated at a steady power of 85MW and when this power can no longer be maintained the reactor is shut down for refueling. So by knowing the average flux for each rabbit, and the total time the rabbit was in the reactor for full-power operation, allows for determination of the final fluence of each rabbit.

The temperature determination is a little more complex, but utilized a very simple method [4]. Silicon carbide is an ideal material to use for passive temperature monitoring because the radiation-produced defects will be annealed out at temperatures slightly higher than the irradiation temperature. Therefore, different properties can be measured during a post-irradiation annealing process, and the properties will change once the annealing temperature surpasses the irradiation temperature. The analysis technique used for this program involved the analysis of the changing behavior of the CTE of the SiC as it approached and surpassed the irradiation temperature. The post-irradiation SiC temperature determination was performed on a dual push-rod dilatometer, and the data used in the analysis is the instantaneous CTE from the heating and cooling segments of the run. An example of the analysis results are shown in Figure 4.1 for a temperature monitor from the rabbit TOK-01, which had a design temperature of 300°C. In this figure, the heating portion of the dilatometer run is the red data, while the blue data is the cooling segment, and the difference between the two is shown with the purple data. At temperatures below 300°C the heating and cooling behavior are the same, but once the temperature goes above the irradiation temperature the CTE decreases as radiation defects are annealed out of the sample. The process of determining the irradiation temperature has been standardized with a computer program that performs the following steps. 1) A numerical curve is fit to the difference of the heating and cooling curves (s-shaped yellow line). 2) The temperature locations of the first, second and third inflection points of this curve are calculated. 3) Straight lines are fit to the heating curve at the three inflection points. 4) The temperatures where the straight lines intersect the cooling data are listed as the maximum (black line at first inflection temperature), median (bright blue line at second inflection temperature), and the minimum temperature (green line at third inflection temperature). Additionally the temperature corresponding to the first inflection point is listed as the transition temperature, because that is the temperature where no new defects are beginning to anneal. The summary of the rabbit information is listed in Section A.1, and the analyzed temperature monitor results are given in Section A.2.

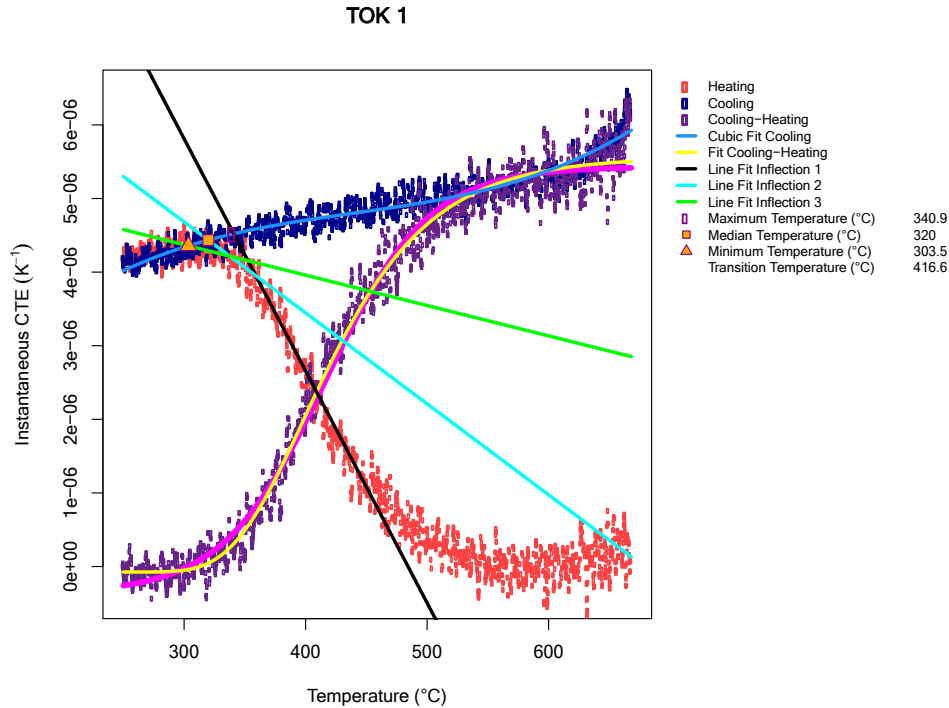


Figure 4.1. Example analysis of passive temperature monitor for rabbit TOK-01.

During the irradiation campaign, it became apparent that high temperature rabbits were not reaching the design temperature. The 900°C rabbits were giving temperatures around 750°C, and the 750°C design rabbits were displaying temperatures around 650°C. An investigation revealed that at these high temperatures the heat loss in the axial direction (along the length of the rabbit) becomes significant. The result was the 2D models of the rabbit cross section were underestimating the necessary gas gap width, which resulted in a lower temperature than designed. This was supported by the results from the 3D models of the as-fabricated rabbits that calculated lower temperatures than the initial targets. The final irradiation envelope is plotted in Figure 4.2, where the colors of the data points are the same as the dashed lines that show the target temperatures. The other deviation from planned is the rabbits with the 300°C design temperature. At the intermediate to high fluence the specimen temperatures were close to 450°C, but these are the same conditions where the changes to the specimens are the most extreme so the rabbits are most likely not correctly modeled with the pre-irradiation designs.

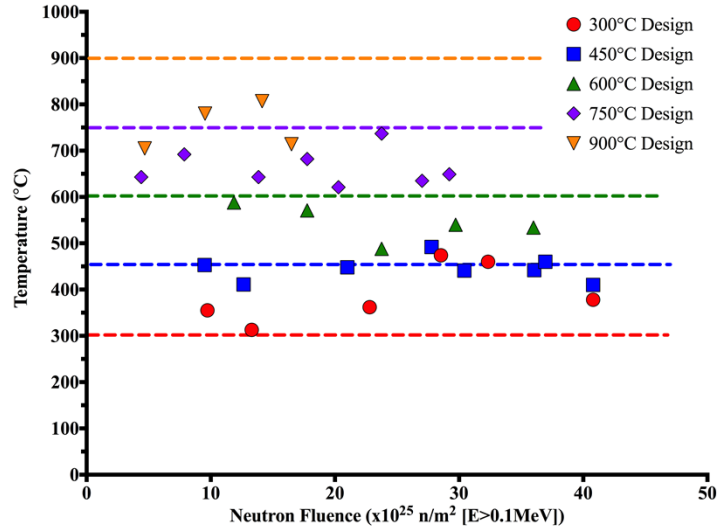


Figure 4.2. Plot of temperature monitor measured temperature and total fluence of each rabbit, where the data points are sorted by shape and color according to the design temperature.

The specimen temperatures were determined on an individual basis from the 3D thermal model results and from the maximum and minimum temperatures from the SiC thermometry, since the multiple specimen geometries resulted in different temperatures within a single capsule. Then the specimens were sorted by temperature, and were grouped into 5 temperature ranges: $362 \pm 43^\circ\text{C}$ (range $264\text{--}413^\circ\text{C}$), $462 \pm 22^\circ\text{C}$ (range $418\text{--}498^\circ\text{C}$), $546 \pm 23^\circ\text{C}$ (range $501\text{--}596^\circ\text{C}$), $659 \pm 27^\circ\text{C}$ (range $603\text{--}697^\circ\text{C}$), and $738 \pm 27^\circ\text{C}$ (range $701\text{--}786^\circ\text{C}$). These ranges were chosen to obtain multiple fluence points within each range, while trying to maintain a relatively small temperature spread. In the program results Excel file, all the property changes have two analysis tabs, one that sorts the specimens according to the actual specimen temperature (same plots presented in this report) and a second where the specimen are sorted according to nominal design temperature.

4.2 IRRADIATION-INDUCED CHANGES TO PROPERTIES

The following sections present the results from the measured property changes, sorted by grouped temperature. Each section, the first set of plots include the changes in length ($\Delta L/L_0$), volume ($\Delta V/V_0$), Young's modulus ($\Delta E/E_0$), shear modulus ($\Delta G/G_0$), electrical resistivity ($\Delta \rho/\rho_0$), strength ($\Delta S/S_0$) plotted versus total neutron fluence. The second set of plots show the coefficient of thermal expansion, and thermal conductivity versus measurement temperature (left plots), and the values measured at the irradiation temperature are plotted versus neutron fluence (right plots). In each plot the individual data points are plotted, except for strength where the average and standard deviation are used. In all the plots the filled points and solid lines represent AG specimens and the open points and dashed lines are the WG. The trend lines shown in all the plots versus fluence are fit either with straight lines or polynomials. These trend lines are only included to aid the reader in following the behavior, since there are currently no physical reasons for either type of fit. All the data used to create these plots are included in the appendices.

4.2.1 362°C±43°C

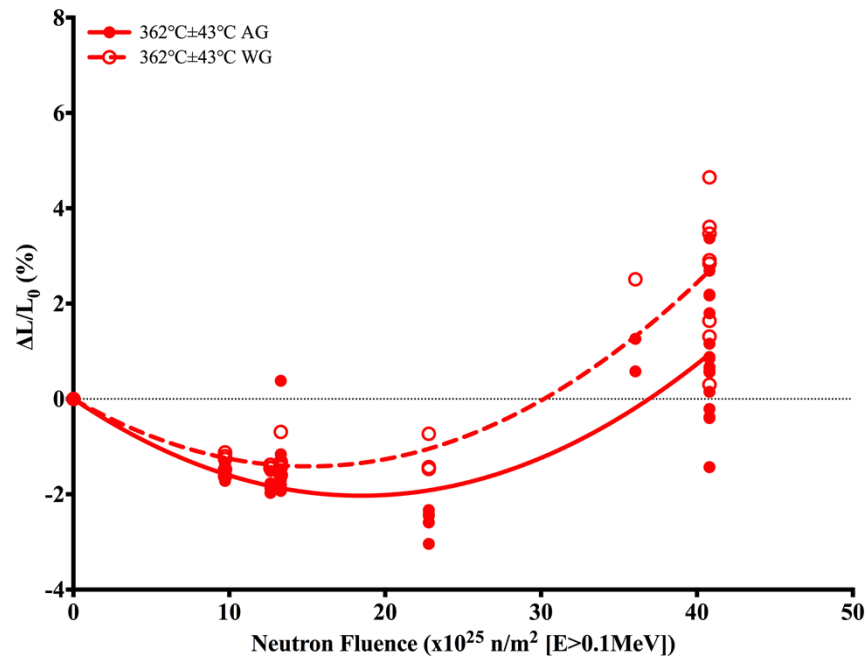


Figure 4.3. Length change of G347A, versus neutron fluence, irradiated at 362°C±43°C.

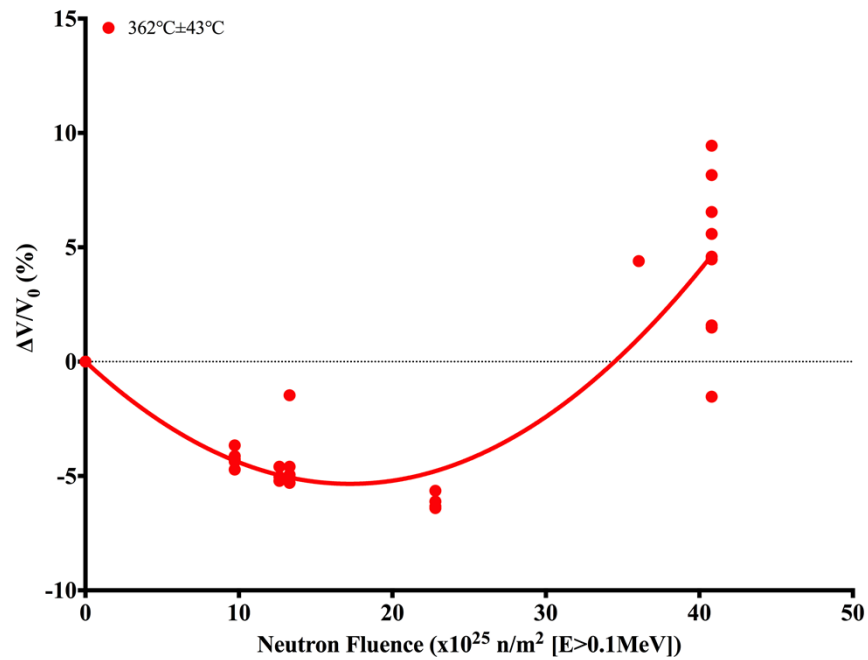


Figure 4.4. Volume change of G347A, versus neutron fluence, irradiated at 362°C±43°C.

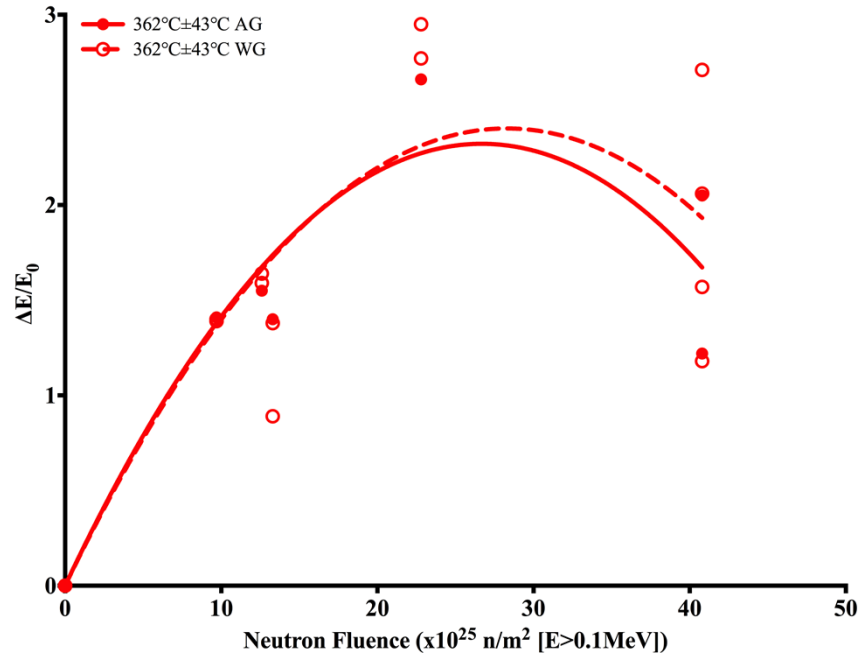


Figure 4.5. Young's modulus change of G347A, versus neutron fluence, irradiated at $362^\circ\text{C} \pm 43^\circ\text{C}$.

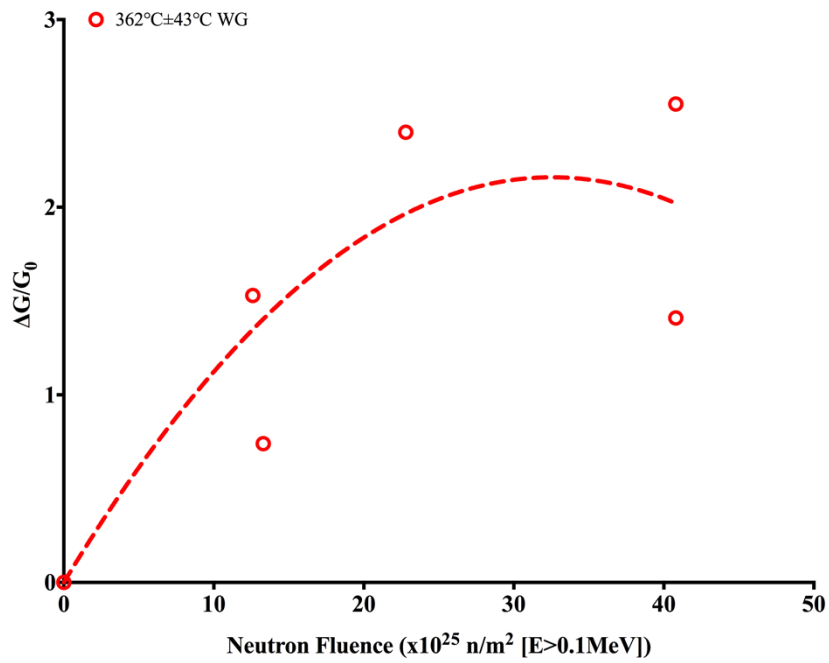


Figure 4.6. Shear modulus change of G347A, versus neutron fluence, irradiated at $362^\circ\text{C} \pm 43^\circ\text{C}$.

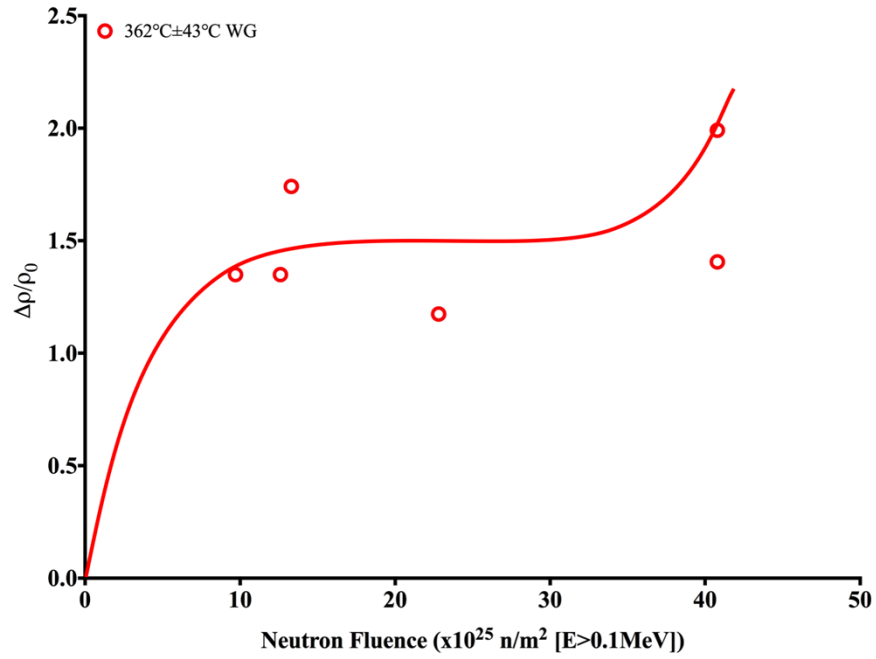


Figure 4.7. Electrical resistivity change of G347A, versus neutron fluence, irradiated at $362^\circ\text{C}\pm 43^\circ\text{C}$.

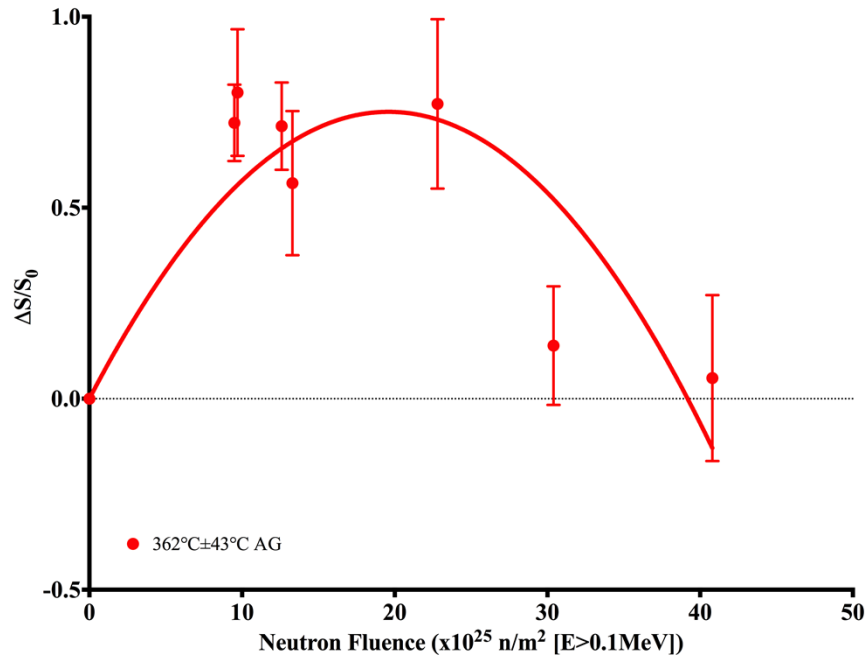


Figure 4.8. Strength changes of G347A, versus neutron fluence, irradiated at $362^\circ\text{C}\pm 43^\circ\text{C}$.

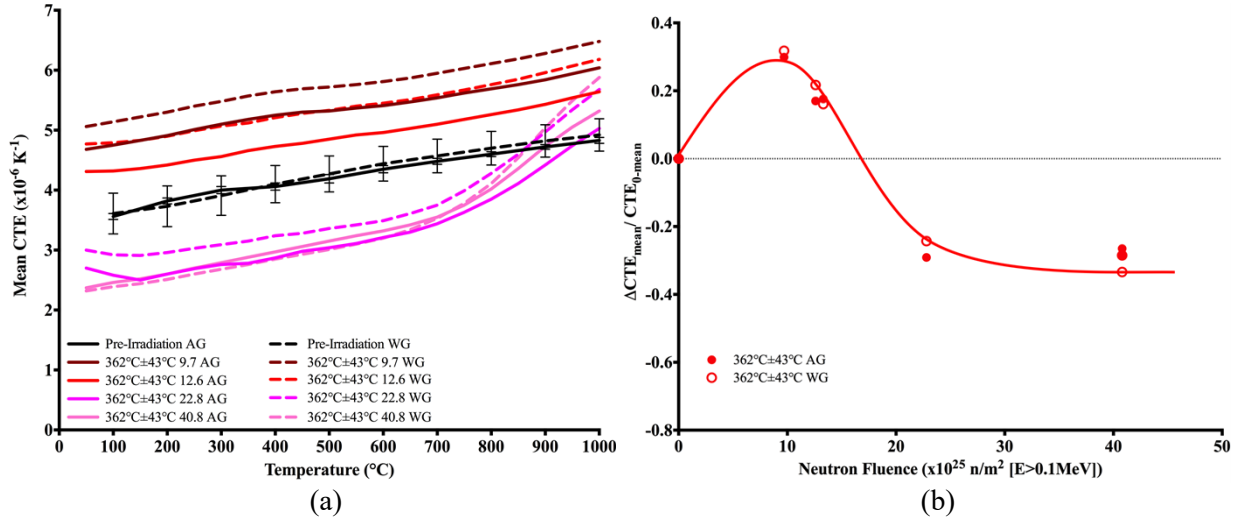


Figure 4.9. (a) Mean CTE versus measurement temperature of G347A, and (b) mean CTE changes versus neutron fluence, irradiated at 362°C±43°C.

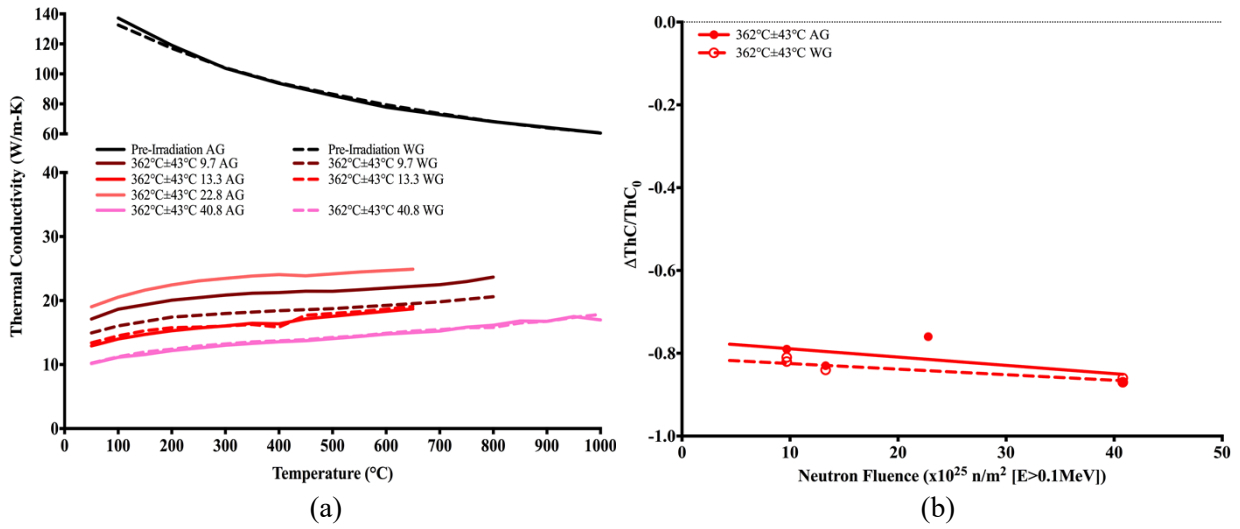


Figure 4.10. (a) Thermal conductivity versus measurement temperature of G347A, and (b) thermal conductivity change versus neutron fluence, irradiated at 362°C±43°C.

4.2.2 462°C±22°C

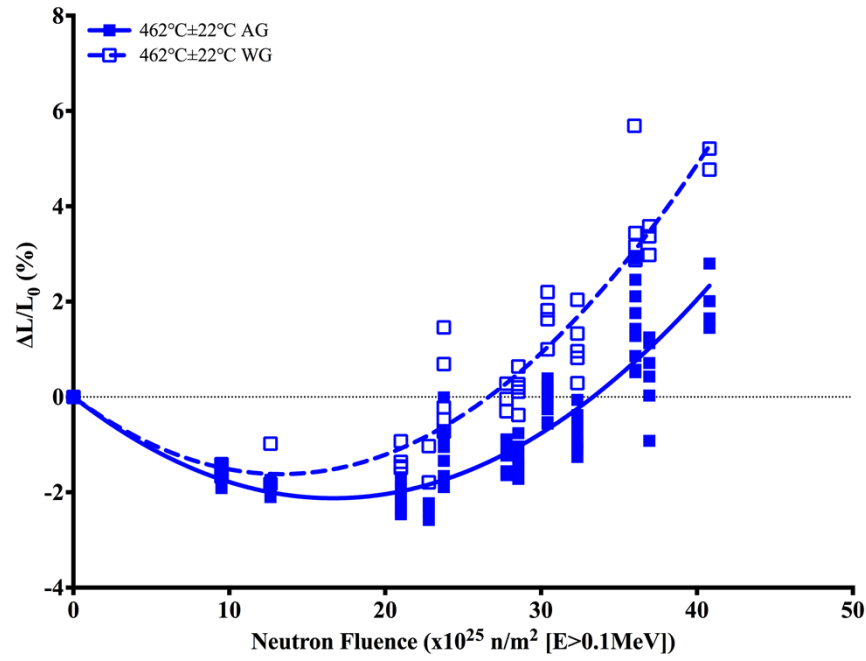


Figure 4.11. Length change of G347A, versus neutron fluence, irradiated at 462°C±22°C.

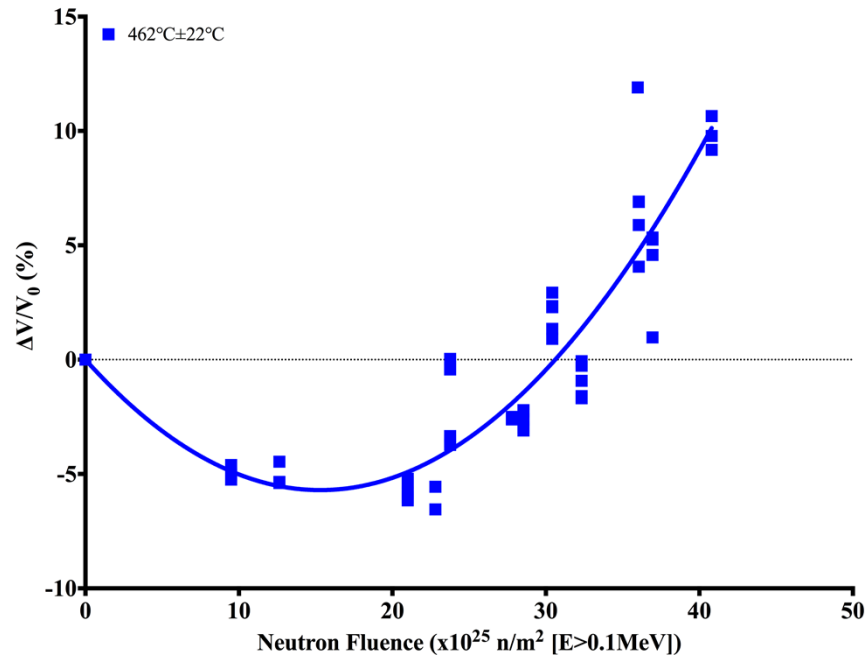


Figure 4.12. Volume change of G347A, versus neutron fluence, irradiated at 462°C±22°C.

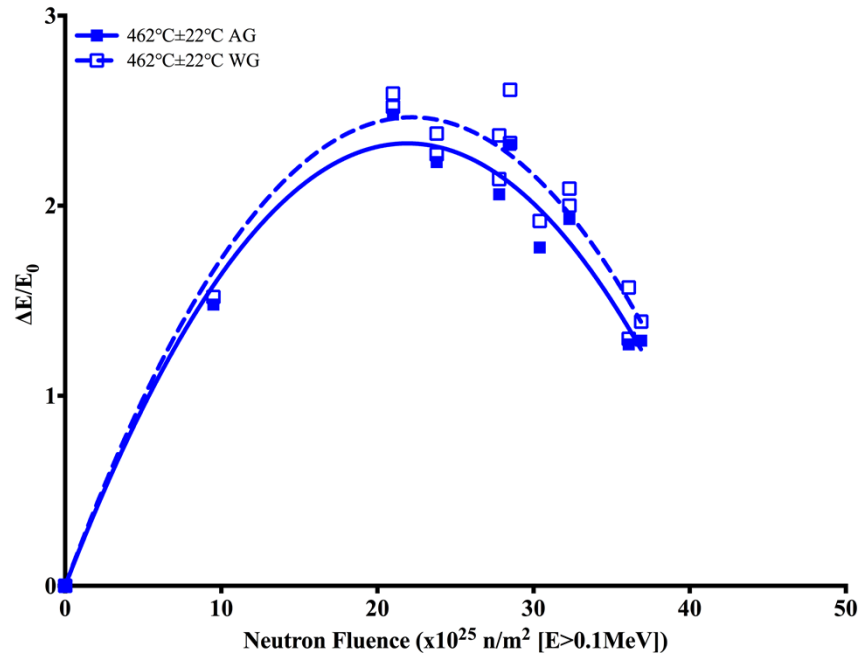


Figure 4.13. Young's modulus change of G347A, versus neutron fluence, irradiated at 462°C±22°C.

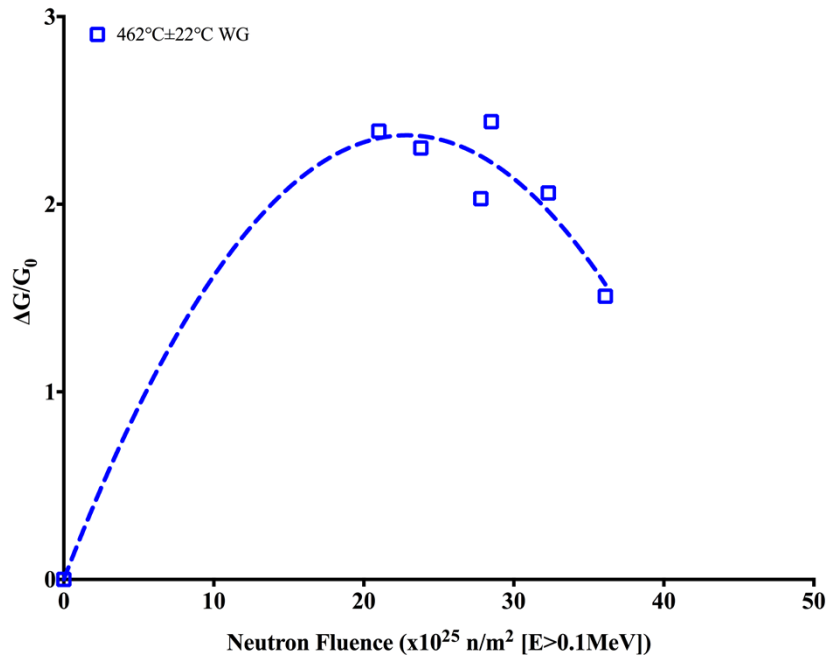


Figure 4.14. Shear modulus change of G347A, versus neutron fluence, irradiated at 462°C±22°C.

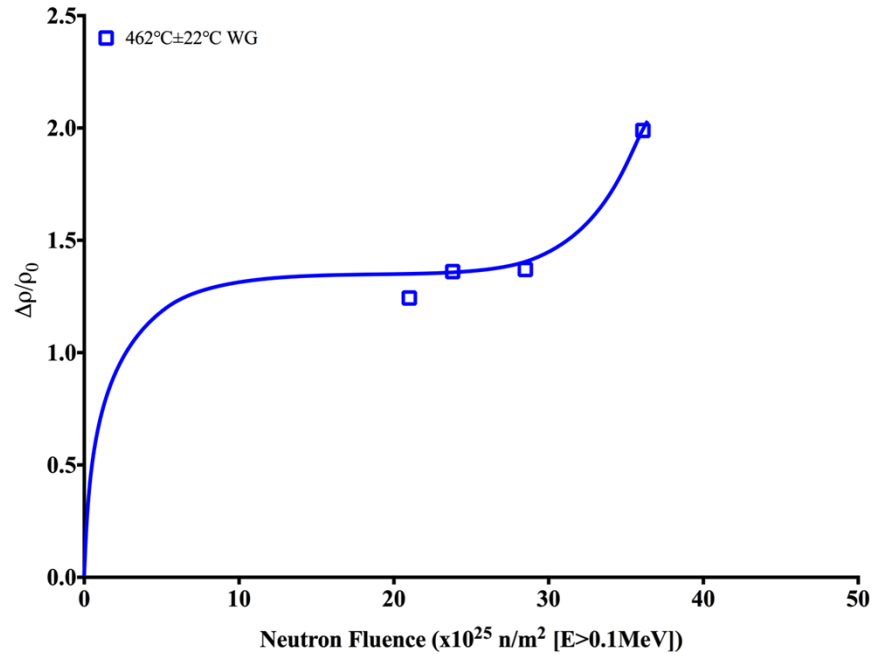


Figure 4.15. Electrical resistivity change of G347A, versus neutron fluence, irradiated at $462^\circ\text{C}\pm 22^\circ\text{C}$.

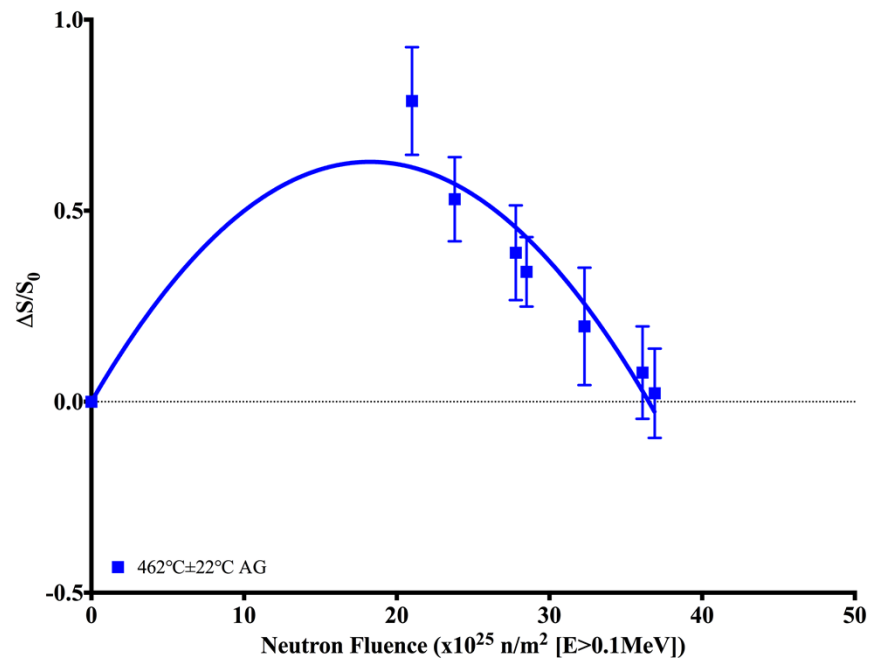


Figure 4.16. Strength changes of G347A, versus neutron fluence, irradiated at $462^\circ\text{C}\pm 22^\circ\text{C}$.

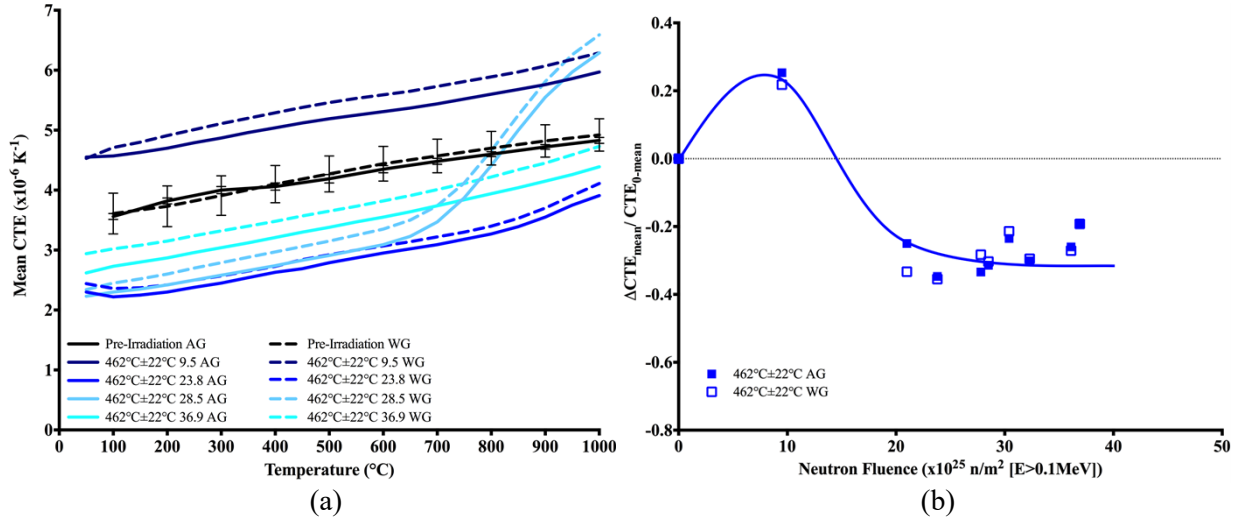


Figure 4.17. (a) Mean CTE versus measurement temperature of G347A, and (b) mean CTE changes versus neutron fluence, irradiated at $462^{\circ}\text{C} \pm 22^{\circ}\text{C}$.

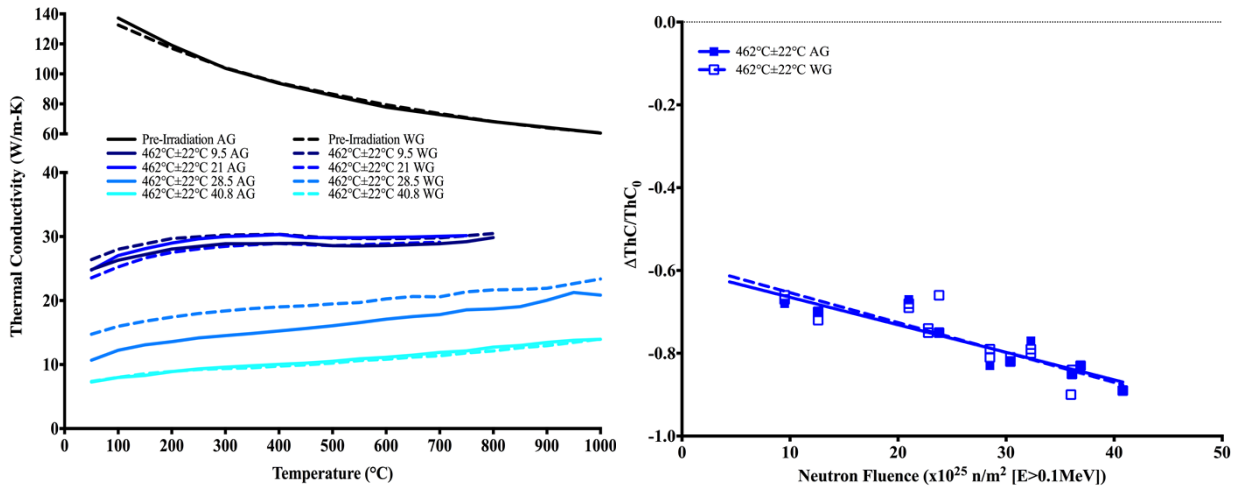


Figure 4.18. (a) Thermal conductivity versus measurement temperature of G347A, and (b) thermal conductivity change versus neutron fluence, irradiated at $462^{\circ}\text{C} \pm 22^{\circ}\text{C}$.

4.2.3 546°C±23°C

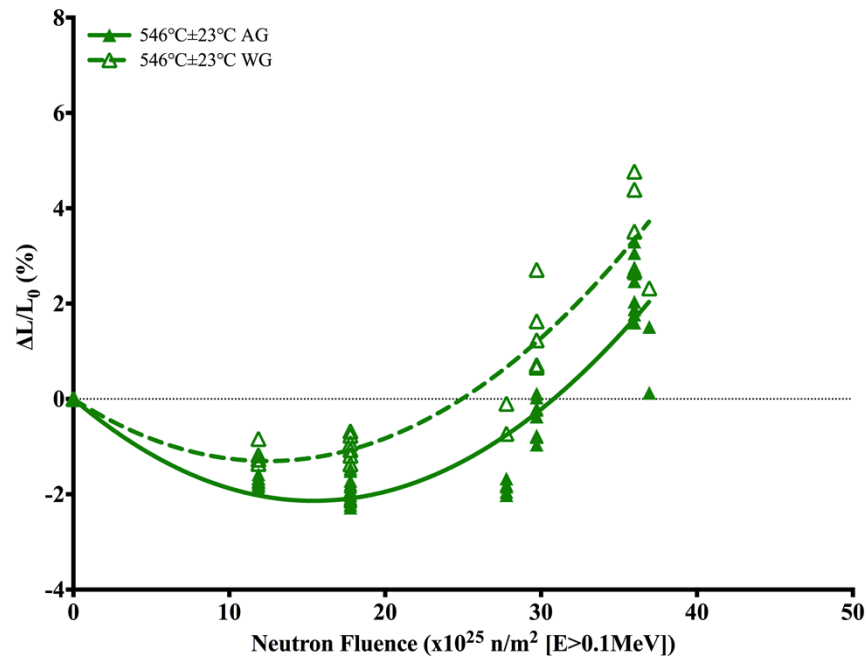


Figure 4.19. Length change of G347A, versus neutron fluence, irradiated at 546°C±23°C.

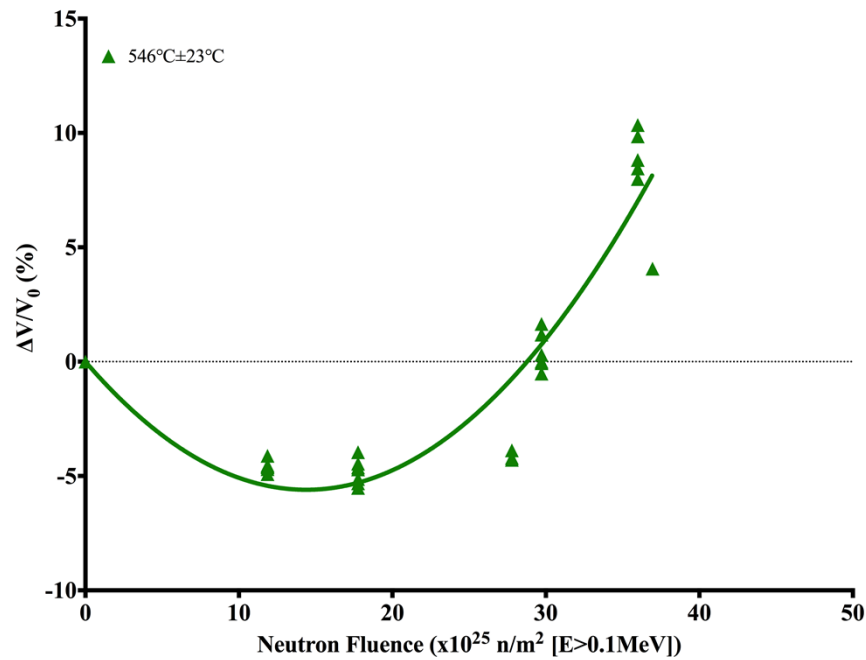


Figure 4.20. Volume change of G347A, versus neutron fluence, irradiated at 546°C±23°C.

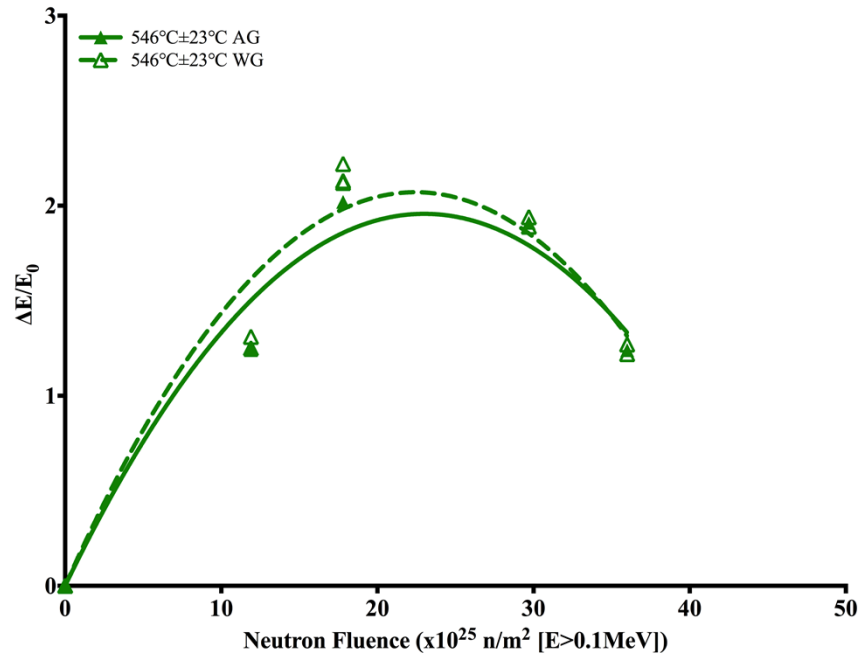


Figure 4.21. Young's modulus change of G347A, versus neutron fluence, irradiated at 546°C±23°C.

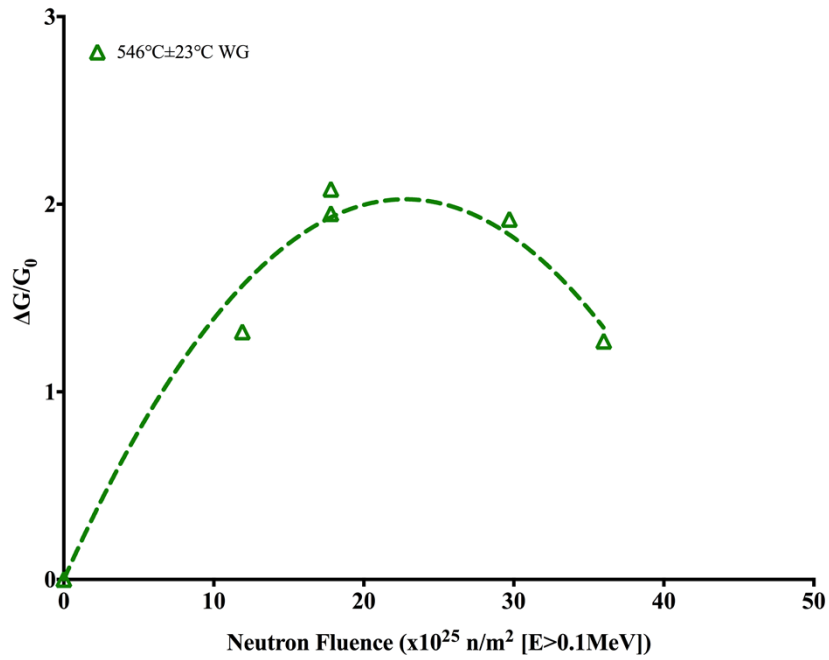


Figure 4.22. Shear modulus change of G347A, versus neutron fluence, irradiated at 546°C±23°C.

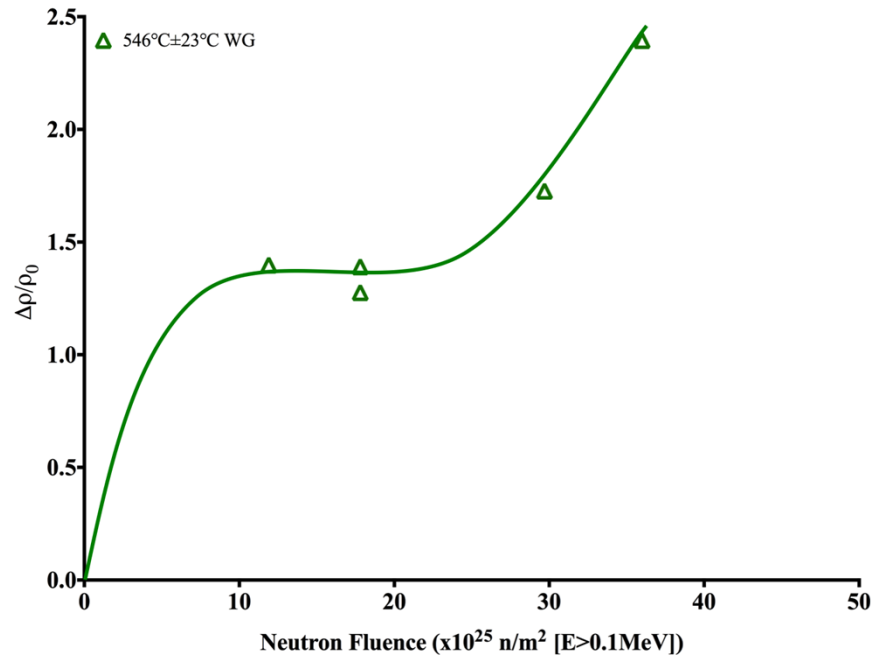


Figure 4.23. Electrical resistivity change of G347A, versus neutron fluence, irradiated at $546^\circ\text{C}\pm 23^\circ\text{C}$.

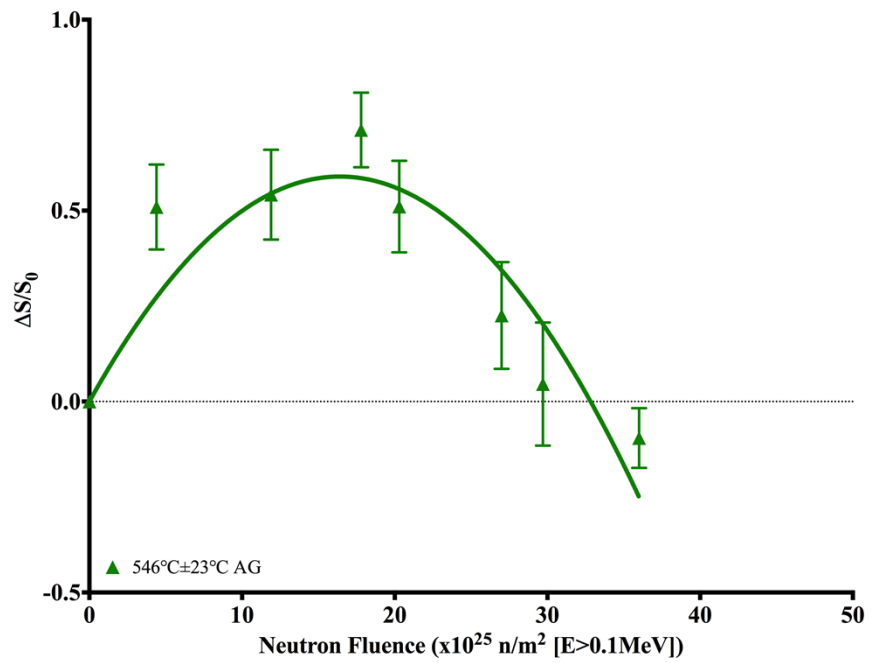


Figure 4.24. Strength changes of G347A, versus neutron fluence, irradiated at $546^\circ\text{C}\pm 23^\circ\text{C}$.

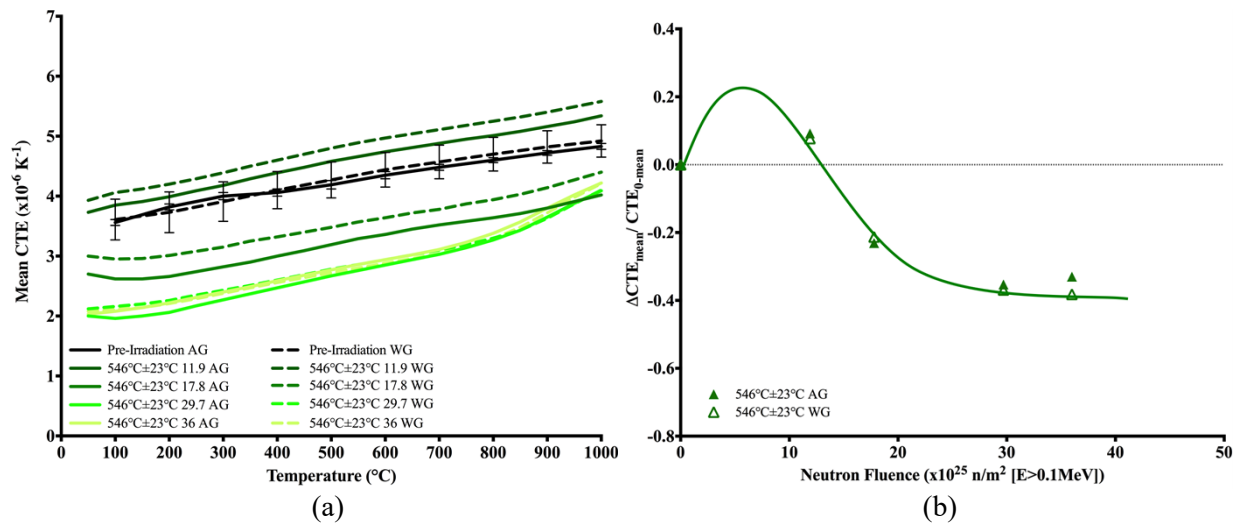


Figure 4.25. (a) Mean CTE versus measurement temperature of G347A, and (b) mean CTE changes versus neutron fluence, irradiated at 546°C±23°C.

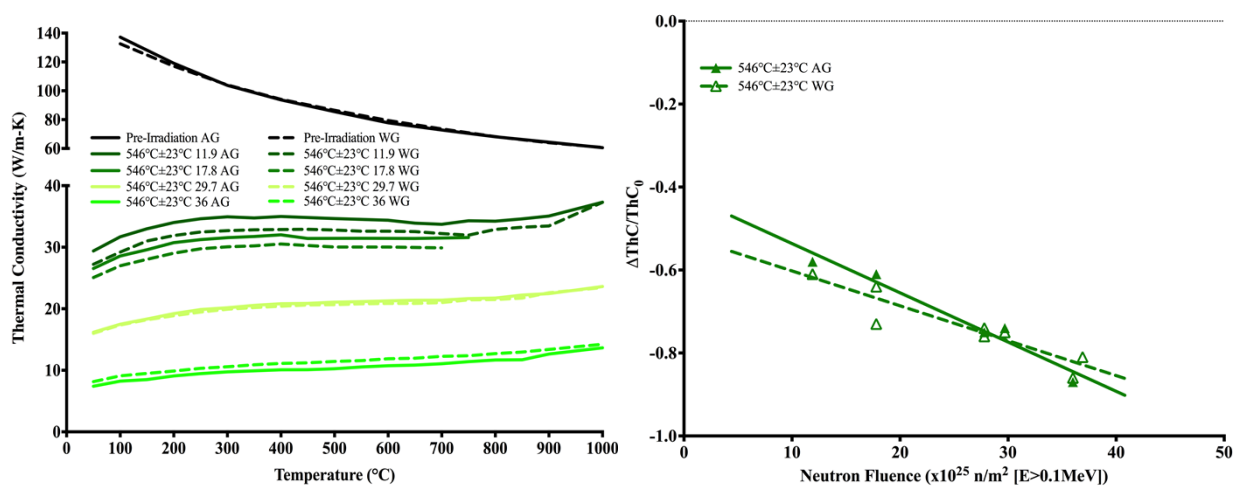


Figure 4.26. (a) Thermal conductivity versus measurement temperature of G347A, and (b) thermal conductivity change versus neutron fluence, irradiated at 546°C±23°C.

4.2.4 659°C±27°C

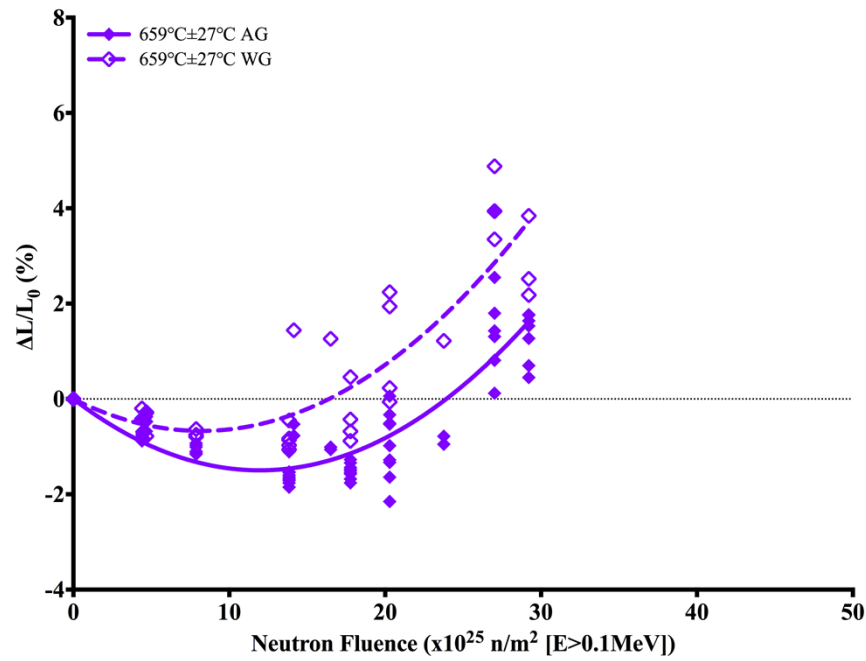


Figure 4.27. Length change of G347A, versus neutron fluence, irradiated at 659°C±27°C.

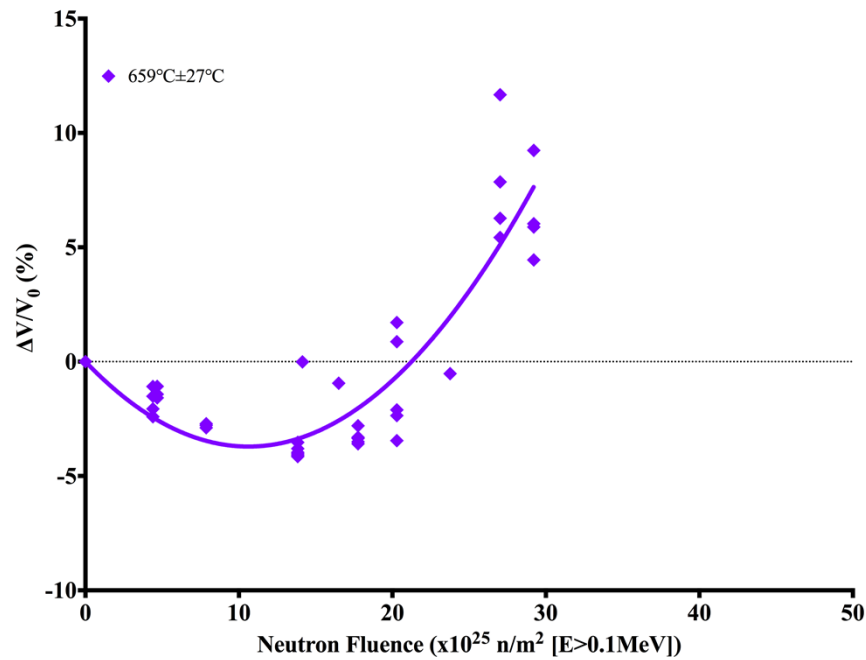


Figure 4.28. Volume change of G347A, versus neutron fluence, irradiated at 659°C±27°C.

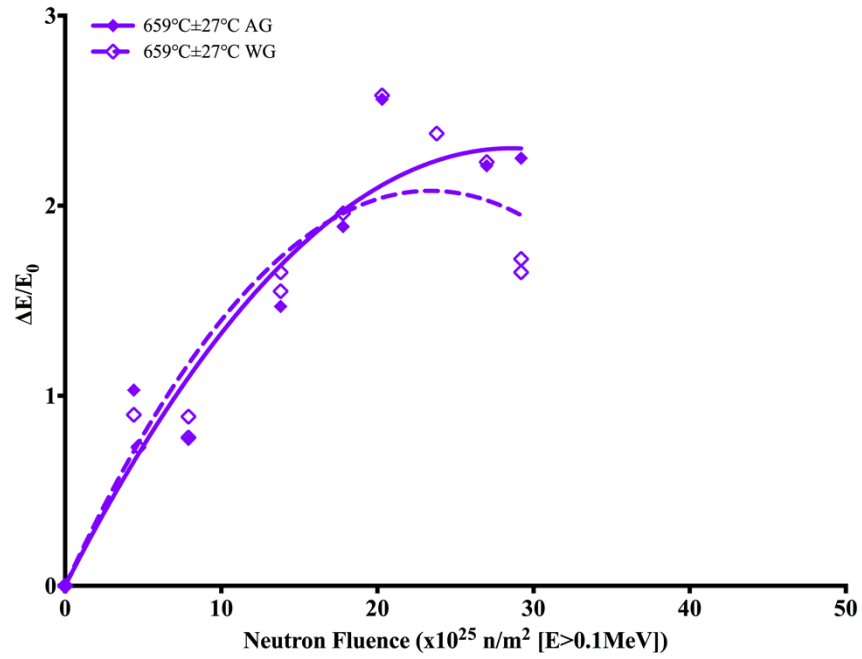


Figure 4.29. Young's modulus change of G347A, versus neutron fluence, irradiated at 659°C±27°C.

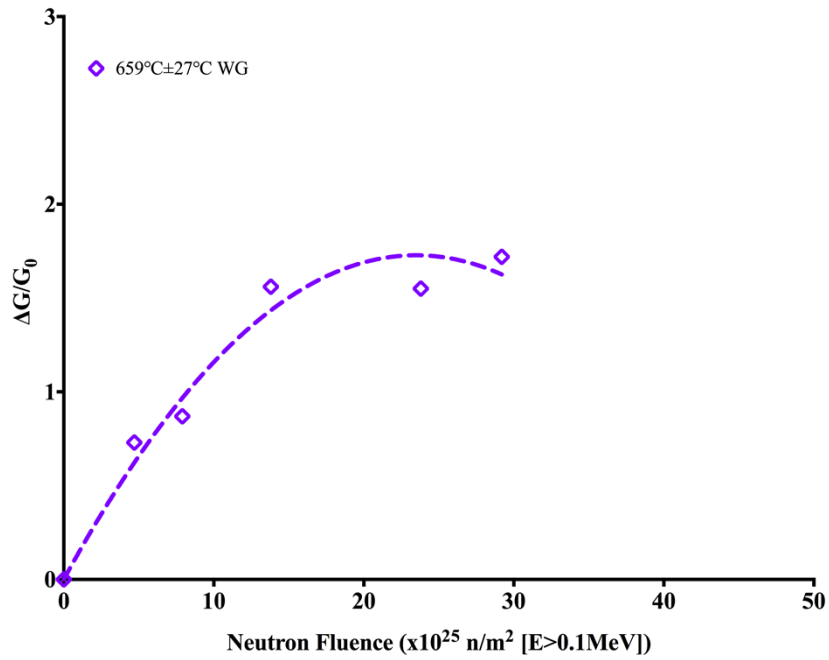


Figure 4.30. Shear modulus change of G347A, versus neutron fluence, irradiated at 659°C±27°C.

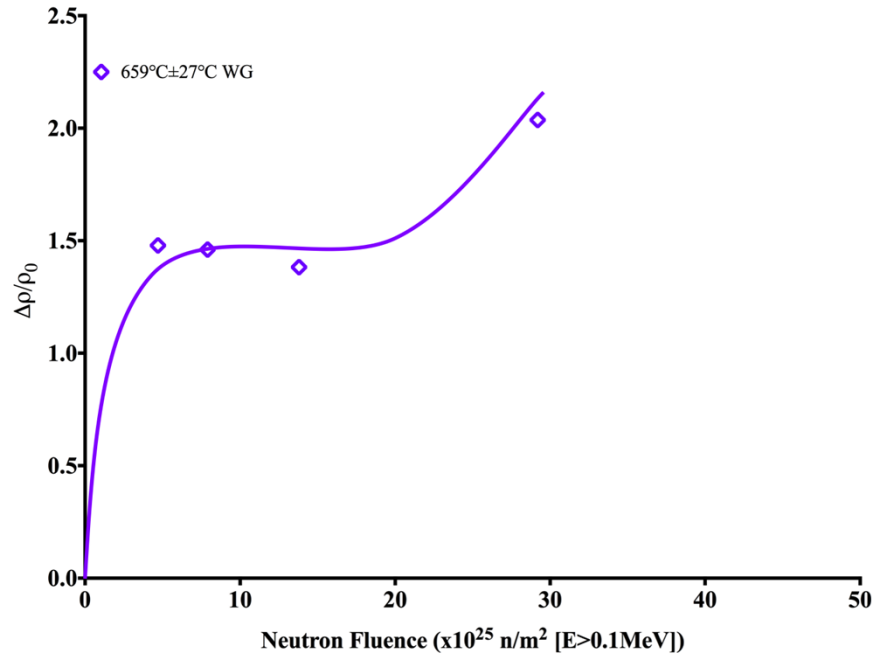


Figure 4.31. Electrical resistivity change of G347A, versus neutron fluence, irradiated at $659^\circ\text{C}\pm 27^\circ\text{C}$.

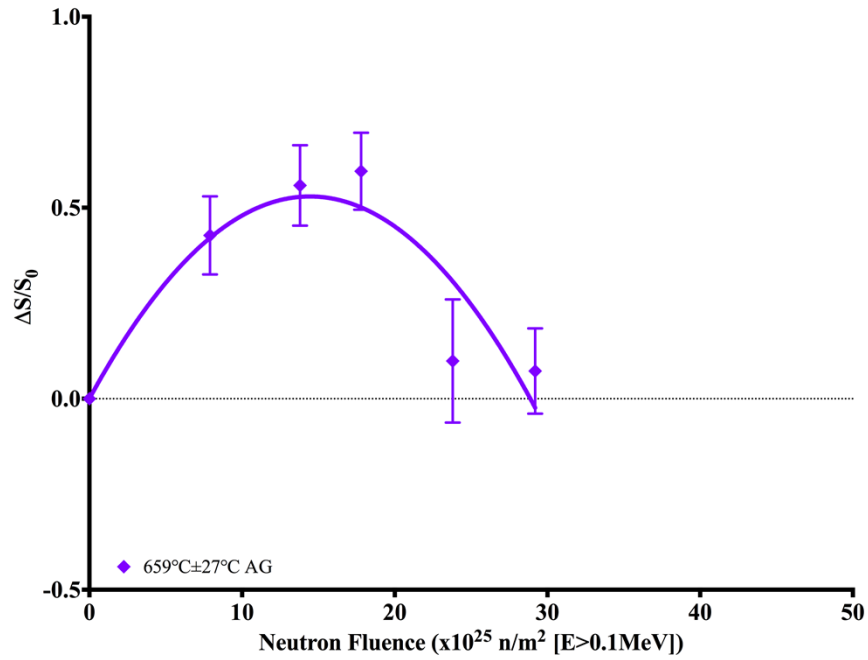


Figure 4.32. Strength changes of G347A, versus neutron fluence, irradiated at $659^\circ\text{C}\pm 27^\circ\text{C}$.

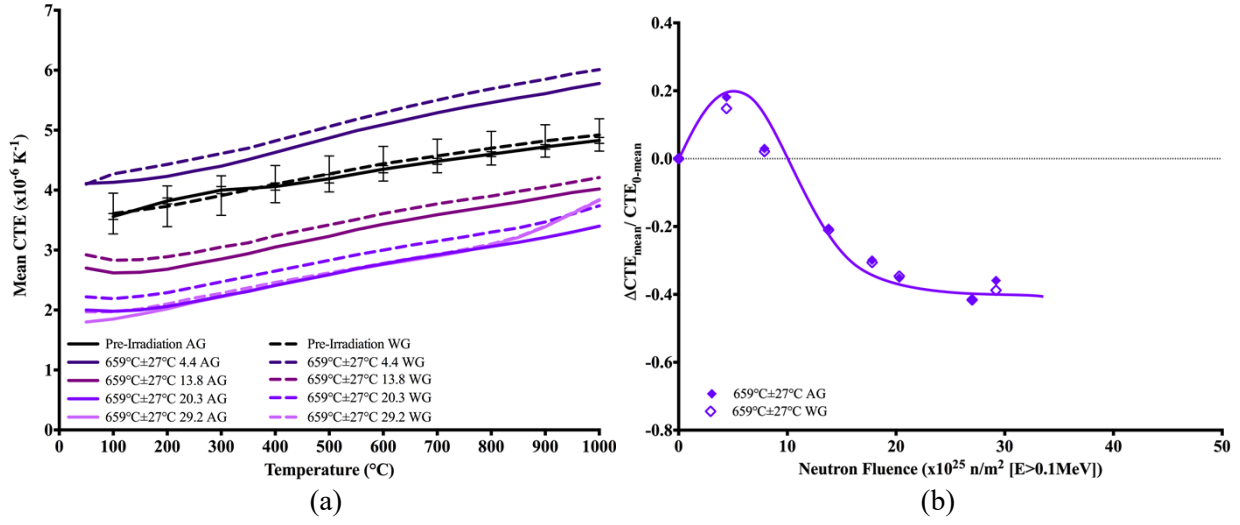


Figure 4.33. (a) Mean CTE versus measurement temperature of G347A, and (b) mean CTE changes versus neutron fluence, irradiated at 659°C±27°C.

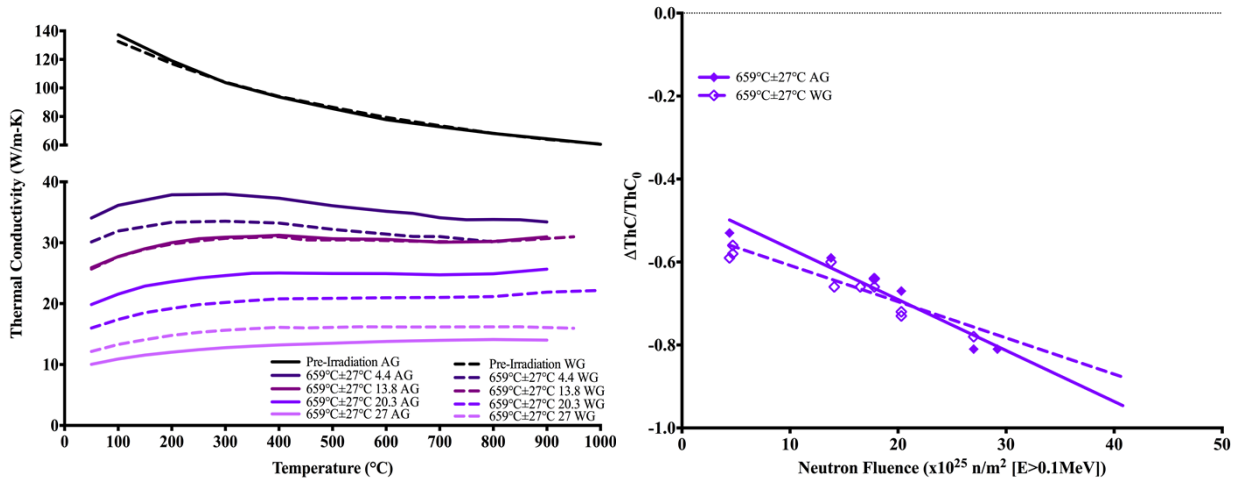


Figure 4.34. (a) Thermal conductivity versus measurement temperature of G347A, and (b) thermal conductivity change versus neutron fluence, irradiated at 659°C±27°C.

4.2.5 738°C±27°C

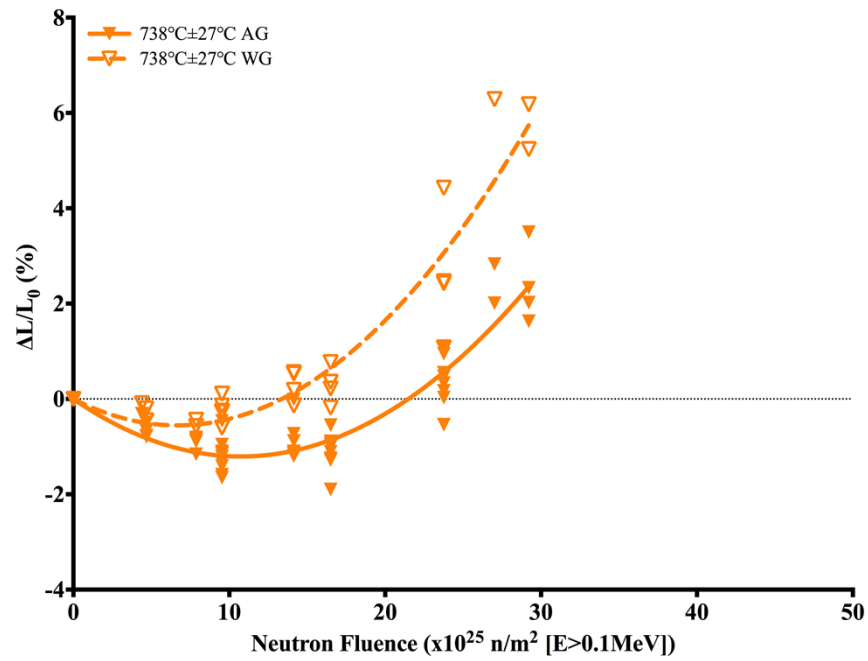


Figure 4.35. Length change of G347A, versus neutron fluence, irradiated at 738°C±27°C.

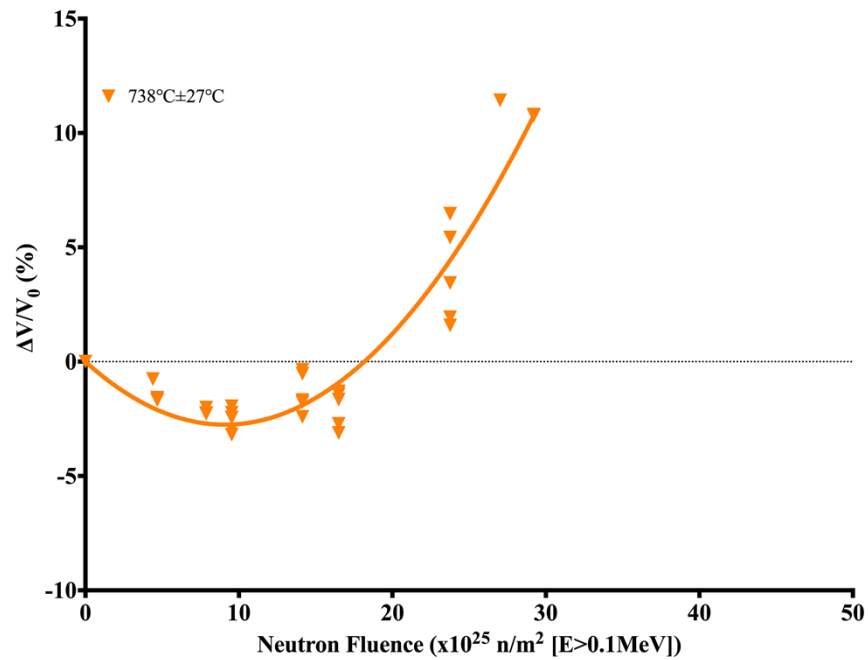


Figure 4.36. Volume change of G347A, versus neutron fluence, irradiated at 738°C±27°C.

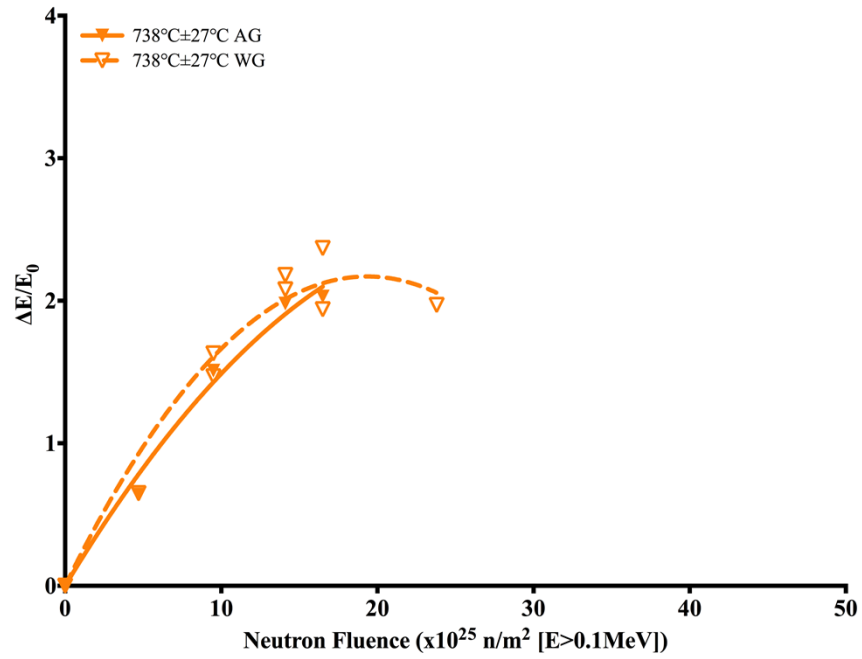


Figure 4.37. Young's modulus change of G347A, versus neutron fluence, irradiated at 738°C±27°C.

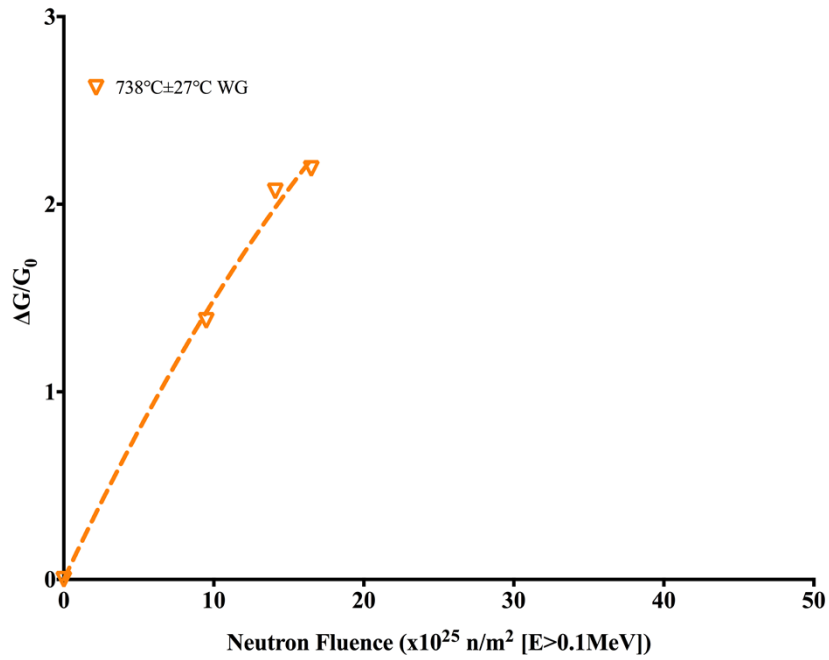


Figure 4.38. Shear modulus change of G347A, versus neutron fluence, irradiated at 738°C±27°C.

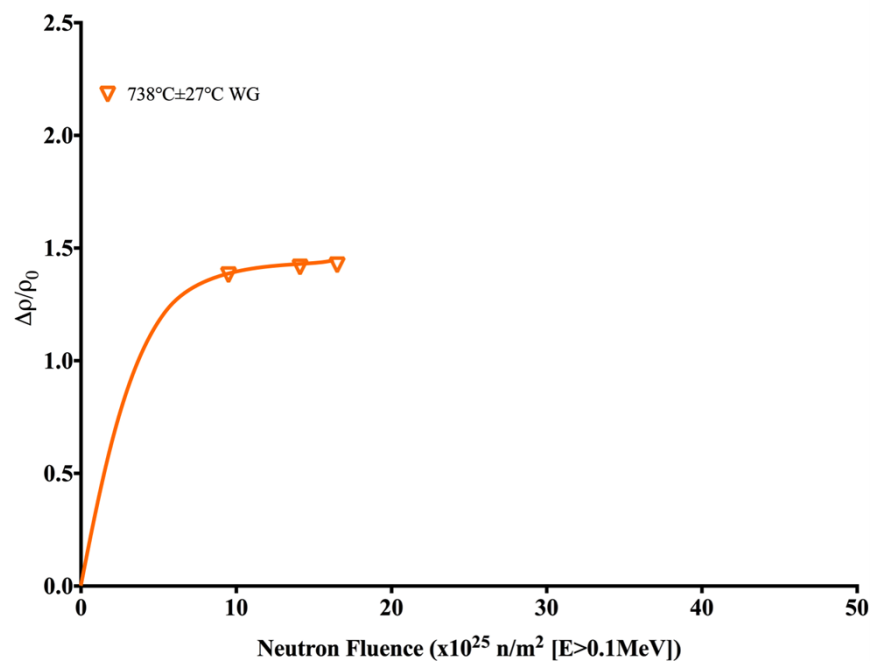


Figure 4.39. Electrical resistivity change of G347A, versus neutron fluence, irradiated at $738^\circ\text{C}\pm 27^\circ\text{C}$.

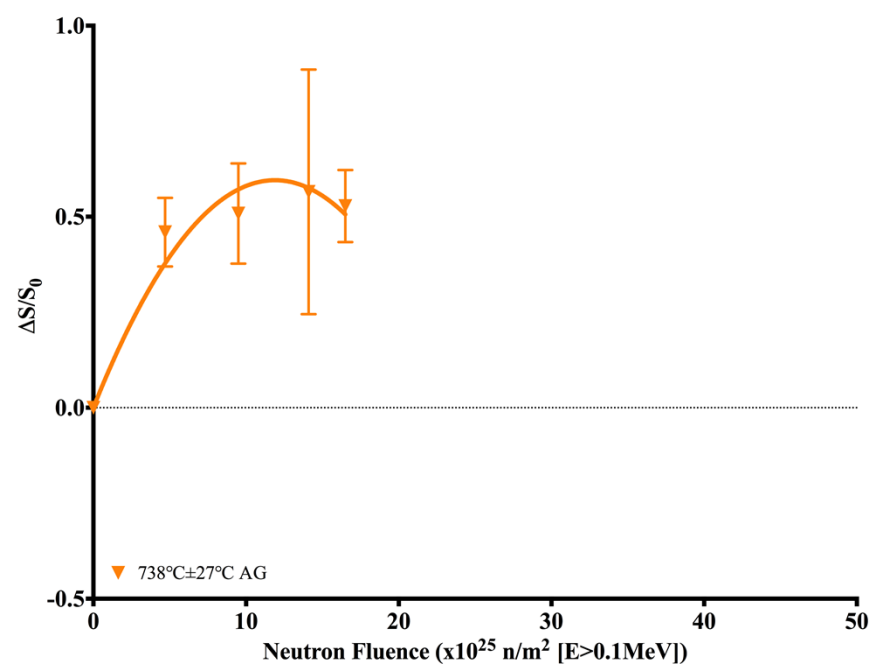


Figure 4.40. Strength changes of G347A, versus neutron fluence, irradiated at $738^\circ\text{C}\pm 27^\circ\text{C}$.

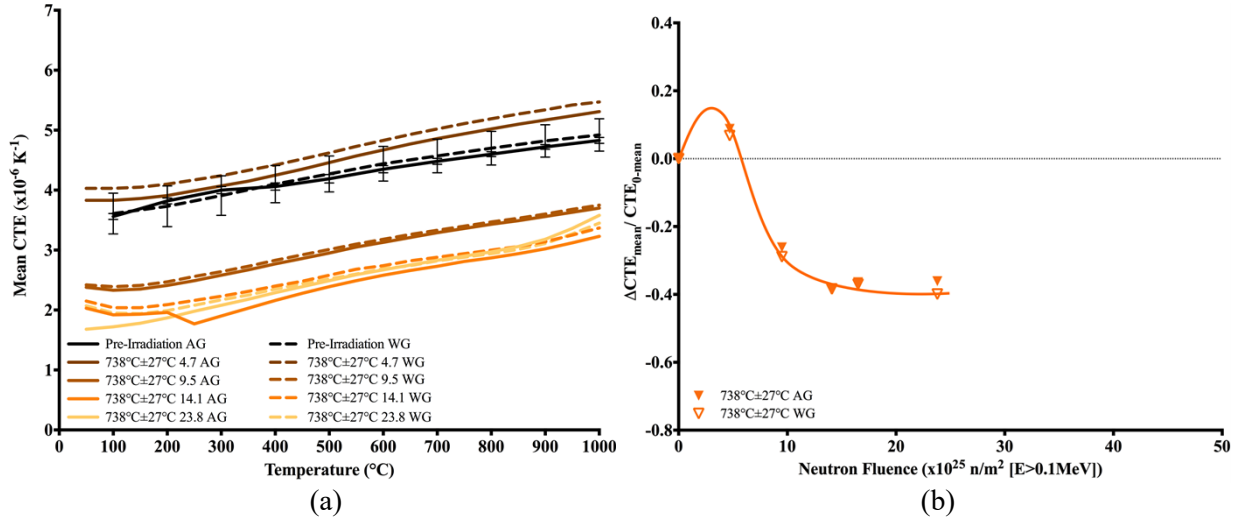


Figure 4.41. (a) Mean CTE versus measurement temperature of G347A, and (b) mean CTE changes versus neutron fluence, irradiated at 738°C±27°C.

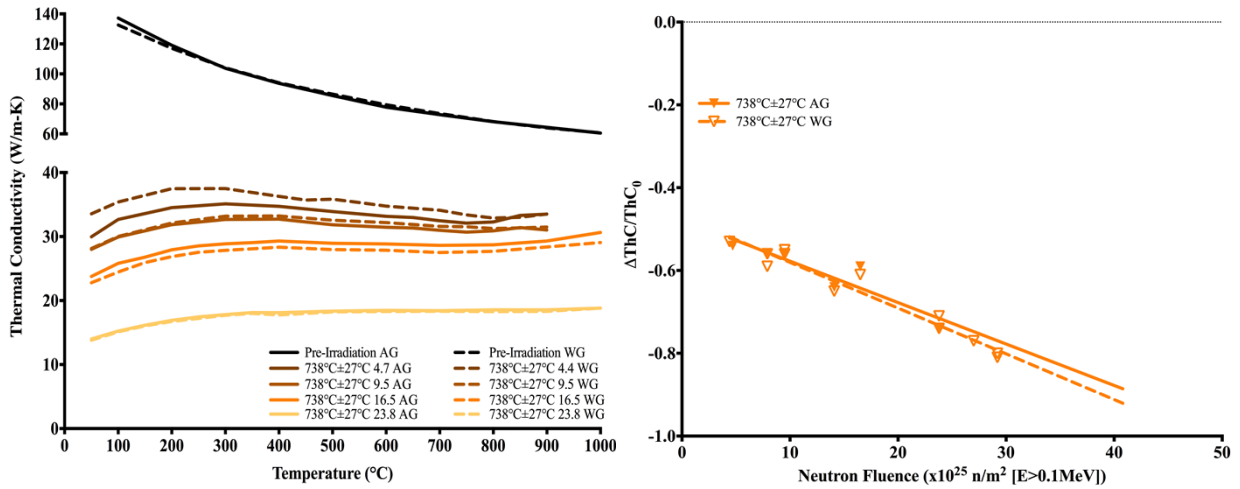


Figure 4.42. (a) Thermal conductivity versus measurement temperature of G347A, and (b) thermal conductivity change versus neutron fluence, irradiated at 738°C±27°C.

4.3 GRADE COMPARISON

This section presents a comparison between the changes in the dimensions, volume, Young's modulus, coefficient of thermal expansion, and the thermal conductivity of G347A and G458A and IG-110. The only temperatures for this comparison are 462±22°C and 659±27°C, since those were the only common temperatures. Overall the changes that occurred for G347A and IG-110 were very similar, while the G458A had a lesser agreement. The most likely cause of the disagreement between G437A and G458A is the different filler materials used for each grade.

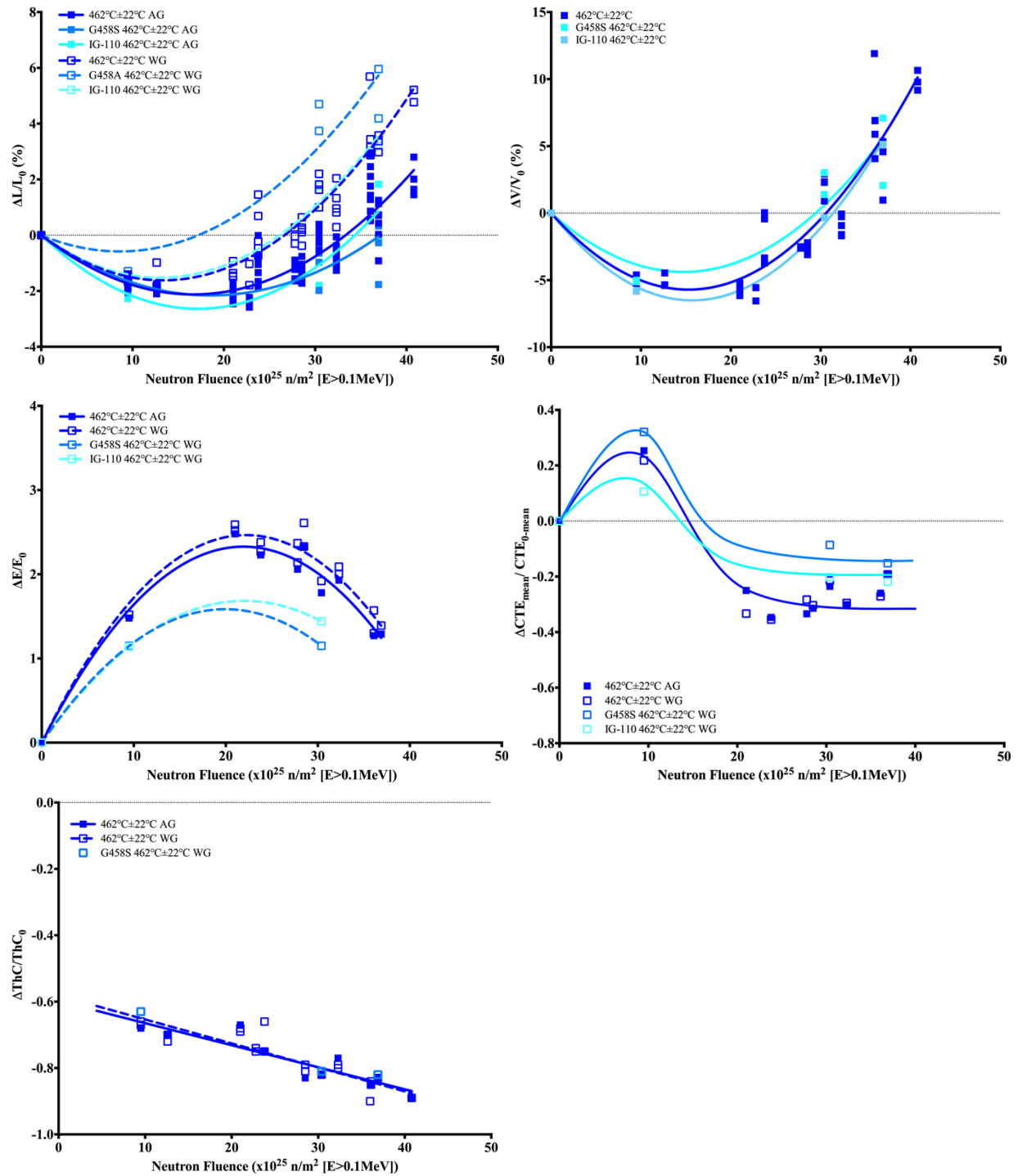


Figure 4.43. Comparison of physical, mechanical, and thermal property changes of the three grades irradiated around 462°C±22°C.

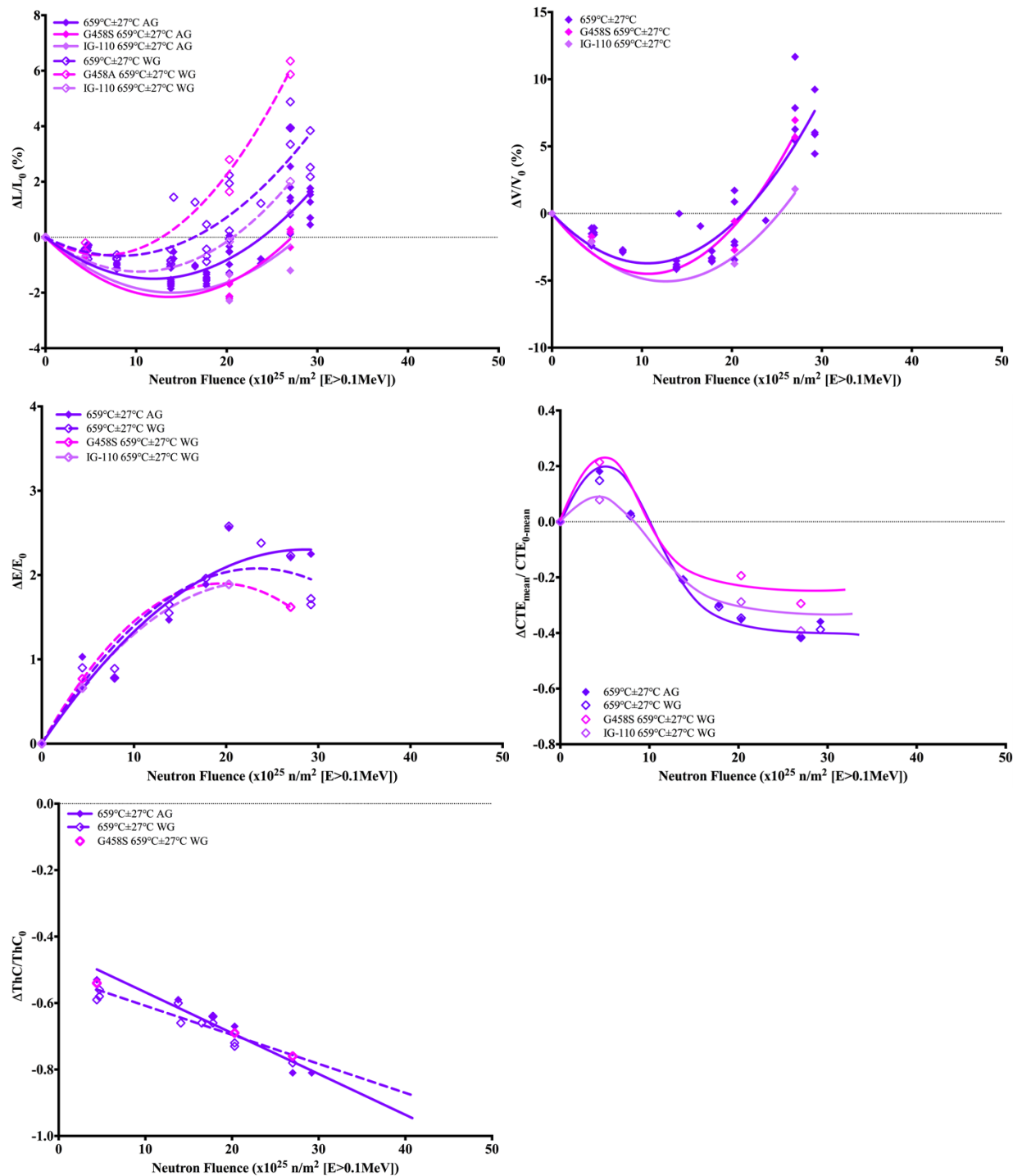


Figure 4.44. Comparison of physical, mechanical, and thermal property changes of the three grades irradiated around $659^\circ\text{C} \pm 27^\circ\text{C}$.

4.4 HISTORICAL BEHAVIOR COMPARISON

In the American Society of Mechanical Engineers (ASME) code for high temperature reactors [5], article HAB-7000, lists the ASTM standards that cover the pre-irradiation specifications for nuclear graphite. These standards include ASTM D7219 [6] and ASTM D7301 [7]. In D7219 (relevant for G347A), the CTE isotropy ratio must be less than 1.1, a density above 1.7 g/cm³, room temperature thermal conductivity of 90 W/m/K, Young's modulus between 8-15 GPa, and tensile, flexural, and compressive strengths, greater than 22, 35, and 65 MPa, respectively. The properties measured by ORNL all fell within the acceptable limits to quantify G347A as nuclear grade graphite.

More importantly is the fact that G347A has exhibited the same irradiation response that has been observed since the 1960's when results on irradiation effects in graphite were first published. Many programs have studied the effect of irradiation on medium and large grained graphite's that were either pressed or extruded [8-23]. All of these programs observed similar trends, even for different grades of graphite. These trends include: the difference in length change relative to the with- or against-grain orientation, an increase of Young's modulus to a peak value that then decreased to an elevated plateau, a rapid rise in the electrical resistivity followed by a plateau, strength increased and then decreased, thermal conductivity underwent sharp decrease to a plateau value, and a peak of CTE followed by a decrease to a plateau. In work with varied irradiation temperature, [14-16, 19, 23], it was found that these changes happened more rapidly at higher irradiation temperatures but the severity of the changes were reduced.

Unlike the previous research, this program has been much more comprehensive in the temperature/fluence levels investigated, and the properties measured. This comprehensiveness allows for a more rigorous investigation into the effects of temperature and fluence on the different physical, mechanical, and thermal properties. The trend lines that were fitted to the data in Figure 4.3 through Figure 4.42 are combined together in Figure 4.45 through Figure 4.52. The only un-expected behavior is shown in the length change, Young's modulus change, CTE change, and the thermal conductivity change; since it has been a commonly held belief that near-isotropic isostatically pressed graphite will have the same property change in all directions. Instead this is the first, and not the last, work that shows this belief to be false. Otherwise all the other trends show the same types of behaviors that have been observed in the past with other graphite.

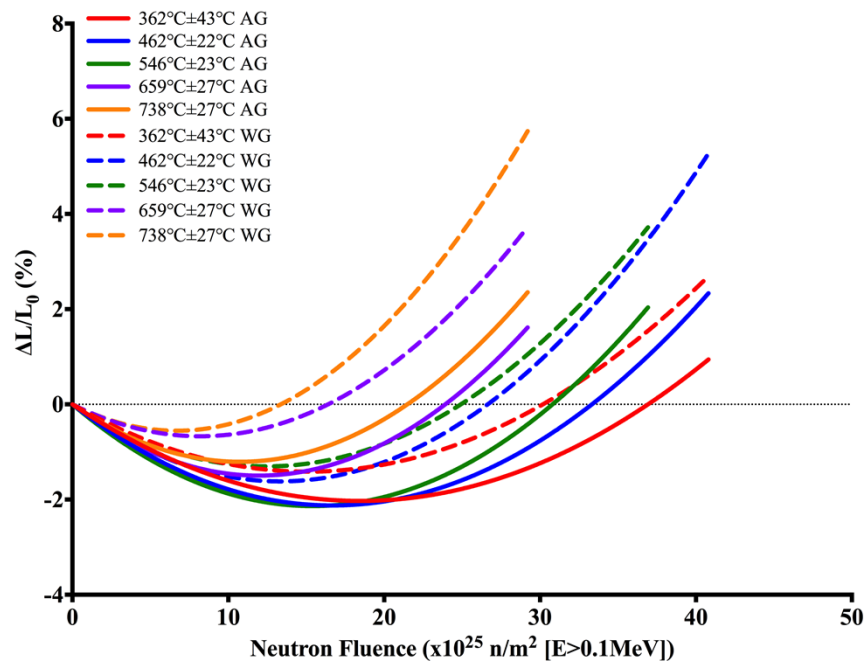


Figure 4.45. Combined trend lines showing temperature effects on length change versus total fluence.

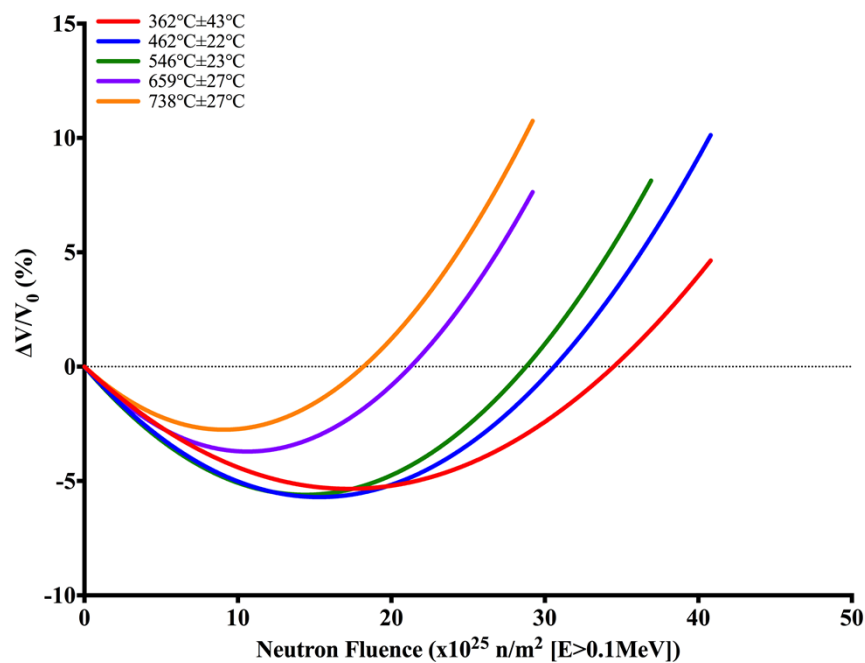


Figure 4.46. Combined trend lines showing temperature effects on volume change versus total fluence.

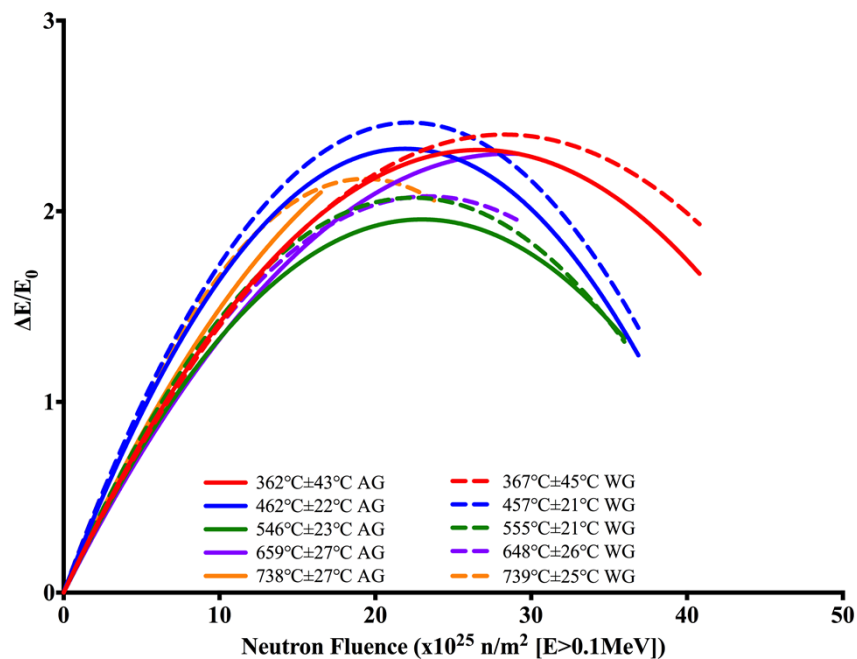


Figure 4.47. Combined trend lines showing temperature effects on Young's modulus change versus total fluence.

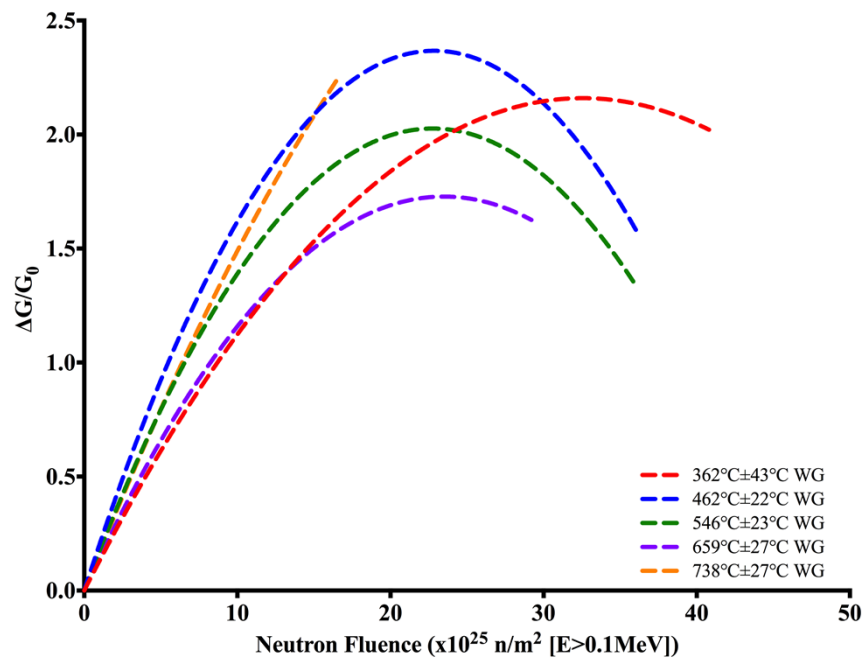


Figure 4.48. Combined trend lines showing temperature effects on shear modulus change versus total fluence.

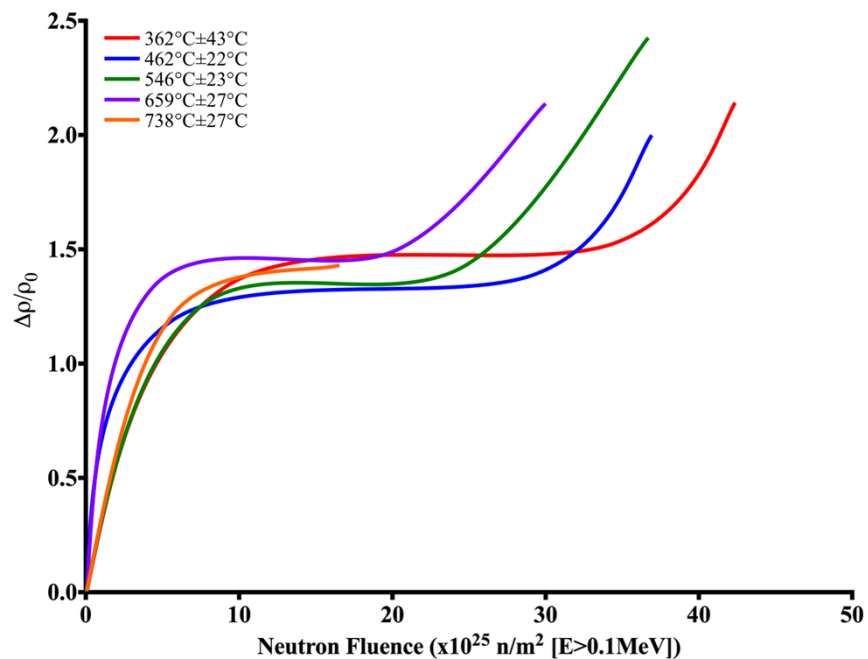


Figure 4.49. Combined trend lines showing temperature effects on electrical resistivity change versus total fluence.

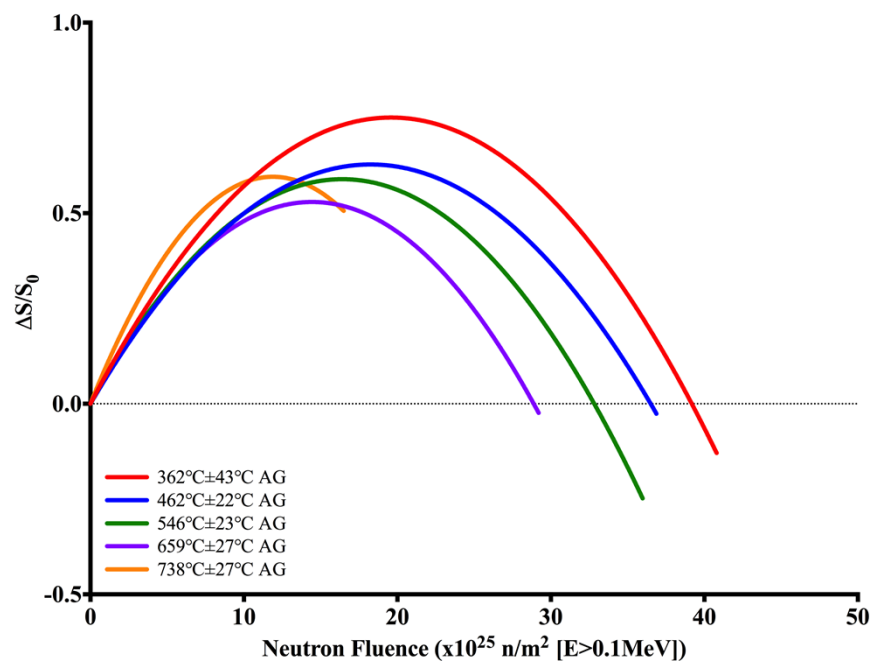


Figure 4.50. Combined trend lines showing temperature effects on strength change versus total fluence.

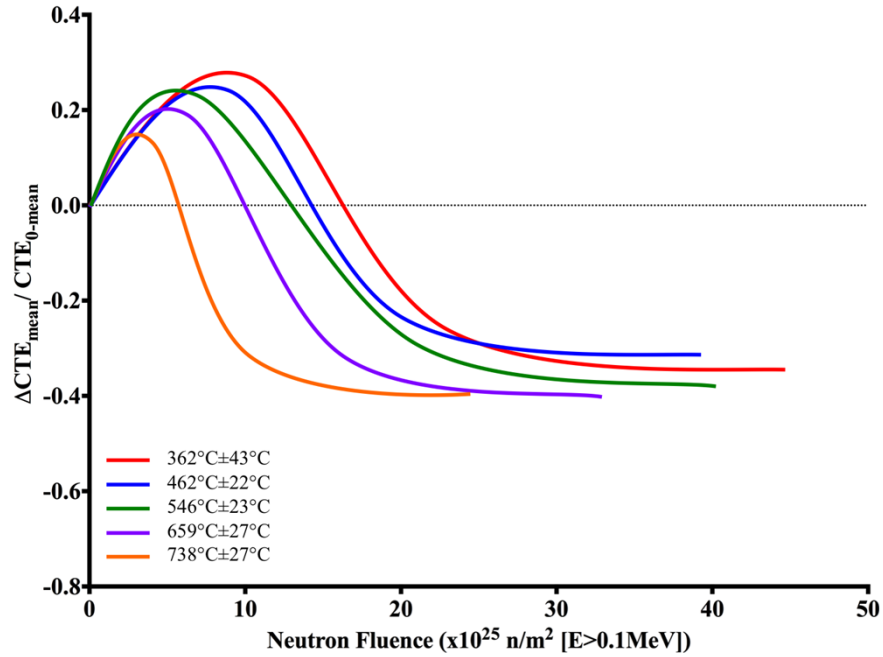


Figure 4.51. Combined trend lines showing temperature effects on the change of mean CTE versus total fluence.

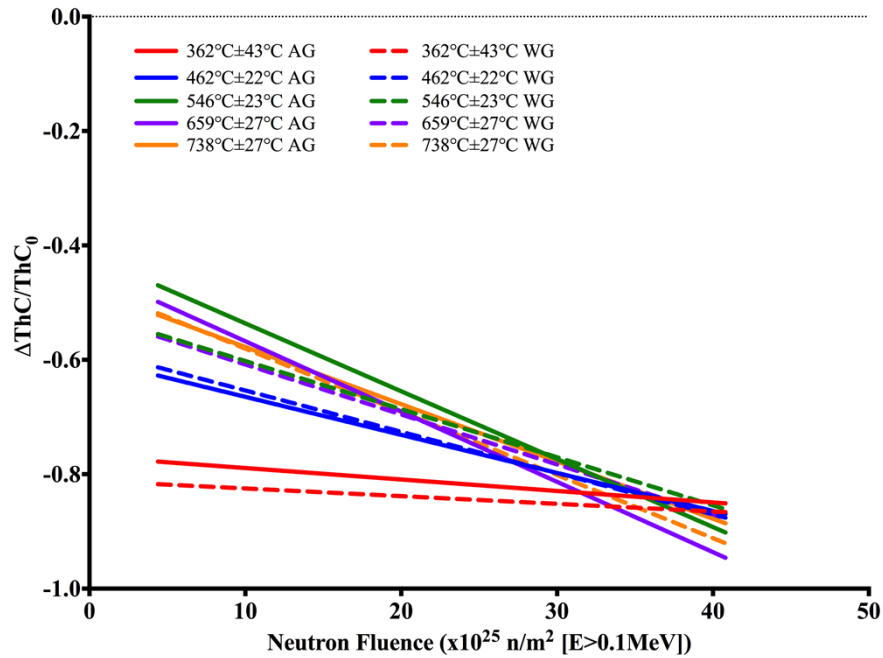


Figure 4.52. Combined trend lines showing temperature effects on the change of thermal conductivity, measured at irradiation temperature, versus total fluence.

The most significant contribution from this program is that it is one of the most comprehensive investigations of the effect of irradiation temperature and neutron fluence on a single graphite grade. An example of the comprehensiveness is the results of neutron fluence and temperature on the thermal conductivity, Figure 4.52. In previous work, the nominal decrease of the room temperature thermal conductivity is lower for higher irradiation temperatures, has a rapid decrease to a plateau that would not change until swelling becomes positive, and that the lower irradiation temperature would reach this plateau value sooner [24]. But this work has shown that the nominal change of thermal conductivity, at irradiation temperature, is similar for all irradiation temperatures.

There are two trends from this work that need to be discussed: 1) the initial decrease is reduced for higher irradiation temperatures, and 2) the continued reduction is more rapid for the higher temperatures. The reduction of thermal conductivity is caused by the presence of basal plane vacancies, crystallite boundaries, or other regions where the basal plane hexagonal geometry is disturbed. The changes to the conductivity are due to a combination of intrinsic and extrinsic defects and how the numbers of these defects change. The intrinsic defects are most likely grain boundaries and crystallite boundaries, while the extrinsic defects are a result of built-up irradiation damage. At high temperatures the irradiation-induced defects are larger, and have a lower density, which is the most probable reason the higher temperature having a smaller decrease at low fluence. Unlike the historical results, this work has shown that the thermal conductivity does not reach a plateau and instead continuously decreases with increasing fluence. This will require further investigation to determine the cause of this disagreement.

5. QUALITY ASSURANCE DOCUMENTATION

The ORNL quality assurance systems and processes used to plan, conduct, and document the subject activities are described in ORNL document # QAP-ORNL-NR&D-01 entitled *Quality Assurance Plan for Nuclear Research and Development Conducted at the Oak Ridge National Laboratory*. This document describes the management system implemented to assure the quality of the work performed for nuclear research endeavors, including the Tokai -funded nuclear science and technology activities at ORNL. The plan is explicitly formulated to identify the ORNL and project-level documents utilized to address the body of requirements associated with the quality standard, ANSI/ISO/ASQ Q9001-2000 entitled *American National Standard – Quality Management Systems - Requirements* (hereafter referred to as ISO 9001) as it applies to the scope of work. The ORNL has been registered to the ISO 9001 standard since 2010 and undergoes annual audits to maintain its registration. The ORNL's Metrology organization is also accredited to the ISO 17025 standard entitled *General Requirements for the Competence of Testing and Calibration Laboratories*.

In addition to the ISO 9001 standard, other documents form a set of references that – in part – are included as inputs to the nuclear Research & Development Quality Assurance plan because they are 1) customer-mandated requirements, 2) have been previously useful in achieving and documenting success in nuclear Science & Technology-related activities, or 3) because they are an explicit component of the requirements set incumbent upon ORNL as a United States Department of Energy (DOE) site.

- ASME NQA-1-2008, *Quality Assurance Requirements for Nuclear Facility Applications*
- ASME NQA-1-2008, Part IV, Subpart 4.2, *Guidance on Graded Application of Quality Assurance (QA) for Nuclear Related Research and Development*, and Subpart 4.3, *Modification of an ISO 9001-2000 Quality Program to Meet NQA-1-2000 Requirements*
- DOE Guide 414.1-2, *Quality Assurance Management System Guide for Use with 10 CFR 830.120 and DOE O 414.1C*
- ORNL Quality Assurance Program Description

6. SUMMARY

The results presented in the document represent one of the most comprehensive graphite irradiation campaigns. This campaign investigated a range of temperatures and fluence that are relevant to both the prismatic and pebble bed core High-Temperature Gas-Cooled Reactors and it also provided a thorough investigation into the effects of the irradiation temperature and fast neutron fluence on multiple physical, mechanical, and thermal properties.

The property changes of G347A are in agreement with the trends that have historically been observed in literature for other nuclear graphite. The fluence-dependent evolutions of G347A properties appeared to be comparable with those for other fine-grain iso-molded graphite's including IG-110.

7. REFERENCES

1. Fechter, M., A. Clark, and Y. Katoh, "Graphite Pre-Irradiation Specimen Size Validation and Testing Program - Results - Tokai Carbon Japan", (January 2012). ORNL/TM-2011/495.
2. Fechter, M., "Graphite Pre-Irradiation Sample Size Validation and Testing Program – Test Specification – Tokai Carbon Japan", (2011). R109-002-01.
3. Fechter, M., "Graphite Post-Irradiation Testing Program – Test Specification – Tokai Carbon Japan", (2012). ORNL/TM-2012/114.
4. Campbell, A.A., W.D. Porter, Y. Katoh, and L.L. Snead, "Method for Analyzing Passive SiC Thermometry with a Continuous Dilatometer to Determine Irradiation Temperature", *NIMB*, (To be published)
5. ASME III-5, 2015, "ASME Boiler and Pressure Vessel Code An International Code", New York, NY,
6. ASTM D7219-08, 2008, "Standard Specification for Isotropic and Near-Isotropic Nuclear Graphites", ASTM International, West Conshohocken, PA, DOI: 10.1520/D7219-08R14, <http://www.astm.org>.
7. ASTM D7301-11, 2011, "Standard Specification for Nuclear Graphite Suitable for Components Subjected to Low Neutron Irradiation Dose", ASTM International, West Conshohocken, PA, 10.1520/D7301-11R15, <http://www.astm.org>.
8. Nightingale, R.E., "Nuclear Graphite", 1962, New York, Academic Press.
9. Kelly, B.T., D. Jones, and A. James, "Irradiation damage to pile grade graphite at 450° C", *Journal of Nuclear Materials*, 7, (1962) 279-291.
10. Bridge, H., B.T. Kelly, and P.T. Nettle, "Effect of high-flux fast-neutron irradiation on the physical properties of graphite", *Carbon*, 2, (1964) 83-93.
11. Simmons, J.H.W., B.T. Kelly, P.T. Nettle, and W.N. Reynolds, *The Irradiation Behavior of Graphite*, in *Third United Nations International Conference on the Peaceful Uses of Atomic Energy*, 1964, United Kingdom, p. Paper #163.
12. Kelly, B.T., W.H. Martin, and P.T. Nettle, "Dimensional Changes in Polycrystalline Graphites under Fast-Neutron Irradiation", *Philosophical Transactions of the Royal Society A*, 260, (1966) 51-71.
13. Nettle, P.T., J.E. Brocklehurst, W.H. Martin, and J.H.W. Simmons, "Irradiation Experience with Isotropic Graphite", Presented at *Symposium on Advanced and High Temperature Gas-Cooled Reactors*, Julich, October 21-25, 1968.
14. Simmons, J.H.W., "Radiation damage in graphite", International Series of Monographs in Nuclear Energy, Vol. 102, 1965, Oxford, New York, Pergamon Press.
15. Kelly, B.T., "Physics of Graphite", 1981, London, Applied Science Publishers.
16. Burchell, T.D. and W.P. Eatherly, "The effects of radiation damage on the properties of GraphNOL N3M", *Journal of Nuclear Materials*, 179-181, Part 1, (1991) 205-208.
17. "Irradiation Damage in Graphite due to Fast Neutrons in Fission and Fusion Systems", (2000). IAEA-TECDOC-1154.
18. Burchell, T.D., "Neutron Irradiation Damage in Graphite and Its Effects on Properties", Presented at *International Carbon Conference CARBON 2002*, Beijing, China, September 15-20, 2002.
19. Haag, G., "Properties of ATR-2E Graphite and Property Changes due to Fast Neutron Irradiation", *Berichte des Forschungszentrums Jülich*, Vol. 4183, 2005, Jülich, FZJ, Institut für Sicherheitsforschung und Reaktortechnik.
20. Burchell, T.D. and L.L. Snead, "The effect of neutron irradiation damage on the properties of grade NBG-10 graphite", *Journal of Nuclear Materials*, 371, (2007) 18-27.
21. Burchell, T.D., "4.10 - Radiation Effects in Graphite", in *Comprehensive Nuclear Materials*, R.J.M. Konings, Editor, 2012, Elsevier, Oxford, p. 299-324.

22. Ishiyama, S., T.D. Burchell, J.P. Strizak, and M. Eto, "The effect of high fluence neutron irradiation on the properties of a fine-grained isotropic nuclear graphite", *Journal of Nuclear Materials*, 230, (1996) 1-7.
23. Kelly, B.T. and T.D. Burchell, "Structure-related property changes in polycrystalline graphite under neutron irradiation", *Carbon*, 32, (1994) 499-505.
24. "Carbon Materials for Advanced Technologies", ed. T.D. Burchell, 1999.

APPENDIX A. RABBIT INFORMATION

A.1 IRRADIATION RESULTS SUMMARY

Rabbit ID	Rabbit Configuration	Target Fluence ($\times 10^{25}$ n/m ² [E>0.1MeV])	Target Temperature (°C)	Actual Fluence ($\times 10^{25}$ n/m ² [E>0.1MeV])	Actual SiC TM Temperature (°C)
TOK-01	GRIC-1	12	300	12.69	320
TOK-02	GRIC-1	20	300	21.76	329
TOK-03	GRIC-1	26	300	27.2	448
TOK-04	GRIC-1	32	300	32.64	429
TOK-05	GRIC-1	40	300	41.2	345
TOK-06	GRIC-1	12	450	12.04	381
TOK-07	GRIC-1	20	450	20.07	420
TOK-08	GRIC-1	26	450	26.5	462
TOK-09	GRIC-1	32	450	34.38	410
TOK-10	GRIC-1	40	450	41.2	389
TOK-11	GRIC-1	10	600	11.36	565
TOK-12	GRIC-1	16	600	17.04	561
TOK-13	GRIC-1	22	600	22.72	461
TOK-14	GRIC-1	28	600	28.4	517
TOK-15	GRIC-1	34	600	36.53	514
TOK-16	GRIC-1	8	750	7.57	639
TOK-17	GRIC-1	12	750	13.25	589
TOK-18	GRIC-1	16	750	17.04	640
TOK-19	GRIC-1	22	750	23	700
TOK-20	GRIC-1	26	750	28	628
TOK-21	GRIC-1	4	900	4.58	659
TOK-22	GRIC-1	8	900	9.15	741
TOK-23	GRIC-1	12	900	13.47	774
TOK-24	GRIC-1	16	900	15.71	681
TOK-25	GRIC-2	8	450	9.07	486
TOK-26	GRIC-2	28	450	29.01	474
TOK-27	GRIC-2	36	450	37	503
TOK-28	GRIC-2	4	750	4.3	688
TOK-29	GRIC-2	18	750	19.34	666
TOK-30	GRIC-2	24	750	25.78	697
TOK-31	GRIC-1	12	300	12.69	261

A.2 TEMPERATURE MONITOR ANALYSIS RESULTS

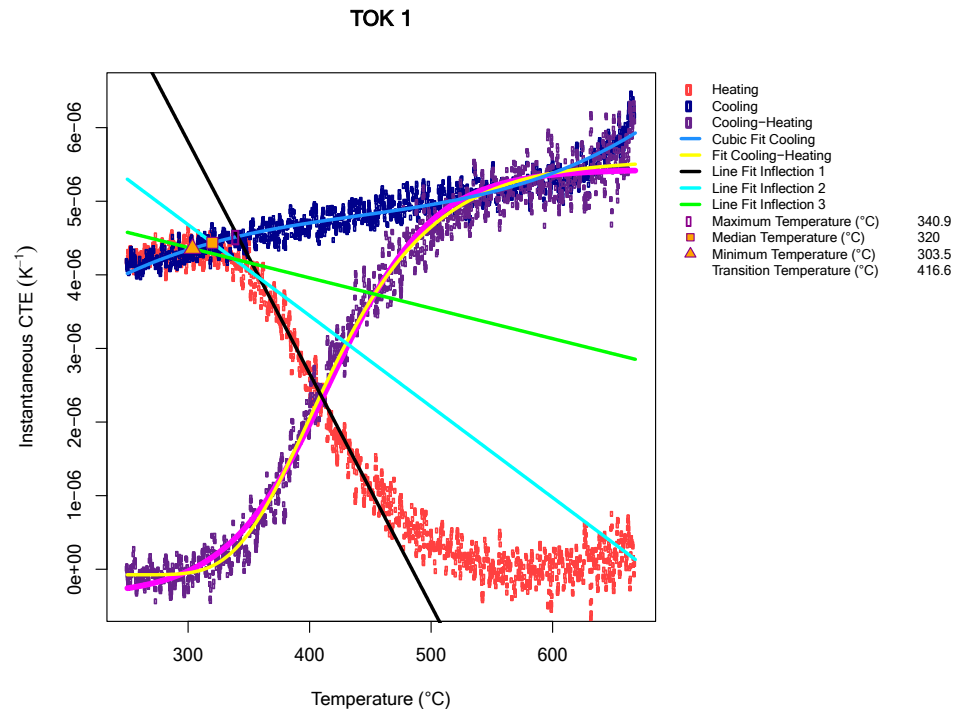


Figure A.1. Temperature monitor analysis from rabbit TOK-01.

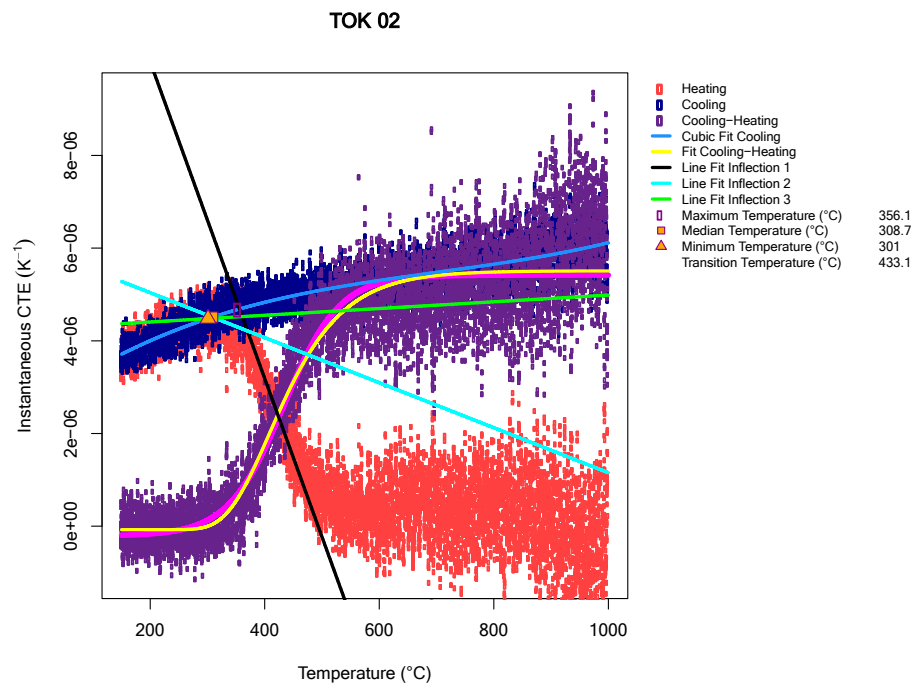


Figure A.2. Temperature monitor analysis from rabbit TOK-02.

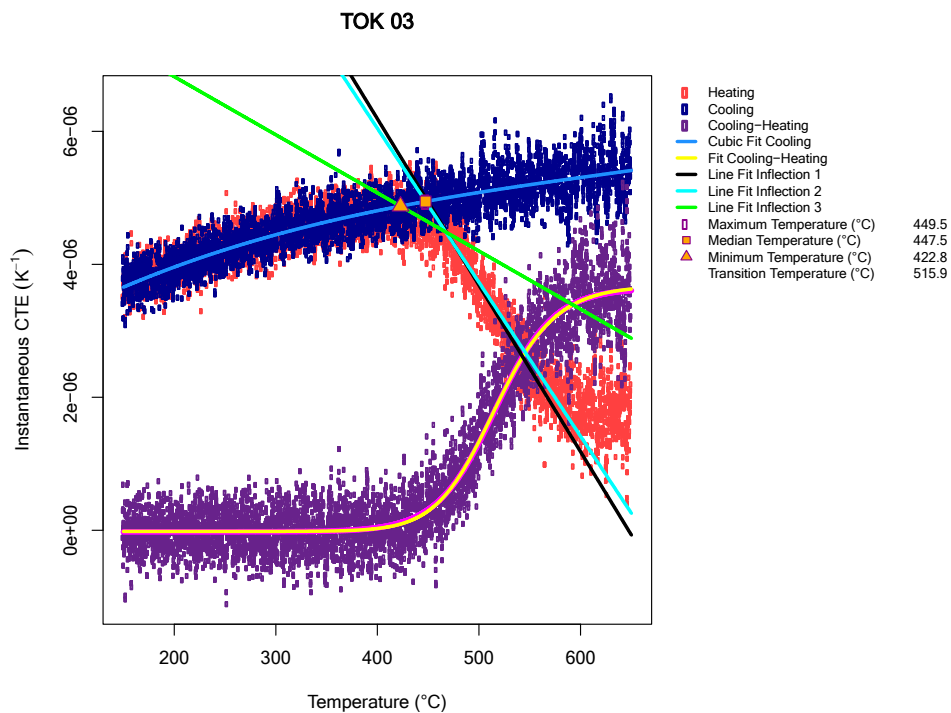


Figure A.3. Temperature monitor analysis from rabbit TOK-03.

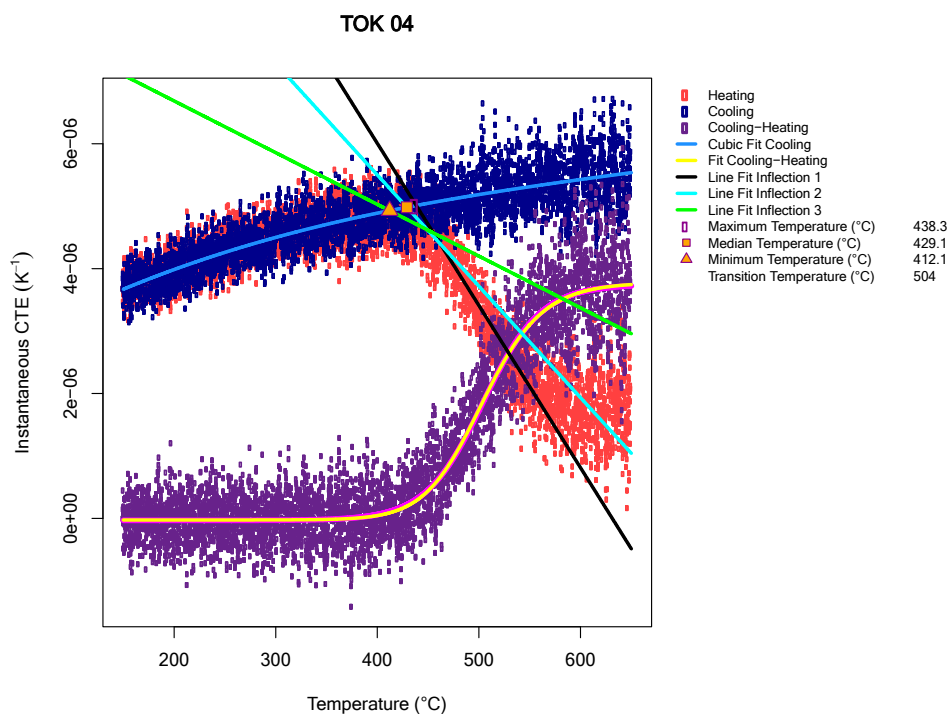


Figure A.4. Temperature monitor analysis from rabbit TOK-04.

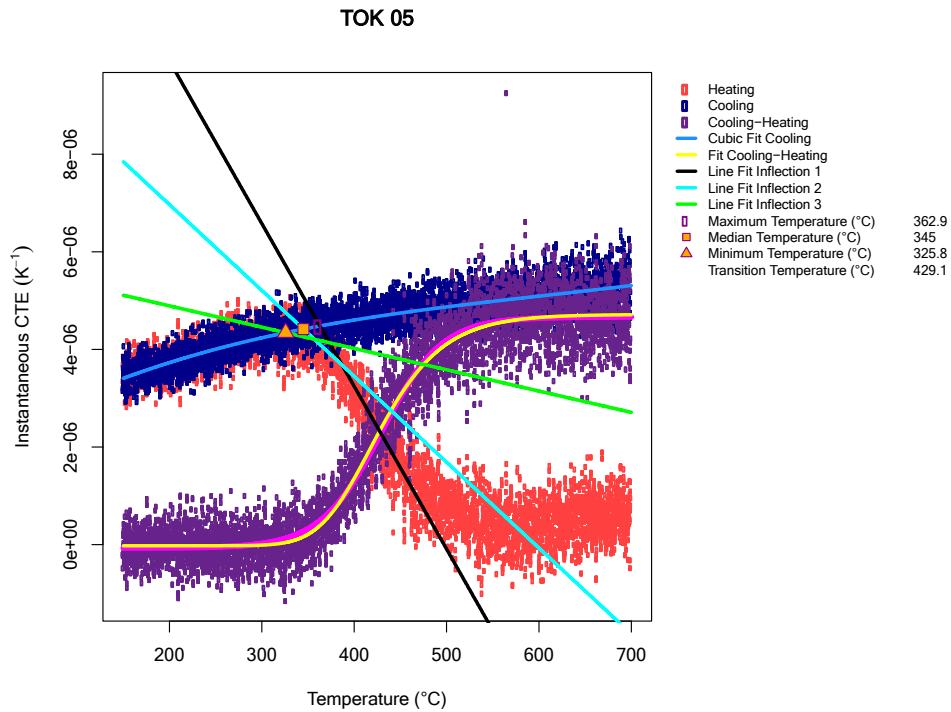


Figure A.5. Temperature monitor analysis from rabbit TOK-05.

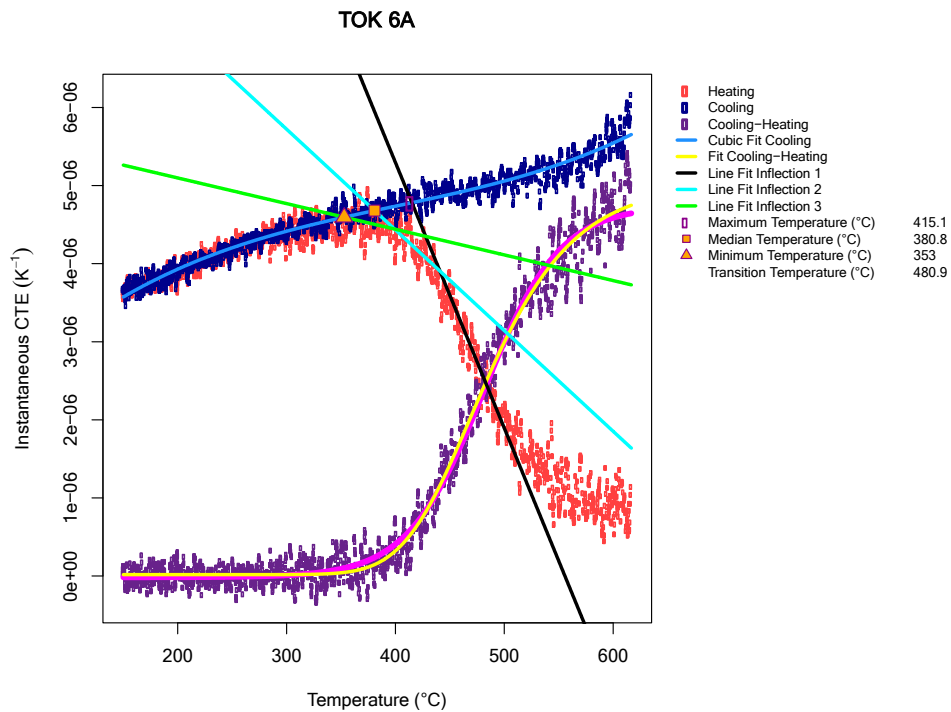


Figure A.6. Temperature monitor analysis from rabbit TOK-06.

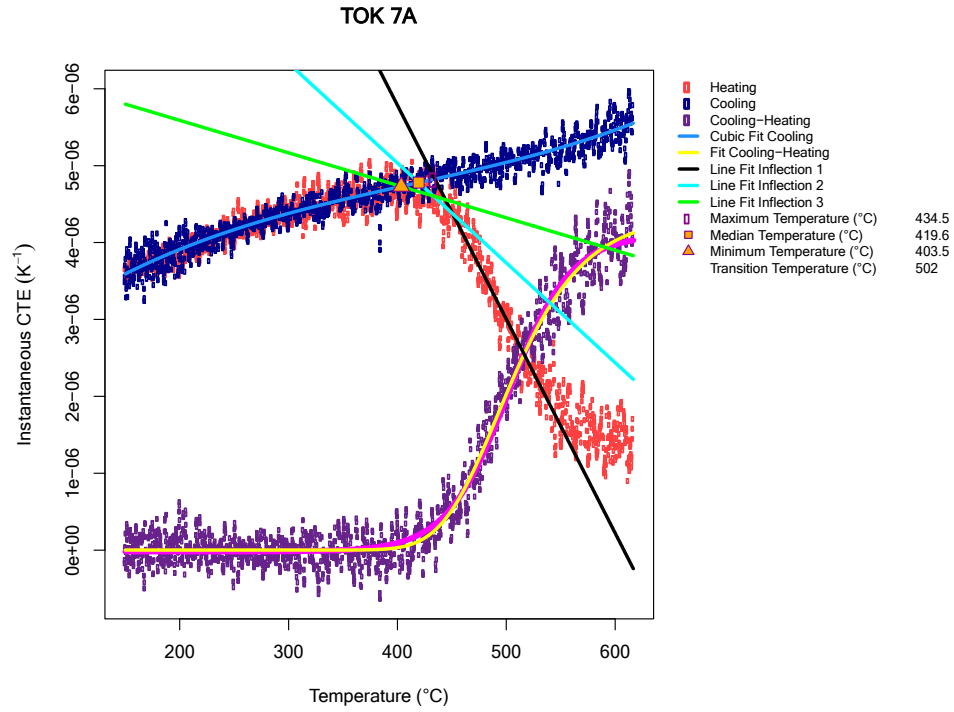


Figure A.7. Temperature monitor analysis from rabbit TOK-07.

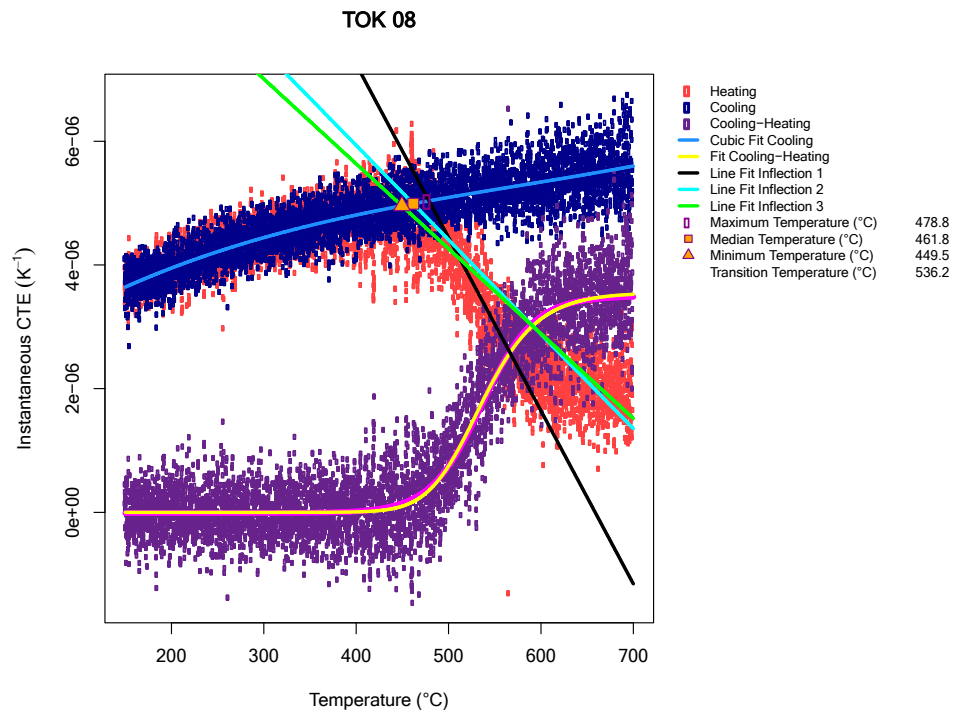


Figure A.8. Temperature monitor analysis from rabbit TOK-08.

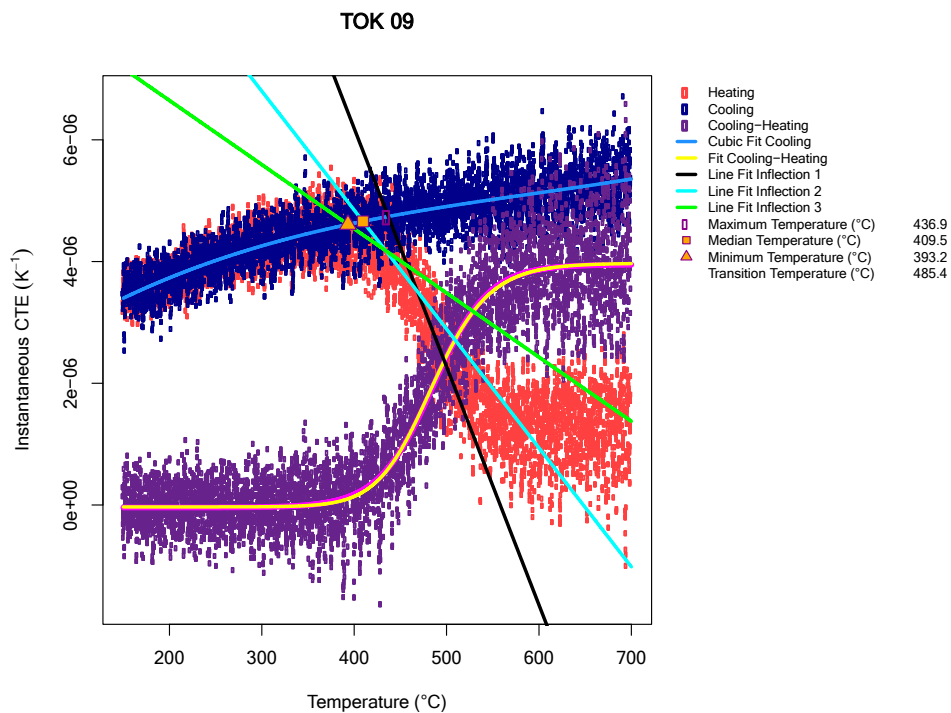


Figure A.9. Temperature monitor analysis from rabbit TOK-09.

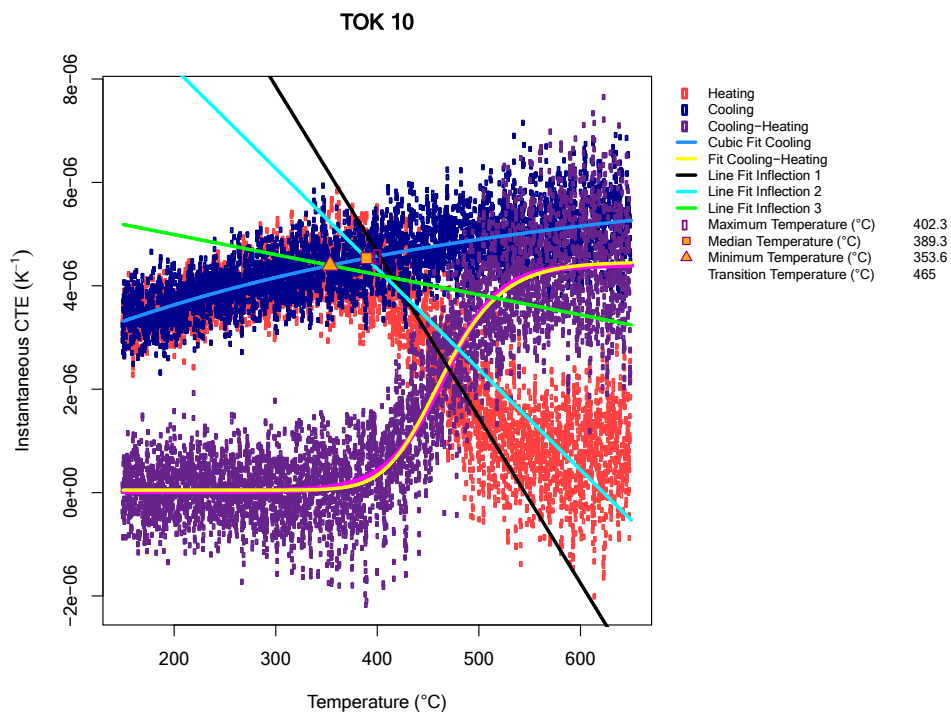


Figure A.10. Temperature monitor analysis from rabbit TOK-10.

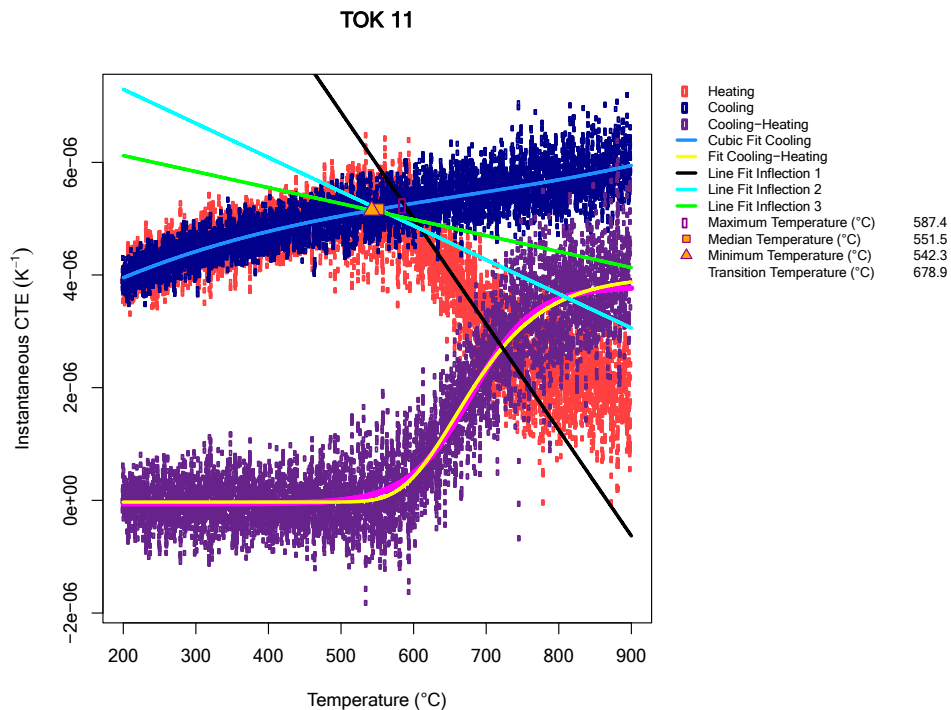


Figure A.11. Temperature monitor analysis from rabbit TOK-11.

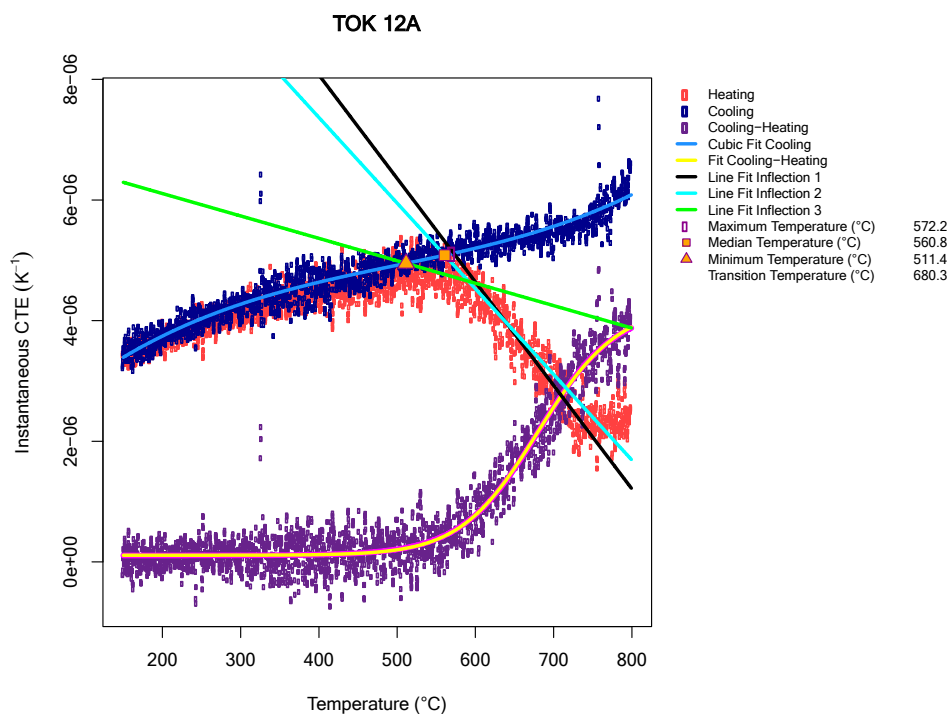


Figure A.12. Temperature monitor analysis from rabbit TOK-12.

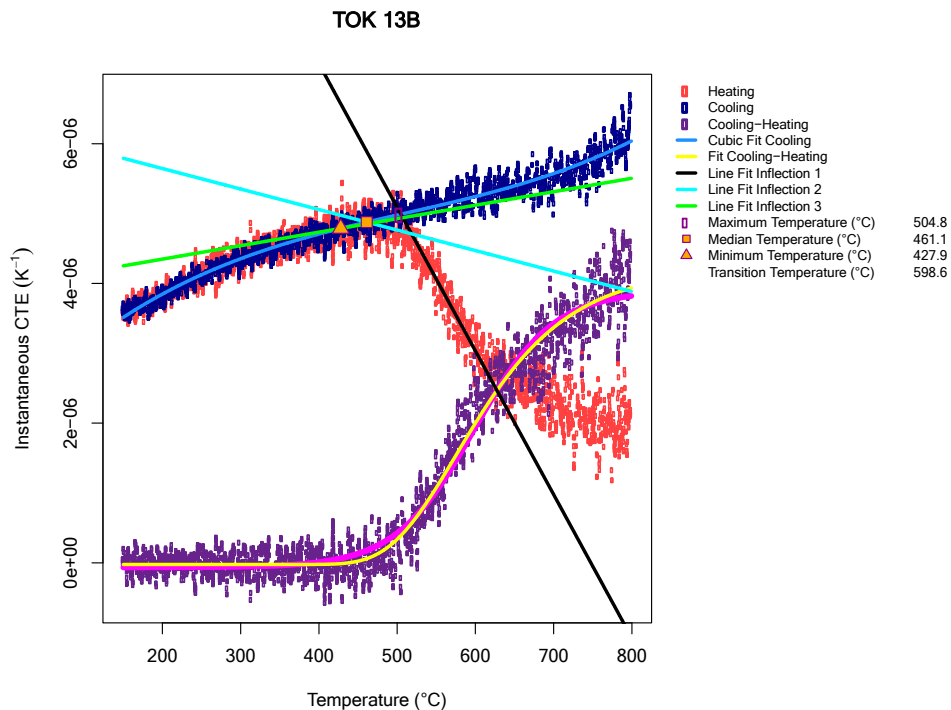


Figure A.13. Temperature monitor analysis from rabbit TOK-13.

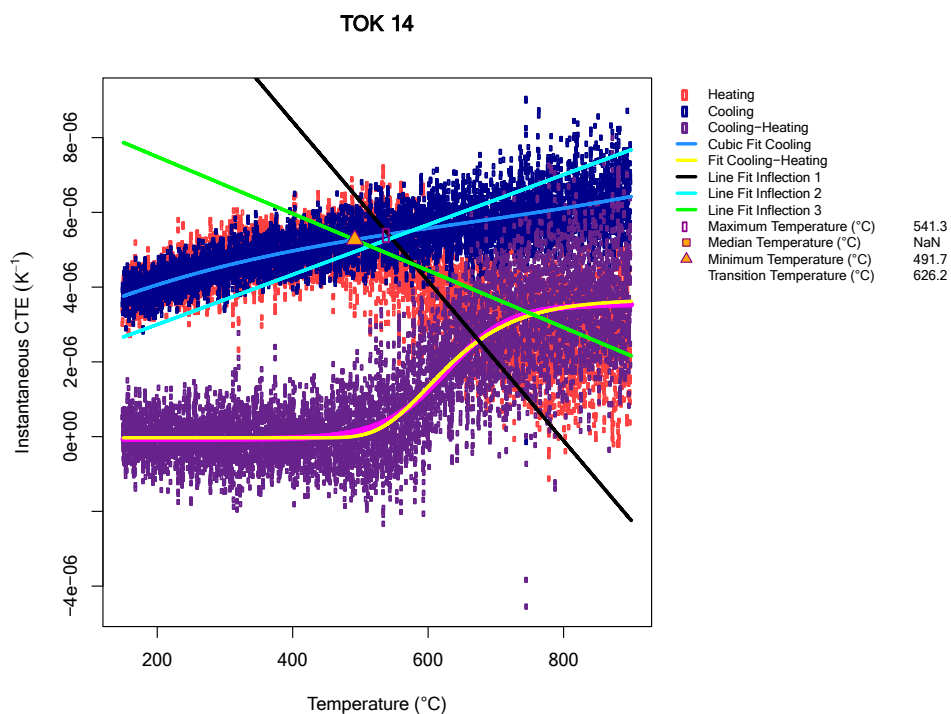


Figure A.14. Temperature monitor analysis from rabbit TOK-14.

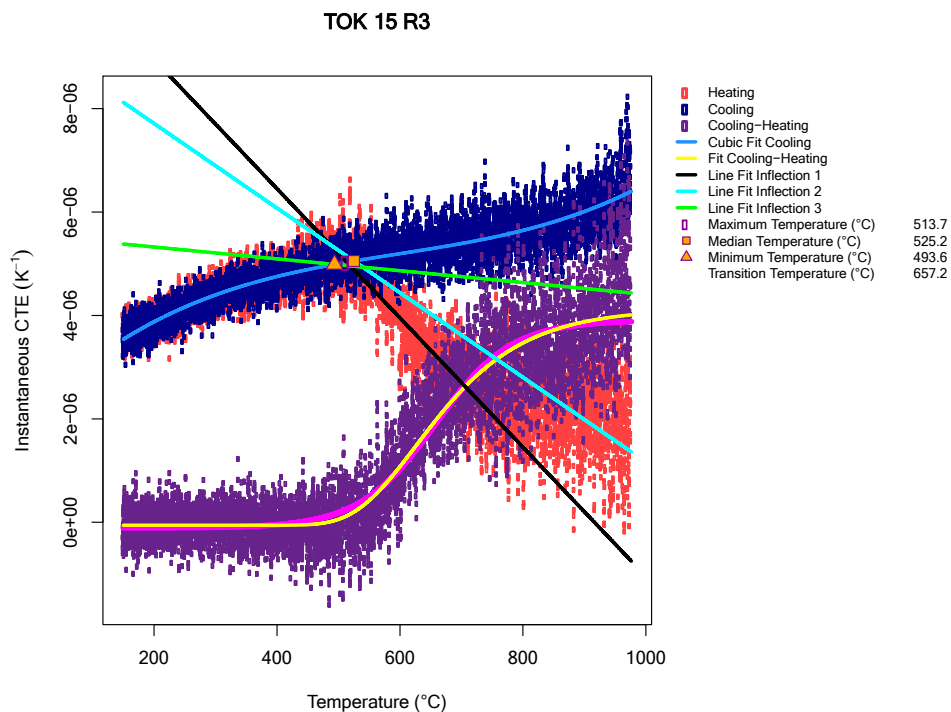


Figure A.15. Temperature monitor analysis from rabbit TOK-15.

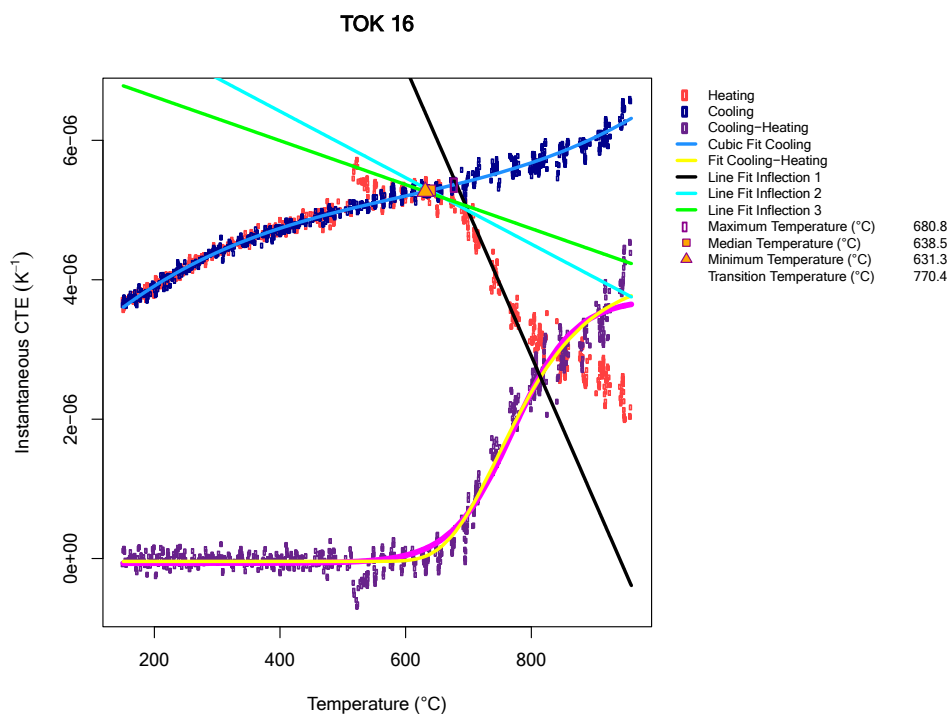


Figure A.16. Temperature monitor analysis from rabbit TOK-16.

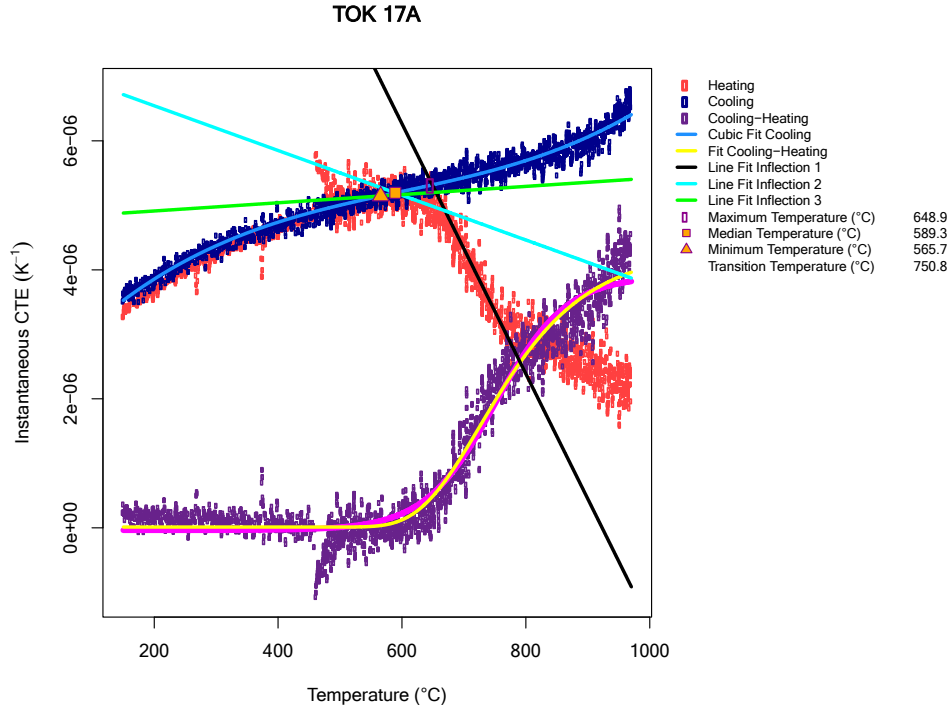


Figure A.17. Temperature monitor analysis from rabbit TOK-17.

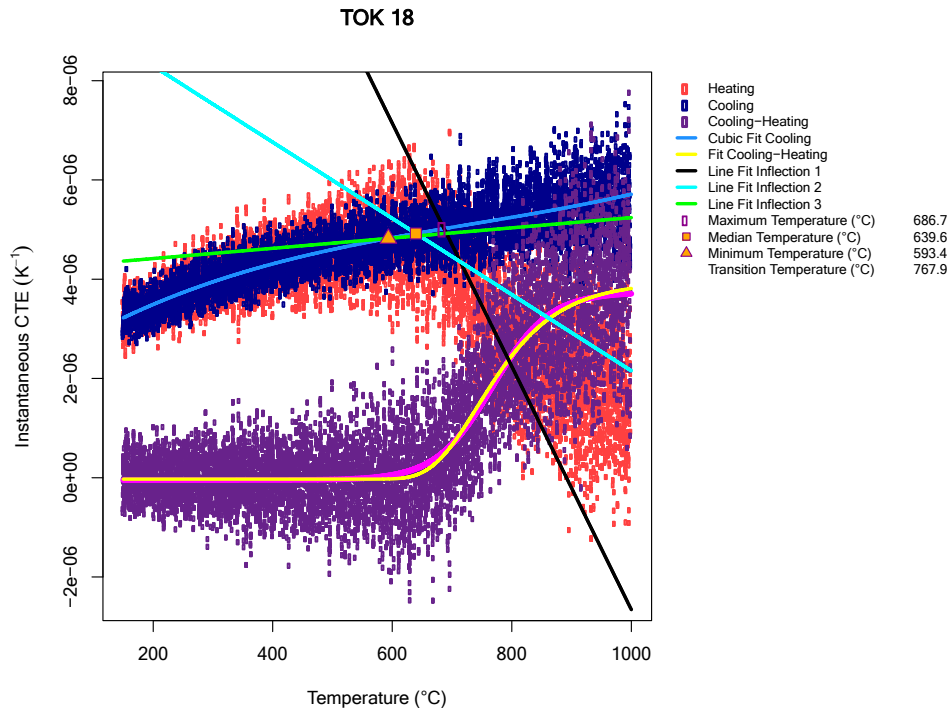


Figure A.18. Temperature monitor analysis from rabbit TOK-18.

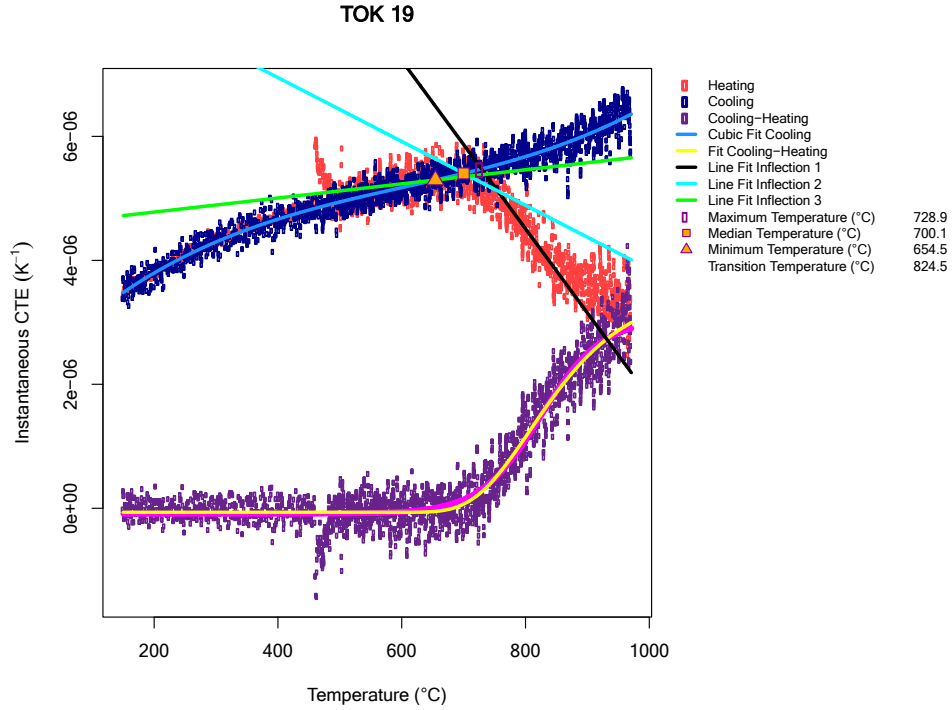


Figure A.19. Temperature monitor analysis from rabbit TOK-19.

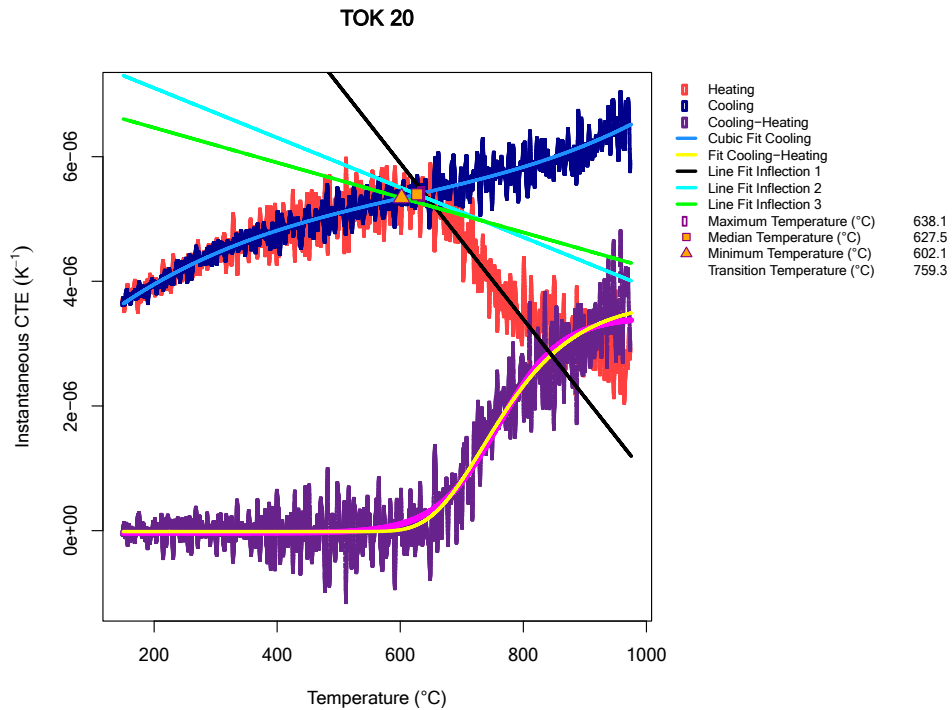


Figure A.20. Temperature monitor analysis from rabbit TOK-20.

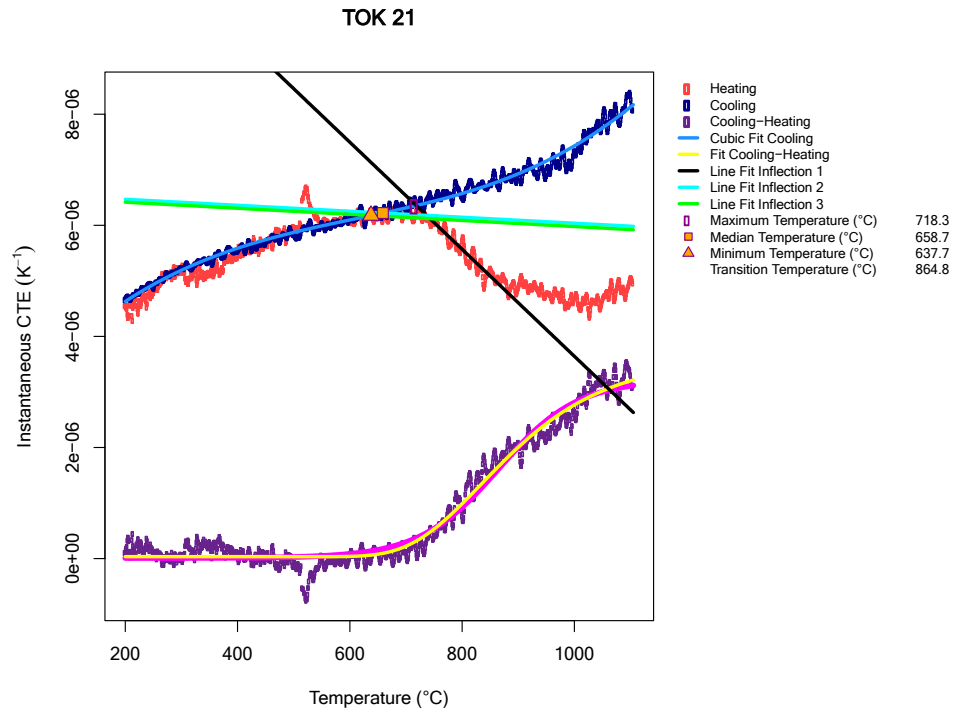


Figure A.21. Temperature monitor analysis from rabbit TOK-21.

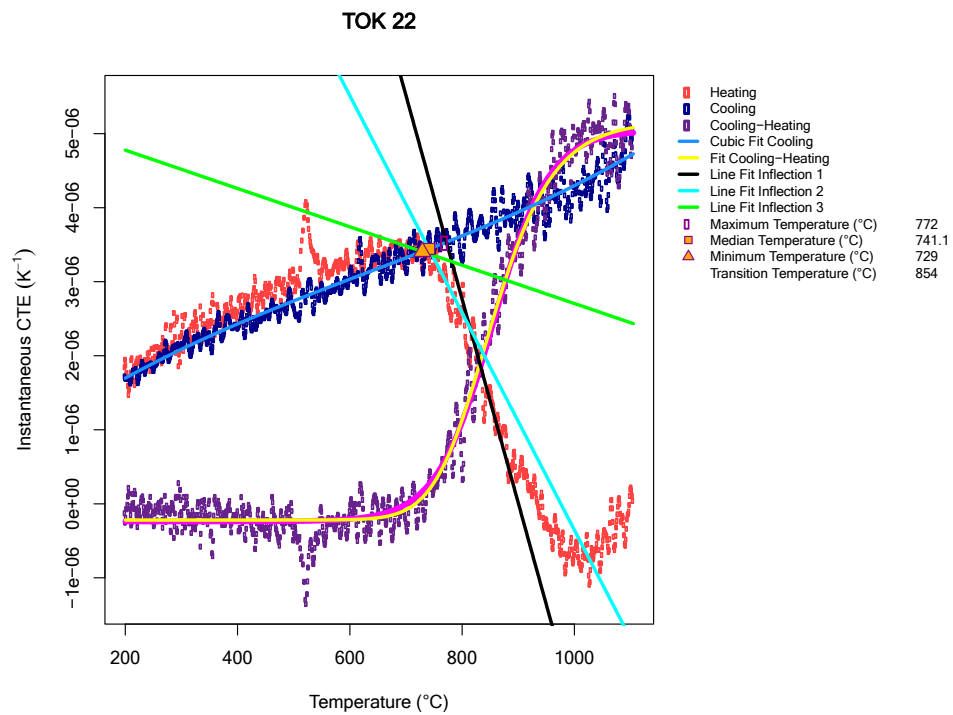


Figure A.22. Temperature monitor analysis from rabbit TOK-22.

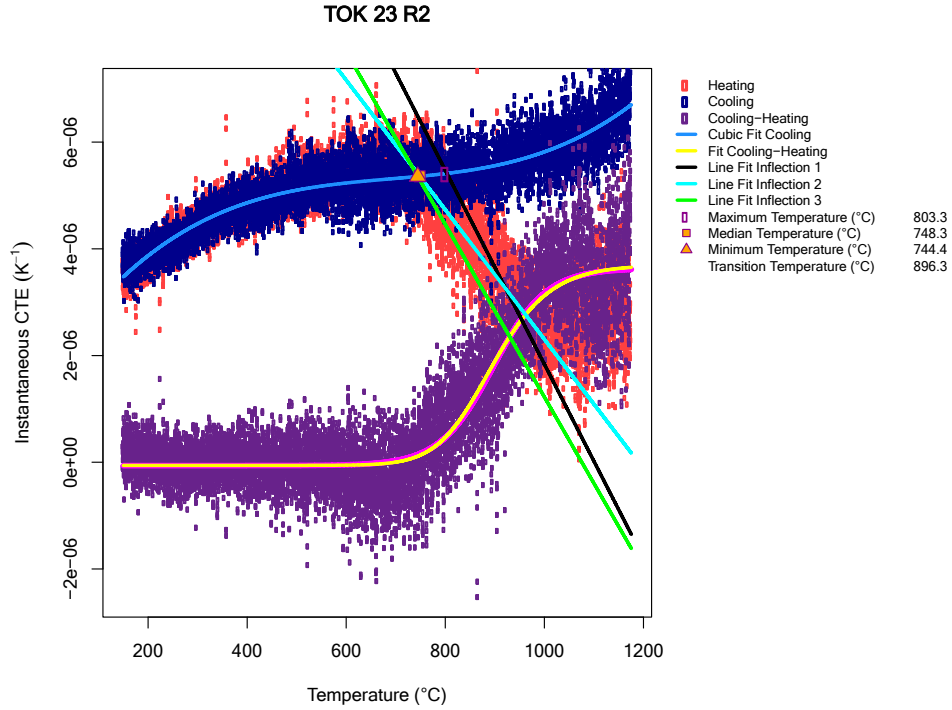


Figure A.23. Temperature monitor analysis from rabbit TOK-23.

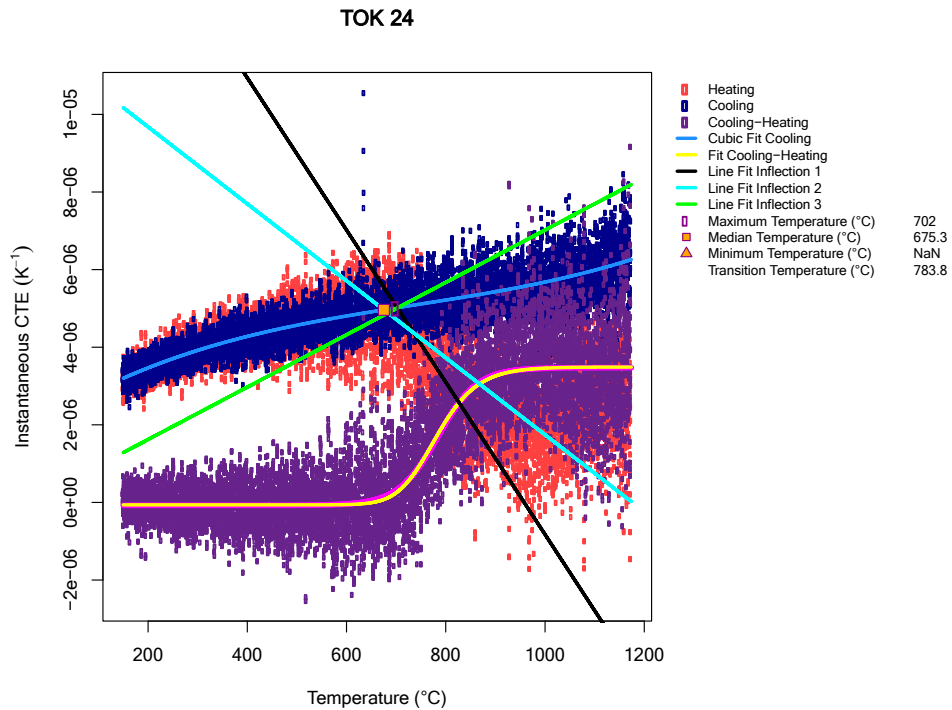


Figure A.24. Temperature monitor analysis from rabbit TOK-24.

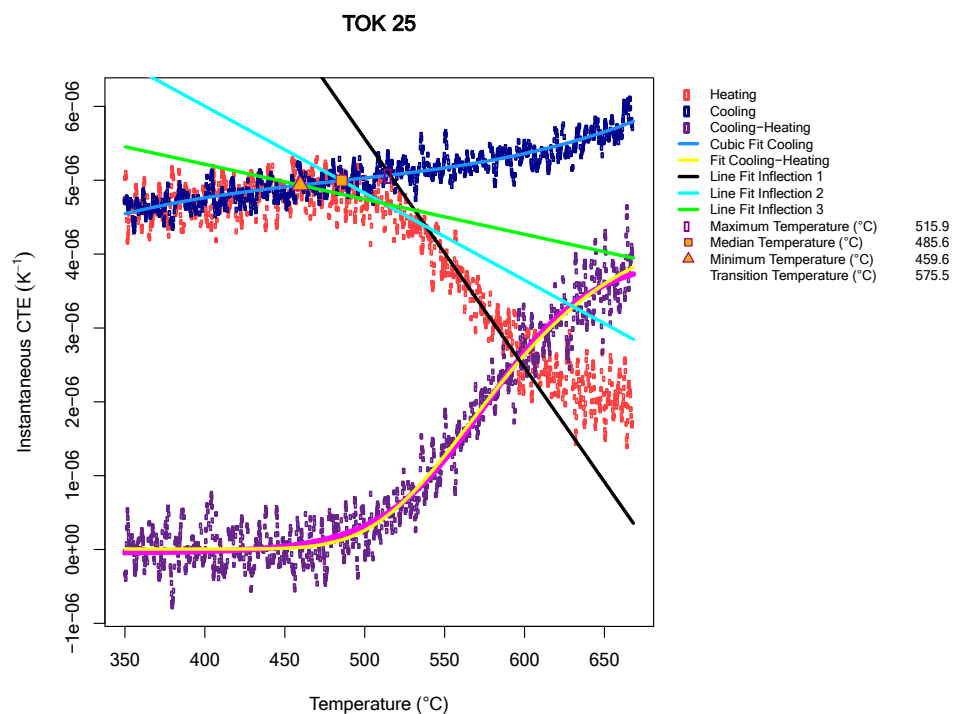


Figure A.25. Temperature monitor analysis from rabbit TOK-25.

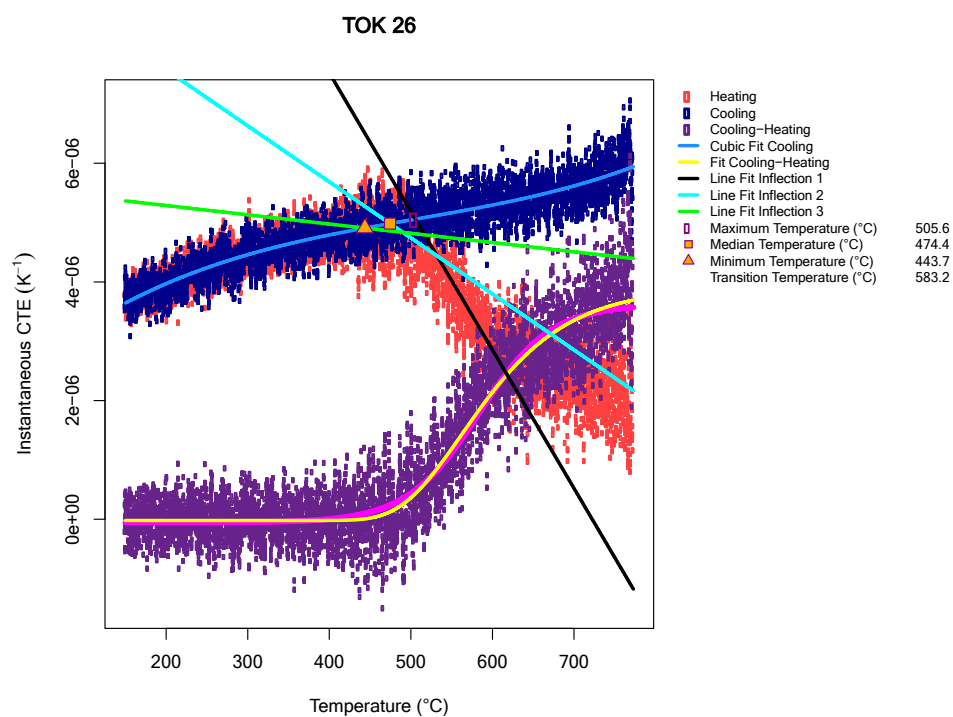


Figure A.26. Temperature monitor analysis from rabbit TOK-26.

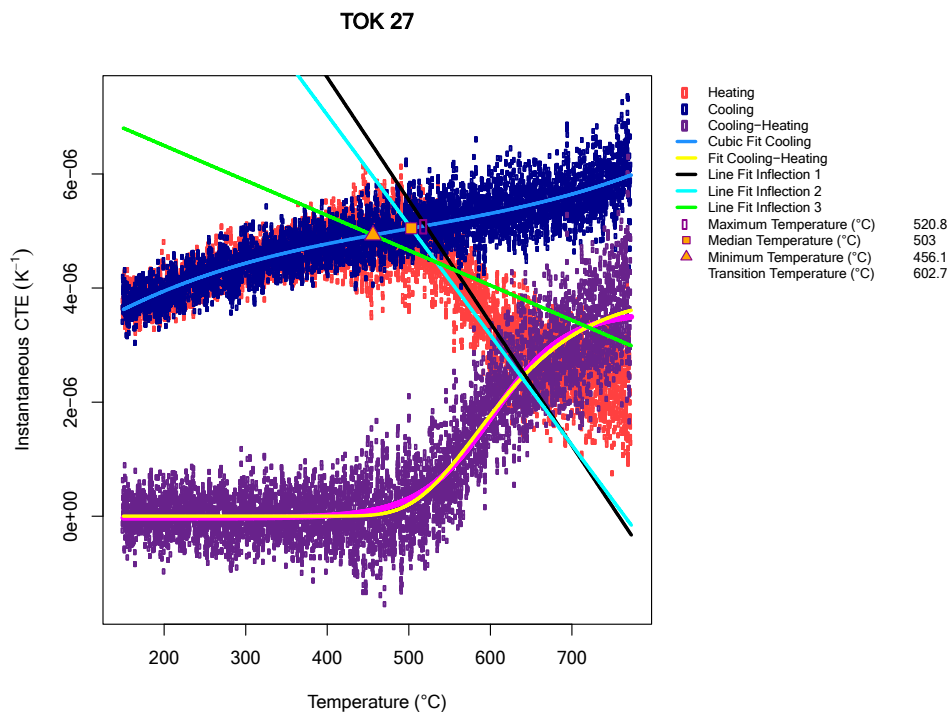


Figure A.27. Temperature monitor analysis from rabbit TOK-27.

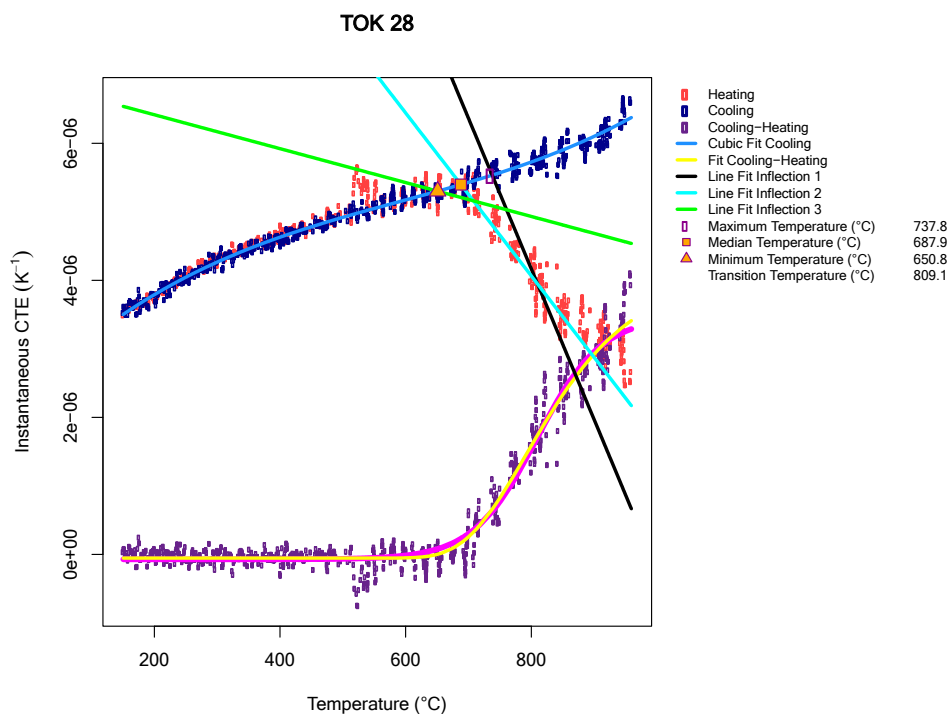


Figure A.28. Temperature monitor analysis from rabbit TOK-28.

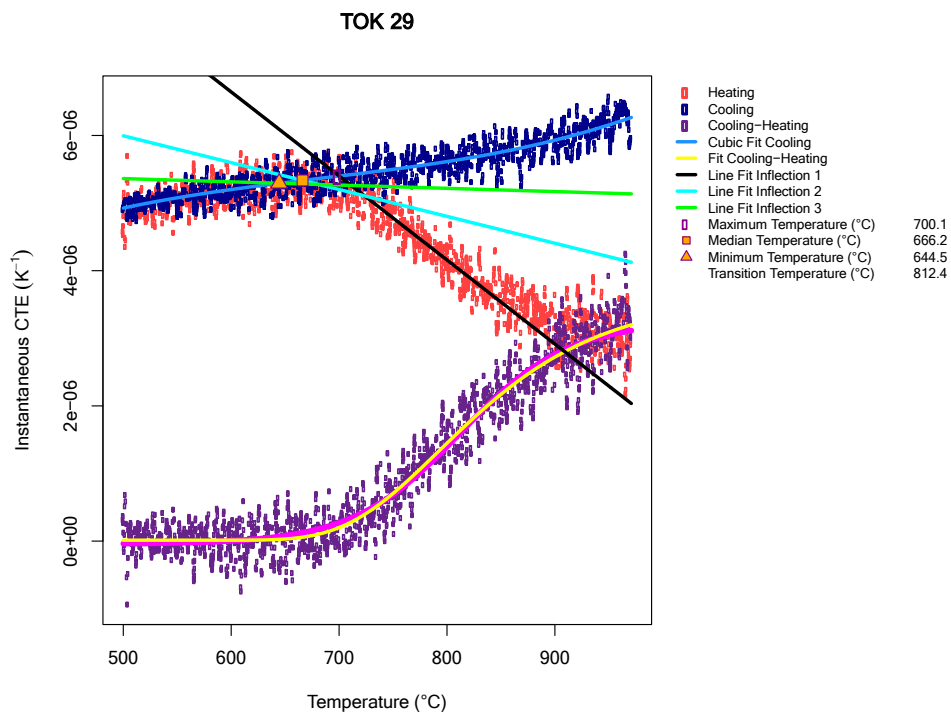


Figure A.29. Temperature monitor analysis from rabbit TOK-29.

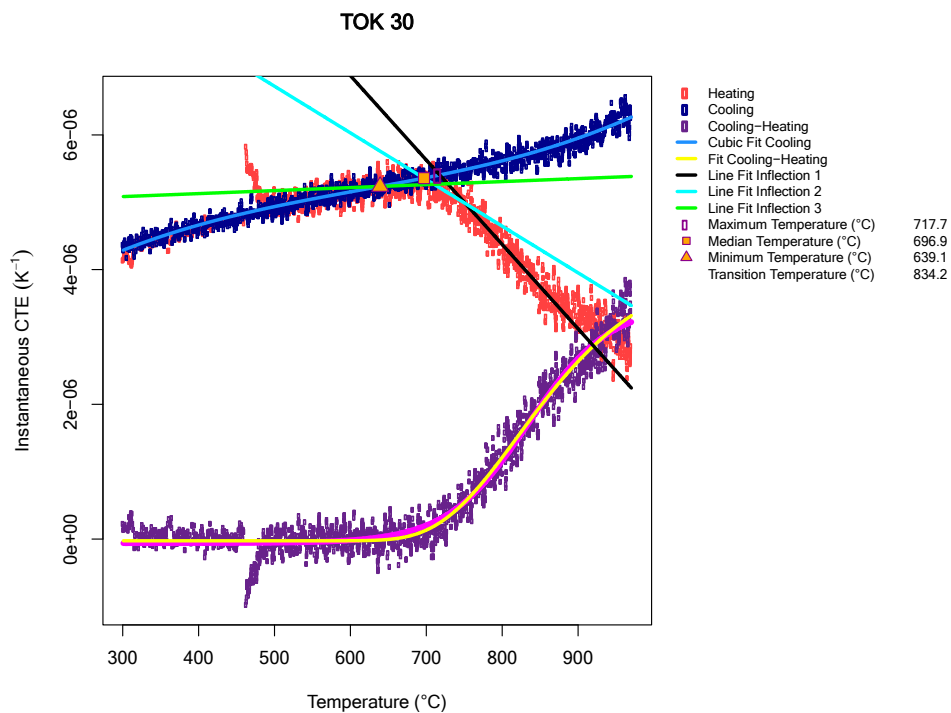


Figure A.30. Temperature monitor analysis from rabbit TOK-30.

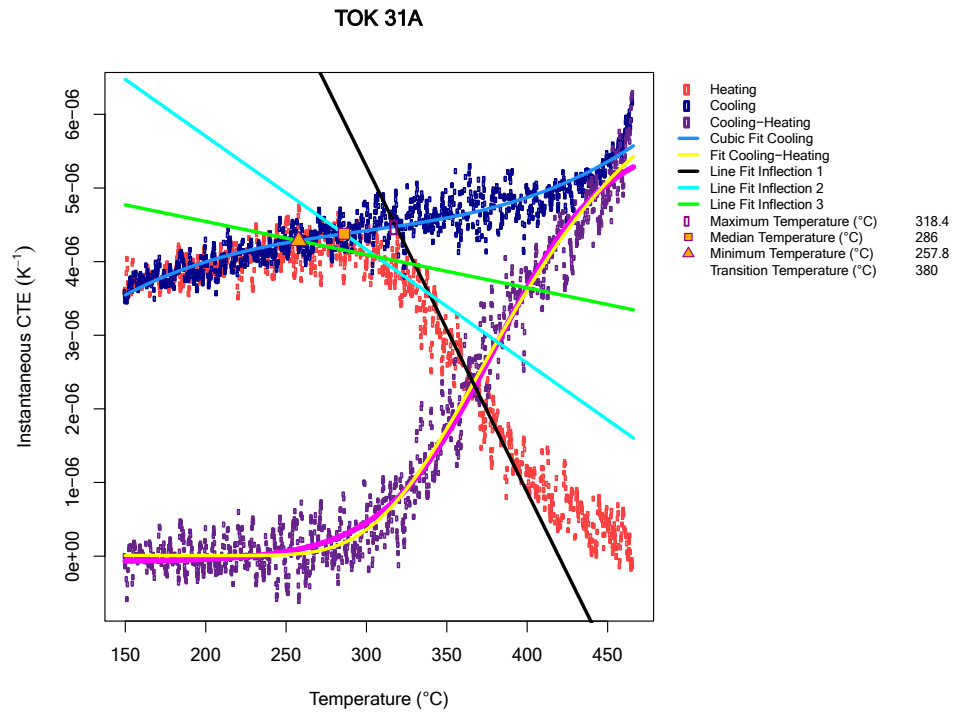


Figure A.31. Temperature monitor analysis from rabbit TOK-31.

APPENDIX B. SPECIMEN RESULTS

B.1 MB-W6

B.1.1 Pre-Irradiation (G347A only)

ID	Orient	Mass (g)	X (mm)	Y (mm)	Z (mm)	Volume (mm ³)	Bulk Density [g/cm ³]	ER [μΩm]	E [GPa]	G [GPa]	Poisson's Ratio
G2W11	WG	0.5275	5.9925	0.9943	47.9800	285.8669	1.8453	9.48	10.43	4.20	0.24
G2W12	WG	0.5275	5.9915	0.9933	47.9820	285.5436	1.8473	9.40	10.51	4.21	0.25
G2W13	WG	0.5260	5.9933	0.9898	47.9770	284.5909	1.8481	9.50	10.46	4.18	0.25
G2W14	WG	0.5265	5.9913	0.9930	47.9770	285.4301	1.8444	9.53	10.37	4.15	0.25
G2W15	WG	0.5267	5.9930	0.9923	47.9760	285.2919	1.8461	9.52	10.42	4.20	0.24
G2W16	WG	0.5262	5.9943	0.9920	47.9790	285.2973	1.8445	9.56	10.40	4.16	0.25
G2W17	WG	0.5250	5.9945	0.9925	47.9830	285.4768	1.8390	9.60	10.22	4.12	0.24
G2W19	WG	0.5236	5.9913	0.9930	47.9805	285.4509	1.8342	9.62	10.32	4.13	0.25
G2W20	WG	0.5253	5.9928	0.9950	47.9825	286.1094	1.8362	9.64	10.25	4.12	0.24
G2W21	WG	0.5269	5.9898	0.9935	47.9815	285.5291	1.8455	9.61	10.31	4.17	0.24
G2W22	WG	0.5254	5.9930	0.9905	47.9815	284.8214	1.8446	9.62	10.37	4.18	0.24
G2W23	WG	0.5250	5.9933	0.9920	47.9790	285.2497	1.8406	9.63	10.22	4.15	0.23
G2W25	WG	0.5251	5.9905	0.9923	47.9695	285.1342	1.8416	9.48	10.44	4.17	0.25
G2W26	WG	0.5250	5.9910	0.9913	47.9855	284.9657	1.8423	9.46	10.42	4.18	0.25
G2W27	WG	0.5251	5.9868	0.9913	47.9765	284.7101	1.8442	9.50	10.45	4.17	0.25
G2W28	WG	0.5265	5.9883	0.9945	47.9780	285.7241	1.8427	9.47	10.45	4.19	0.25
G2W29	WG	0.5262	5.9890	0.9900	47.9665	284.3987	1.8501	9.41	10.50	4.20	0.25
G2W30	WG	0.5270	5.9905	0.9925	47.9735	285.2299	1.8476	9.43	10.44	4.21	0.24
G2W31	WG	0.5266	5.9875	0.9938	47.9795	285.4818	1.8445	9.45	10.50	4.18	0.25
G2W32	WG	0.5272	5.9875	0.9913	47.9680	284.6953	1.8518	9.41	10.48	4.23	0.24
G2W33	WG	0.5271	5.9918	0.9980	47.9825	286.9241	1.8372	9.50	10.29	4.14	0.24
G2W34	WG	0.5267	5.9865	0.9983	47.9835	286.7505	1.8368	9.48	10.27	4.13	0.24
G2W35	WG	0.5255	5.9880	0.9970	47.9780	286.4304	1.8347	9.43	10.39	4.15	0.25
G2W36	WG	0.5260	5.9880	0.9980	47.9790	286.7237	1.8347	9.48	10.33	4.14	0.25
G2W37	WG	0.5255	5.9878	0.9975	47.9840	286.5979	1.8336	9.49	10.28	4.13	0.24

B.1.2 Post-Irradiation (G347A only)

ID	Fluence (x10 ²⁵ n/m ² [E>0.1MeV])	Irradiation Temperature (°C)	Mass (g)	X (mm)	Y (mm)	Z (mm)	Volume (mm ³)	Bulk Density [g/cm ³]	ER [μΩm]	E [GPa]	G [GPa]	Poisson's Ratio
G2W11	9.73	323	0.5278	5.9028	0.9778	47.4020	273.6	1.929	22.27	24.88		
G2W12	22.80	330				<i>47.6320</i>	<i>269.4</i>		20.44	41.55	14.31	0.45
G2W12-1			0.2974	5.8465	0.9675	26.8550	151.9	1.958				
G2W13	28.54	442	0.5256	5.8905	0.9795	47.7957	275.8	1.906	22.52	37.75	14.40	0.31
G2W14	32.33	428				<i>48.6165</i>	<i>285.0</i>			31.13	12.72	0.22
G2W14-1			0.3639	5.9250	0.9893	33.6053	197.0	1.847				
G2W15	40.80	346	0.5249	5.9075	0.9883	48.1177	280.9	1.869	22.90	38.67	14.89	0.30
G2W16	12.64	382	0.5266	5.8883	0.9770	47.3145	272.2	1.935	22.46	27.49	10.53	0.30
G2W17	21.00	419	0.5251	5.8572	0.9754	47.2843	270.1	1.944	21.54	36.64	14.00	0.31
G2W19	27.78	463				<i>48.1168</i>	<i>278.3</i>			34.73	12.49	0.39
G2W19-1			0.2783	5.8975	0.9808	25.5757	147.9	1.881				
G2W20	36.06	413	0.5244	6.0275	1.0075	49.1853	298.7	1.756	28.82	26.39	10.34	0.28
G2W21	40.80	381				<i>49.3462</i>	<i>304.2</i>		28.74	26.48	10.08	0.31
G2W21-1			0.4179	6.0428	1.0203	39.1357	241.3	1.732				
G2W22	11.87	578	0.5170	5.8928	0.9735	47.3740	271.8	1.902	23.07	23.91	9.70	0.23
G2W23	17.77	561	0.5248	5.8685	0.9770	47.4075	271.8	1.931	21.92	32.85	12.78	0.29
G2W25	23.76	478	0.5249	5.8773	0.9848	47.6205	275.6	1.904	22.39	35.33	13.77	0.28
G2W26	29.72	530	0.5154	5.9433	0.9915	48.3277	284.8	1.810	25.79	30.10	12.23	0.23
G2W27	35.99	524	0.5169	6.0928	1.0240	49.6587	309.8	1.668	32.25	23.75	9.44	0.26
G2W28	7.87	652	0.5265	5.9303	0.9830	47.5970	277.5	1.898	23.30	19.72	7.84	0.26
G2W29	13.84	603	0.5261	5.8883	0.9790	47.4578	273.6	1.923	22.43	27.83	10.74	0.30
G2W30	17.77	642				<i>47.6052</i>	<i>273.9</i>		22.54	32.63	12.40	0.32
G2W30-1			0.4764	5.8835	0.9780	43.0360	247.6	1.924				
G2W31	23.76	697				<i>48.5644</i>	<i>284.0</i>			35.44	10.66	0.66
G2W31-1			0.1990	5.9407	0.9843	18.3530	107.3	1.854				
G2W32	29.21	625	0.5164	6.0143	1.0088	49.0133	297.4	1.737	28.57	28.53	11.51	0.24
G2W33	4.68	681	0.5278	5.9635	0.9913	47.8470	282.8	1.866	23.55	17.75	7.14	0.24
G2W34	9.54	756				<i>47.6941</i>	<i>277.6</i>		22.58	25.40	9.81	0.29
G2W34-1			0.4437	5.9288	0.9818	40.1790	233.9	1.897				
G2W35	14.14	783	0.5260	5.9170	0.9860	47.9093	279.5	1.882	22.78	33.04	12.73	0.30
G2W36	16.50	690				<i>47.8917</i>	<i>278.9</i>		22.98	34.79	13.19	0.32
G2W36-1			0.4741	5.9113	0.9853	43.1630	251.4	1.886				
G2W37	13.30	281	0.5257	5.9183	1.0013	47.6535	282.4	1.862	26.03	19.46	7.21	0.35

Specimen ID's in bold red text broke before dimensional inspection could be performed. The broken piece was cut to be rectangular, and then mass and dimensional inspection was performed. The cut piece is indicated with the -1 after the specimen ID. The mass and dimensions of the cut piece were used to calculate the density. With the density then the expected total length (Z) and full specimen volume were calculated using the bulk density, mass, X, and Y dimensions from the cut piece. All the subsequent measurements were performed on the cut specimen (electrical resistivity and modulus). The calculated volume was used for pre- and post-irradiation volume comparison. The dimensions used for the pre- and post-irradiation length change comparison are: measured X and Y, and expected total length of the unbroken specimen.

B.2 SB-W3

B.2.1 Pre-Irradiation Dimensions

ID	Mater.	Orient.	Mass (g)	X (mm)	Y (mm)	Z (mm)	Volume (mm ³)	Bulk Density [g/cm ³]	E [GPa]
11W00	IG-110	WG	0.3060	2.8987	2.3980	25.0355	173.7865	1.7608	
11W01	IG-110	WG	0.3065	2.8968	2.3960	25.0020	173.4025	1.7675	
11W02	IG-110	WG	0.3065	2.8943	2.3990	24.9990	173.3044	1.7683	
11W03	IG-110	WG	0.3066	2.8995	2.3970	24.9980	173.5937	1.7660	
11W04	IG-110	WG	0.3064	2.8955	2.3970	24.9925	173.3341	1.7675	13.43
11W05	IG-110	WG	0.3065	2.8958	2.3990	24.9980	173.6406	1.7651	
11W06	IG-110	WG	0.3056	2.8955	2.4020	25.0030	173.6423	1.7597	
11W07	IG-110	WG	0.3058	2.8958	2.3970	25.0320	173.8949	1.7582	9.06
11W08	IG-110	WG	0.3060	2.8953	2.4040	25.0140	173.7399	1.7614	9.05
11W09	IG-110	WG	0.3065	2.8945	2.4030	25.0265	173.9809	1.7616	9.02
11W10	IG-110	WG	0.3064	2.8945	2.4020	24.9950	173.8342	1.7628	8.95
11W11	IG-110	WG	0.3065	2.8993	2.4050	25.0035	173.79	1.7591	8.76
41W00	G458S	WG	0.3190	2.8988	2.3953	24.9410	173.40	1.8423	11.95
41W01	G458S	WG	0.3080	2.8928	2.3948	25.0085	173.30	1.7775	9.55
41W02	G458S	WG	0.3079	2.8945	2.3945	25.0135	173.59	1.7758	9.54
41W03	G458S	WG	0.3186	2.8980	2.3948	24.9655	173.33	1.8390	
41W04	G458S	WG	0.3184	2.9013	2.3930	24.9790	173.64	1.8361	
41W05	G458S	WG	0.3191	2.9020	2.3943	24.9870	173.64	1.8377	
41W06	G458S	WG	0.3204	2.9018	2.3938	24.9615	173.89	1.8480	
41W07	G458S	WG	0.3204	2.9008	2.3963	24.9775	173.74	1.8456	
41W08	G458S	WG	0.3190	2.8988	2.3948	24.9995	173.98	1.8379	
41W09	G458S	WG	0.3196	2.9023	2.3970	25.0220	173.83	1.8361	12.24
41W10	G458S	WG	0.3206	2.9003	2.3928	24.9710	174.23	1.8498	12.34
41W11	G458S	WG	0.3200	2.9015	2.3983	25.0030	173.17	1.8393	12.14
G1A00	G347S	AG	0.3149	2.8860	25.0565	2.3865	173.24	1.8248	
G1A01	G347S	AG	0.3173	2.8970	24.9870	2.3893	173.37	1.8346	
G1A02	G347S	AG	0.3184	2.8970	25.0080	2.4003	173.26	1.8308	
G1A03	G347S	AG	0.3184	2.8970	25.0705	2.4003	173.42	1.8263	
G1A04	G347S	AG	0.3192	2.8975	25.0220	2.3955	173.61	1.8378	
G1A05	G347S	AG	0.3194	2.8995	25.0925	2.3988	173.38	1.8303	
G1A06	G347S	AG	0.3192	2.8995	25.0035	2.3980	173.62	1.8358	
G1A07	G347S	AG	0.3196	2.9028	24.9980	2.3995	173.54	1.8356	
G1A08	G347S	AG	0.3191	2.9018	25.0135	2.3945	174.07	1.8363	9.67

ID	Mater.	Orient.	Mass (g)	X (mm)	Y (mm)	Z (mm)	Volume (mm ³)	Bulk Density [g/cm ³]	E [GPa]
G1A09	G347S	AG	0.3195	2.9015	25.0185	2.3985	173.29	1.8350	9.74
G1A10	G347S	AG	0.3193	2.8993	25.0760	2.3975	173.98	1.8321	9.85
G1A11	G347S	AG	0.3198	2.9015	25.0365	2.3985	172.58	1.8353	9.81
G1W00	G347S	WG	0.3184	2.8860	2.3865	25.0565	172.95	1.8359	
G1W01	G347S	WG	0.3171	2.8970	2.3893	24.9870	173.89	1.8396	
G1W02	G347S	WG	0.3095	2.8970	2.4003	25.0080	174.33	1.7848	
G1W03	G347S	WG	0.3191	2.8970	2.4003	25.0705	173.68	1.8339	
G1W04	G347S	WG	0.3197	2.8975	2.3955	25.0220	174.52	1.8374	
G1W05	G347S	WG	0.3195	2.8995	2.3988	25.0925	173.85	1.8347	
G1W06	G347S	WG	0.3193	2.8995	2.3980	25.0035	174.11	1.8358	
G1W07	G347S	WG	0.3197	2.9028	2.3995	24.9980	173.80	1.8357	
G1W08	G347S	WG	0.3186	2.9018	2.3945	25.0135	174.11	1.8365	
G1W09	G347S	WG	0.3194	2.9015	2.3985	25.0185	174.30	1.8390	
G1W10	G347S	WG	0.3199	2.8993	2.3975	25.0760	174.24	1.8389	
G1W11	G347S	WG	0.3199	2.9015	2.3985	25.0365	173.40	1.8382	
G1W12	G347S	WG	0.3199	2.8948	2.3955	25.0060	172.36	1.8393	
G1W13	G347S	WG	0.3197	2.8920	2.3838	25.0025	173.40	1.8390	
G1W14	G347S	WG	0.3196	2.8945	2.3950	25.0135	173.99	1.8383	9.41
G1W15	G347S	WG	0.3198	2.8993	2.4005	24.9995	174.01	1.8402	9.42
G1W20	G347S	WG							
G1W21	G347S	WG							
G1W22	G347S	WG							
G1W23	G347S	WG							
G1W24	G347S	WG							

B.2.2 Pre-irradiation CTE

ID	Mater.	Orient.	Mean CTE x10 ⁻⁶ K ⁻¹ (references to 25°C)									
			100°C	200°C	300°C	400°C	500°C	600°C	700°C	800°C	900°C	1000°C
11W09	IG-110	WG	3.69	4.03	4.28	4.39	4.54	4.70	4.84	4.94	5.05	5.12
11W10	IG-110	WG	3.62	3.90	4.14	4.28	4.44	4.56	4.71	4.82	4.93	5.02
11W11	IG-110	WG	3.91	4.22	4.46	4.57	4.69	4.81	4.91	5.01	5.10	5.19
41W09	G458S	WG	3.13	3.35	3.57	3.63	3.79	3.89	4.01	4.11	4.20	4.29
41W10	G458S	WG	3.03	3.36	3.64	3.70	3.80	3.92	4.02	4.15	4.27	4.36
41W11	G458S	WG	3.08	3.42	3.67	3.73	3.83	3.89	4.01	4.15	4.26	4.35
G1A09	G347S	AG	3.55	3.65	3.82	3.99	4.16	4.32	4.45	4.57	4.68	4.77
G1A10	G347S	AG	3.59	3.68	3.83	4.00	4.17	4.33	4.47	4.59	4.70	4.80
G1A11	G347S	AG	3.51	3.66	3.84	4.01	4.18	4.34	4.47	4.60	4.70	4.80
G1W09	G347S	WG	3.89	4.02	4.18	4.34	4.49	4.63	4.75	4.87	4.97	5.06
G1W20	G347S	WG	3.82	3.98	4.15	4.32	4.49	4.64	4.77	4.90	5.00	5.10
G1W21	G347S	WG	3.79	3.95	4.13	4.30	4.46	4.60	4.74	4.85	4.95	5.05
G1W22	G347S	WG	3.95	4.04	4.17	4.34	4.50	4.66	4.79	4.92	5.03	5.13
G1W23	G347S	WG	3.89	4.02	4.18	4.34	4.50	4.64	4.77	4.89	4.99	5.08
G1W24	G347S	WG	3.93	4.04	4.20	4.37	4.52	4.67	4.80	4.92	5.03	5.12

B.2.3 Post-Irradiation Dimensions

ID	Mater.	Orient.	Fluence (x10 ²⁵ n/m ² [E>0.1MeV])	Irradiation Temperature (°C)	Mass (g)	X (mm)	Y (mm)	Z (mm)	Volume (mm ³)	Bulk Density [g/cm ³]	E [GPa]
11W00	IG-110	WG	9.50	468	0.3063	2.8328	2.3535	24.5468	163.65	1.8719	20.76
11W01	IG-110	WG	30.42	456	0.3066	2.8445	2.4383	24.9160	172.81	1.7742	23.73
11W02	IG-110	WG	36.95	475				25.4558	182.19		1.63
11W02-1					0.1238	2.8910	2.4757	10.2837	73.60	1.6820	
11W03	IG-110	WG	4.40	664	0.3072	2.8728	2.3793	24.8540	169.88	1.8081	16.07
11W05	IG-110	WG	20.29	642	0.3074	2.8295	2.3953	24.6610	167.14	1.8392	28.09
11W06	IG-110	WG	27.02	656		2.8607	2.4502	25.0673	176.80	1.7283	0.31
11W06-1					0.1642	2.8713	2.4563	13.5720	95.72	1.7154	
11W06-2					0.1191	2.8500	2.4440	9.8200	68.40	1.7412	
41W03	G458S	WG	9.50	444	0.3188	2.8383	2.3638	24.5055	164.41	1.9391	24.31
41W04	G458S	WG	30.42	432	0.3186	2.8733	2.5055	24.8180	178.66	1.7832	24.27
41W05	G458S	WG	36.95	451		2.9236	2.5368	25.0302	185.94	1.7159	1.80
41W05-1					0.161	2.9227	2.5417	12.6040	93.63	1.7196	
41W05-2					0.1372	2.9245	2.5320	10.8210	80.13	1.7123	
41W06	G458S	WG	4.40	623	0.3209	2.8760	2.3810	24.7963	169.80	1.8899	19.95
41W07	G458S	WG	20.29	601	0.3212	2.8393	2.4355	24.4230	168.88	1.9016	32.58
41W08	G458S	WG	27.02	615	0.3190	2.9043	2.5353	24.9088	183.40	1.7391	29.56
G1A00	G347S	AG	9.50	453	0.3151	2.8320	2.46015	2.3470	163.52	1.9271	24.23
G1A02	G347S	AG	30.42	441	0.3154	2.9020	24.9433	2.4243	175.48	1.7973	27.18
G1A03	G347S	AG	36.95	460	0.3137	2.9298	25.0790	2.4813	182.31	1.7207	22.37
G1A04	G347S	AG	4.40	643	0.3196	2.8738	24.8258	2.3758	169.49	1.8857	19.78
G1A05	G347S	AG	20.29	621	0.3200	2.8625	24.5535	2.3973	168.49	1.8992	34.74
G1A06	G347S	AG	27.02	635	0.3177	2.9375	25.0340	2.4925	183.29	1.7333	31.32
G1W03	G347S	WG	9.50	458	0.3195	2.8418	2.3570	24.6653	165.21	1.9339	23.77
G1W04	G347S	WG	30.42	446	0.3196	2.8823	2.4015	25.4780	176.35	1.8123	27.45
G1W05	G347S	WG	36.95	465	0.3194	2.9200	2.4288	25.8393	183.25	1.7430	22.50
G1W06	G347S	WG	4.40	641	0.3200	2.8780	2.3770	24.8990	170.33	1.8784	17.88
G1W07	G347S	WG	20.29	619	0.3205	2.8640	2.3760	25.0560	170.50	1.8797	33.75
G1W08	G347S	WG	27.02	633	0.3185	2.9253	2.4375	25.8508	184.32	1.7279	30.46

Specimen ID's in bold red text broke before dimensional inspection could be performed. The broken piece was cut to be rectangular, and then mass and dimensional inspection was performed. The cut piece is indicated with the -1 and -2 (when 2 pieces were cut) after the specimen ID. The mass and dimensions of the cut piece/s were used to calculate the density (average shown in italics). The expected total length (Z) and full specimen volume were calculated using the bulk density, mass, X, and Y dimensions from the cut piece (or average values when 2 cut pieces). The resulting moduli from the cut pieces are suspect because the specimens were smaller than minimum dimension required by equipment. The calculated volume was used for pre- and post-irradiation volume comparison. The dimensions used for the pre- and post-irradiation length change comparison are: measured X and Y (or average X and Y when 2 pieces were cut), and expected total length of the unbroken specimen.

B.2.4 Post-Irradiation CTE

ID	Mater.	Orient.	Mean CTE x10 ⁻⁶ K ⁻¹ (references to 25°C)									
			100°C	200°C	300°C	400°C	500°C	600°C	700°C	800°C	900°C	1000°C
11W00	IG-110	WG	4.37	4.52	4.70	4.88	5.03	5.15	5.27	5.41	5.54	5.72
11W01	IG-110	WG	3.11	3.20	3.33	3.49	3.66	3.83	4.01	4.19	4.36	4.56
11W02-1	IG-110	WG	2.89	3.01	3.21	3.40	3.60	3.79	3.97	4.12	4.25	4.43
11W03	IG-110	WG	4.22	4.31	4.45	4.63	4.83	5.04	5.22	5.39	5.54	5.67
11W05	IG-110	WG	2.61	2.65	2.80	2.97	3.15	3.31	3.46	3.62	3.82	4.05
11W06-2	IG-110	WG	1.86	1.99	2.21	2.43	2.63	2.81	2.97	3.16	3.52	4.06
41W03	G458S	WG	4.37	4.50	4.68	4.85	5.02	5.13	5.26	5.40	5.54	5.73
41W04	G458S	WG	2.92	3.03	3.18	3.34	3.51	3.67	3.87	4.13	4.42	4.75
41W05-2	G458S	WG	2.59	2.74	2.93	3.10	3.27	3.46	3.66	3.90	4.17	4.49
41W06	G458S	WG	3.77	3.83	3.97	4.17	4.46	4.69	4.90	5.09	5.25	5.41
41W07	G458S	WG	2.36	2.43	2.59	2.77	2.95	3.11	3.26	3.40	3.57	3.80
41W08	G458S	WG	1.97	2.04	2.21	2.39	2.57	2.72	2.86	3.07	3.49	4.02
G1A00	G347S	AG	4.57	4.70	4.87	5.04	5.19	5.31	5.44	5.60	5.76	5.97
G1A02	G347S	AG	2.58	2.71	2.87	3.04	3.21	3.38	3.59	3.88	4.24	4.62
G1A03	G347S	AG	2.73	2.87	3.04	3.21	3.38	3.55	3.74	3.94	4.15	4.39
G1A04	G347S	AG	4.13	4.23	4.40	4.63	4.87	5.09	5.29	5.46	5.61	5.78
G1A05	G347S	AG	1.98	2.06	2.23	2.41	2.59	2.77	2.92	3.06	3.21	3.40
G1A06	G347S	AG	1.71	1.82	1.99	2.17	2.35	2.51	2.66	2.79	3.05	3.49
G1W03	G347S	WG	4.71	4.91	5.11	5.29	5.46	5.59	5.73	5.89	6.07	6.29
G1W04	G347S	WG	2.92	3.05	3.21	3.38	3.55	3.73	3.94	4.24	4.58	4.99
G1W05	G347S	WG	3.02	3.15	3.32	3.48	3.65	3.82	4.01	4.22	4.45	4.73
G1W06	G347S	WG	4.27	4.43	4.61	4.82	5.06	5.29	5.50	5.69	5.85	6.01
G1W07	G347S	WG	2.19	2.29	2.47	2.65	2.83	3.00	3.15	3.30	3.47	3.74
G1W08	G347S	WG	1.85	1.96	2.15	2.34	2.52	2.68	2.82	2.99	3.41	4.03

Specimen ID's in bold red text broke before dimensional inspection could be performed. The cut piece that was closest to 10 mm length were used for CTE measurements, which corresponds to the cut specimen ID's given in B.2.3.

B.3 SB-W4

B.3.1 Pre-irradiation Dimensions (G347A only)

ID	Mater.	Orient.	Mass (g)	X (mm)	Y (mm)	Z (mm)	Volume (mm ³)	Bulk Density [g/cm ³]	E [GPa]
G0A06	G347S	AG	0.6072	2.8985	29.9943	3.7915	329.63	1.8420	11.28
G0A07	G347S	AG	0.6079	2.9008	29.9910	3.7925	329.93	1.8423	11.26
G0A08	G347S	AG	0.6076	2.9013	29.9963	3.7930	330.09	1.8408	11.24
G0W03	G347S	WG	0.6090	2.9003	3.8005	29.9978	330.65	1.8417	11.13
G0W04	G347S	WG	0.6095	2.9023	3.8015	30.0260	331.27	1.8400	11.23
G0W05	G347S	WG	0.6100	2.9015	3.7973	30.0015	330.55	1.8455	11.19
G0A10	G347S	AG	0.6059	2.8998	29.9978	3.7913	329.79	1.8372	11.27
G0A11	G347S	AG	0.6059	2.9003	29.9928	3.7890	329.59	1.8384	11.24
G0A12	G347S	AG	0.6063	2.9008	29.9893	3.7915	329.83	1.8383	11.24
G0A13	G347S	AG	0.6062	2.9028	29.9945	3.7903	330.00	1.8370	11.20
G0A14	G347S	AG	0.6062	2.9013	29.9885	3.7913	329.85	1.8378	11.26
G0A16	G347S	AG	0.6046	2.8895	29.9935	3.7905	328.51	1.8404	11.30
G0A17	G347S	AG	0.6051	2.8938	29.9945	3.7930	329.22	1.8380	11.28
G0A18	G347S	AG	0.6053	2.8938	29.9913	3.7930	329.18	1.8389	11.31
G0A19	G347S	AG	0.6052	2.8968	29.9925	3.7928	329.52	1.8367	11.30
G0A20	G347S	AG	0.6075	2.8965	29.9908	3.7923	329.43	1.8440	11.51
G0A21	G347S	AG	0.6091	2.8963	29.9855	3.7923	329.34	1.8495	11.61
G0A22	G347S	AG	0.6093	2.8983	29.9848	3.7930	329.62	1.8485	11.58
G0A28	G347S	AG	0.6099	2.8983	29.9838	3.7970	329.96	1.8485	11.56
G0A29	G347S	AG	0.6102	2.8995	29.9850	3.7938	329.83	1.8499	11.51
G0A30	G347S	AG	0.6103	2.8983	29.9965	3.7940	329.84	1.8502	11.54
G0A31	G347S	AG	0.6103	2.8995	29.9983	3.7955	330.13	1.8488	11.55
G0A32	G347S	AG	0.6104	2.8995	29.9950	3.7923	329.81	1.8507	11.52
G0A33	G347S	AG	0.6103	2.8988	29.9958	3.7945	329.93	1.8497	11.54
G0A34	G347S	AG	0.6103	2.8990	29.9945	3.7935	329.86	1.8503	11.53
G0A35	G347S	AG	0.6100	2.9000	29.9980	3.7938	330.03	1.8484	9.00
G0A36	G347S	AG	0.6099	2.9015	29.9960	3.7965	330.42	1.8458	11.51
G0A37	G347S	AG	0.6098	2.8998	29.9985	3.7938	330.01	1.8478	11.51
G0A38	G347S	AG	0.6099	2.9015	29.9988	3.7950	330.32	1.8464	11.52
G0A39	G347S	AG	0.6097	2.9015	29.9968	3.7958	330.37	1.8455	11.51
G0A59	G347S	AG	0.6084	2.8993	29.9960	3.7993	330.41	1.8412	11.34
G0W15	G347S	WG	0.6121	2.9058	3.7990	29.9960	331.12	1.8484	11.22
G0W16	G347S	WG	0.6119	2.9043	3.8010	29.9943	331.11	1.8479	11.12

ID	Mater.	Orient.	Mass (g)	X (mm)	Y (mm)	Z (mm)	Volume (mm ³)	Bulk Density [g/cm ³]	E [GPa]
G0W17	G347S	WG	0.6117	2.9063	3.8010	29.9968	331.36	1.8461	11.10
G0W18	G347S	WG	0.6112	2.9058	3.8003	30.0028	331.31	1.8448	11.13
G0W19	G347S	WG	0.6110	2.9028	3.7980	29.9940	330.67	1.8477	11.22
G0W23	G347S	WG	0.6085	2.9013	3.8005	29.9923	330.70	1.8399	10.95
G0W24	G347S	WG	0.6091	2.9010	3.8025	29.9940	330.87	1.8411	11.08
G0W25	G347S	WG	0.6092	2.9013	3.7990	29.9935	330.58	1.8426	11.20
G0W26	G347S	WG	0.6093	2.9028	3.8000	29.9960	330.87	1.8414	11.22
G0W27	G347S	WG	0.6104	2.9045	3.8025	29.9963	331.29	1.8425	11.24
G0W28	G347S	WG	0.6104	2.9023	3.8003	29.9920	330.79	1.8451	11.25
G0W29	G347S	WG	0.6113	2.9043	3.7980	29.9938	330.84	1.8478	11.21
G0W30	G347S	WG	0.6071	2.8963	3.8005	29.9980	330.19	1.8387	11.00
G0W32	G347S	WG	0.6083	2.9018	3.7993	29.9965	330.70	1.8395	11.11
G0W33	G347S	WG	0.6089	2.8983	3.8013	29.9978	330.48	1.8424	11.20
G0W34	G347S	WG	0.6078	2.9005	3.8003	29.9955	330.63	1.8383	11.10
G0W35	G347S	WG	0.6090	2.9010	3.8033	29.9950	330.94	1.8401	11.19
G0W36	G347S	WG	0.6094	2.9028	3.8000	29.9970	330.88	1.8418	11.13
G0W37	G347S	WG	0.6095	2.9040	3.8015	29.9990	331.18	1.8403	11.09
G0W38	G347S	WG	0.6098	2.9048	3.8013	29.9923	331.16	1.8413	11.16
G0W39	G347S	WG	0.6122	2.9053	3.8015	29.9953	331.28	1.8480	11.16
G0W40	G347S	WG	0.6098	2.8975	3.8025	29.9978	330.51	1.8451	11.06
G0W41	G347S	WG	0.6104	2.8978	3.8038	30.0045	330.72	1.8457	11.15
G0W42	G347S	WG	0.6104	2.8998	3.8025	29.9978	330.76	1.8454	11.15
G0W63	G347S	WG	0.6092	2.8953	3.7955	29.9948	329.61	1.8481	11.25

B.3.2 Pre-Irradiation CTE (G347A only)

ID	Mater.	Orient.	Mean CTE x10 ⁻⁶ K ⁻¹ (references to 25°C)									
			100°C	200°C	300°C	400°C	500°C	600°C	700°C	800°C	900°C	1000°C
G0A06	G347S	AG	3.49	3.76	3.92	3.98	4.10	4.29	4.43	4.55	4.68	4.80
G0A07	G347S	AG	3.61	3.89	4.06	4.10	4.22	4.34	4.47	4.59	4.70	4.79
G0A08	G347S	AG	3.58	3.81	4.03	4.09	4.26	4.42	4.55	4.66	4.77	4.89
G0W03	G347S	WG	3.89	4.01	4.16	4.33	4.47	4.61	4.73	4.84	4.94	5.04
G0W04	G347S	WG	3.86	3.99	4.16	4.32	4.47	4.61	4.74	4.85	4.95	5.04
G0W05	G347S	WG	3.86	3.99	4.16	4.31	4.46	4.59	4.72	4.83	4.93	5.02

B.3.3 Post-Irradiation Dimensions (G347A only)

ID	Orient.	Fluence ($\times 10^{25}$ n/m ² [E>0.1MeV])	Irradiation Temperature (°C)	Mass (g)	X (mm)	Y (mm)	Z (mm)	Volume (mm ³)	Bulk Density [g/cm ³]	E [GPa]
G0A10	AG	9.73	355	0.6064	2.8563	29.5690	3.7435	316.16	1.9181	27.11
G0A11	AG	22.80	362	0.6055	2.8327	29.2618	3.7332	309.44	1.9566	41.18
G0A12	AG	28.54	474	0.6063	2.8660	29.5053	3.7990	321.25	1.8873	37.29
G0A13	AG	32.33	460	0.6065	2.9010	29.7073	3.8268	329.79	1.8390	32.80
G0A14	AG	40.80	378	0.6068	2.9175	29.8760	3.8408	334.77	1.8126	34.31
G0A16	AG	12.64	411	0.6053	2.8370	29.4325	3.7360	311.96	1.9403	28.84
G0A17	AG	21.00	448	0.6056	2.8324	29.2821	3.7414	310.31	1.9516	39.23
G0A18	AG	27.78	492	0.6065	2.8680	29.5000	3.7915	320.78	1.8907	34.65
G0A19	AG	36.06	442	0.6058	2.9478	30.2513	3.9128	348.91	1.7362	25.66
G0A20	AG	40.80	410	0.6078	2.9593	30.3377	3.9688	356.30	1.7059	25.52
G0A21	AG	11.87	588	0.6094	2.8478	29.4630	3.7408	313.86	1.9416	26.03
G0A22	AG	17.77	571	0.6106	2.8425	29.3198	3.7523	312.72	1.9524	35.01
G0A28	AG	23.76	488	0.6107	2.8503	29.4175	3.7885	317.66	1.9224	37.30
G0A29	AG	29.72	540	0.6112	2.8768	29.6973	3.8405	328.10	1.8628	33.54
G0A30	AG	35.99	534	0.6108	2.9528	30.4767	3.9750	357.71	1.7075	25.86
G0A31	AG	7.87	692	0.6112	2.8668	29.7198	3.7670	320.94	1.9043	20.49
G0A32	AG	13.84	643	0.6110	2.8533	29.5163	3.7608	316.72	1.9290	28.51
G0A33	AG	17.77	682	0.6110	2.8533	29.5333	3.7783	318.38	1.9191	33.31
G0A34	AG	23.76	737			29.8313		336.3		1.55
G0A34-1				0.3513	2.8998	17.1703	3.8873	193.5	1.815	
G0A35	AG	29.21	665	0.6112	2.9368	30.2083	3.9393	349.47	1.7489	29.24
G0A36	AG	4.68	705	0.6110	2.8830	29.8485	3.7793	325.22	1.8787	18.89
G0A37	AG	9.54	780	0.6109	2.8648	29.6675	3.7883	321.96	1.8975	28.94
G0A38	AG	14.14	807	0.6111	2.8693	29.6398	3.8153	324.46	1.8834	34.34
G0A39	AG	16.50	714	0.6109	2.8743	29.6240	3.8250	325.69	1.8757	34.82
G0A59	AG	13.30	313	0.6090	2.8448	29.4293	3.7470	313.69	1.9412	27.24
G0W15	WG	9.73	355	0.6124	2.8570	3.7370	29.6590	316.66	1.9339	26.94
G0W16	WG	22.80	362	0.6111	2.8331	3.7027	29.5662	310.15	1.9704	41.88
G0W17	WG	28.54	474	0.6118	2.8583	3.7458	30.0297	321.51	1.9029	36.96
G0W18	WG	32.33	460	0.6114	2.8783	3.7703	30.2473	328.24	1.8627	34.34
G0W19	WG	40.80	378	0.6113	2.8968	3.8038	30.4873	335.93	1.8198	34.28
G0W23	WG	12.64	411	0.6093	2.8440	3.7290	29.5578	313.47	1.9436	28.36
G0W24	WG	21.00	448	0.6098	2.8375	3.7163	29.5462	311.57	1.9570	39.04
G0W25	WG	27.78	492	0.6096	2.8685	3.7530	29.9040	321.93	1.8936	35.14
G0W26	WG	36.06	442	0.6095	2.9743	3.8543	30.8570	353.73	1.7231	25.76

ID	Orient.	Fluence ($\times 10^{25}$ n/m ² [E>0.1MeV])	Irradiation Temperature (°C)	Mass (g)	X (mm)	Y (mm)	Z (mm)	Volume (mm ³)	Bulk Density [g/cm ³]	E [GPa]
G0W27	WG	40.80	410	0.6105	3.0023	3.8858	31.0793	362.57	1.6838	24.55
G0W28	WG	11.87	588	0.6102	2.8493	3.7313	29.5843	314.52	1.9401	25.31
G0W29	WG	17.77	571	0.6119	2.8418	3.7183	29.5828	312.58	1.9574	34.95
G0W30	WG	23.76	488	0.6070	2.8443	3.7498	29.8558	318.42	1.9063	35.95
G0W32	WG	29.72	540	0.6086	2.8795	3.8033	30.1950	330.68	1.8405	32.61
G0W33	WG	35.99	534	0.6092	2.9573	3.9178	30.8027	356.87	1.7071	24.88
G0W34	WG	7.87	692	0.6083	2.8685	3.7620	29.8058	321.64	1.8913	19.80
G0W35	WG	13.84	643	0.6090	2.8568	3.7383	29.7043	317.22	1.9197	28.48
G0W36	WG	17.77	682	0.6098	2.8598	3.7518	29.7318	318.99	1.9115	32.88
G0W37	WG	23.76	737	0.6102	2.9090	3.8140	30.3230	336.43	1.8137	32.96
G0W38	WG	29.21	665	0.6103	2.9523	3.8683	30.7477	351.14	1.7381	29.59
G0W39	WG	4.68	705	0.6127	2.8823	3.7760	29.9353	325.80	1.8807	18.47
G0W40	WG	9.54	780	0.6102	2.8515	3.7595	29.9183	320.73	1.9026	29.14
G0W41	WG	14.14	807	0.6113	2.8645	3.7760	30.0623	325.16	1.8798	34.31
G0W42	WG	16.50	714	0.6113	2.8710	3.7688	30.0628	325.28	1.8793	32.82
G0W63	WG	13.30	313	0.6091	2.8430	3.7275	29.5653	313.31	1.9439	26.77

Specimen ID in bold red text broke before dimensional inspection could be performed. The broken piece was cut to be rectangular, and then mass and dimensional inspection was performed. The cut piece is indicated with the -1 after the specimen ID. The mass and dimensions of the cut piece were used to calculate the density. The expected total length (Y) and full specimen volume were calculated using the bulk density, mass, X, and Z dimensions from the cut piece. The resulting moduli from the cut pieces are suspect because the specimens were smaller than minimum dimension required by equipment. The calculated volume was used for pre- and post-irradiation volume comparison. The dimensions used for the pre- and post-irradiation length change comparison are: measured X and Z, and expected total length of the unbroken specimen.

B.3.4 Post-Irradiation CTE (G347A only)

ID	Orient.	Mean CTE x10 ⁻⁶ K ⁻¹ (references to 25°C)									
		100°C	200°C	300°C	400°C	500°C	600°C	700°C	800°C	900°C	1000°C
G0A10	AG	4.75	4.91	5.10	5.25	5.32	5.41	5.54	5.69	5.84	6.04
G0A11	AG	2.58	2.60	2.76	2.87	3.04	3.21	3.44	3.85	4.42	5.03
G0A12	AG	2.30	2.42	2.58	2.74	2.91	3.09	3.47	4.41	5.55	6.29
G0A13	AG	2.33	2.46	2.63	2.80	2.97	3.17	3.53	4.27	5.24	5.98
G0A14	AG	2.46	2.60	2.79	2.97	3.15	3.32	3.55	4.02	4.73	5.32
G0A16	AG	4.32	4.42	4.56	4.73	4.85	4.96	5.10	5.26	5.43	5.64
G0A17	AG	2.63	2.70	2.86	3.03	3.17	3.31	3.50	3.82	4.29	4.82
G0A18	AG	2.16	2.30	2.48	2.66	2.83	2.99	3.25	3.75	4.55	5.35
G0A19	AG	2.48	2.61	2.79	2.96	3.14	3.31	3.56	3.93	4.38	4.87
G0A20	AG	2.40	2.53	2.71	2.90	3.05	3.21	3.44	3.79	4.25	4.75
G0A21	AG	3.85	3.99	4.18	4.39	4.58	4.74	4.88	5.01	5.16	5.34
G0A22	AG	2.62	2.66	2.82	3.00	3.19	3.36	3.52	3.64	3.80	4.02
G0A28	AG	2.22	2.30	2.45	2.63	2.79	2.95	3.09	3.27	3.55	3.91
G0A29	AG	1.96	2.06	2.27	2.47	2.67	2.85	3.03	3.27	3.65	4.09
G0A30	AG	2.08	2.22	2.40	2.59	2.77	2.94	3.11	3.38	3.80	4.22
G0A31	AG	3.61	3.66	3.81	4.02	4.24	4.45	4.64	4.81	4.92	5.07
G0A32	AG	2.62	2.68	2.85	3.05	3.23	3.43	3.59	3.73	3.88	4.02
G0A33	AG	2.26	2.33	2.50	2.68	2.85	3.02	3.16	3.31	3.46	3.64
G0A34-1	AG	1.72	1.87	2.08	2.29	2.49	2.67	2.83	2.97	3.18	3.58
G0A35	AG	1.85	2.02	2.22	2.41	2.59	2.76	2.90	3.08	3.39	3.83
G0A36	AG	3.83	3.91	4.07	4.25	4.46	4.67	4.86	5.02	5.17	5.31
G0A37	AG	2.33	2.41	2.58	2.77	2.95	3.13	3.29	3.43	3.56	3.70
G0A38	AG	1.92	1.96	1.90	2.16	2.39	2.58	2.73	2.87	3.02	3.23
G0A39	AG	1.97	2.05	2.20	2.37	2.54	2.69	2.84	2.96	3.10	3.32
G0A59	AG	4.39	4.55	4.70	4.76	4.66	4.63	4.64	4.68	4.74	4.86
G0W15	WG	5.14	5.30	5.48	5.64	5.72	5.81	5.95	6.11	6.28	6.48
G0W16	WG	2.92	2.96	3.09	3.24	3.36	3.49	3.75	4.28	4.97	5.68
G0W17	WG	2.45	2.60	2.79	2.97	3.15	3.35	3.74	4.66	5.81	6.59
G0W18	WG	2.50	2.65	2.83	3.01	3.19	3.39	3.74	4.46	5.44	6.20
G0W19	WG	2.39	2.51	2.68	2.85	3.01	3.20	3.53	4.11	5.04	5.88
G0W23	WG	4.79	4.90	5.07	5.21	5.33	5.45	5.59	5.76	5.96	6.18
G0W24	WG	1.88	2.13	2.54	2.79	3.06	3.28	3.53	3.91	4.43	5.00
G0W25	WG	2.62	2.75	2.91	3.07	3.24	3.41	3.73	4.33	5.10	5.70
G0W26	WG	2.58	2.74	2.93	3.11	3.29	3.48	3.74	4.12	4.60	5.10
G0W27	WG	2.54	2.68	2.87	3.06	3.23	3.39	3.62	3.96	4.40	4.93
G0W28	WG	4.06	4.20	4.39	4.60	4.80	4.97	5.11	5.25	5.40	5.58

ID	Condition	Mean CTE x10⁻⁶K⁻¹ (references to 25°C)									
G0W29	WG	2.95	3.01	3.15	3.32	3.48	3.64	3.78	3.94	4.14	4.40
G0W30	WG	2.36	2.42	2.57	2.73	2.92	3.07	3.22	3.40	3.70	4.11
G0W32	WG	2.16	2.26	2.43	2.60	2.78	2.94	3.10	3.30	3.63	4.10
G0W33	WG	2.11	2.21	2.38	2.56	2.72	2.88	3.04	3.29	3.72	4.21
G0W34	WG	3.80	3.86	4.01	4.23	4.45	4.67	4.86	5.02	5.12	5.28
G0W35	WG	2.83	2.89	3.05	3.24	3.42	3.61	3.77	3.90	4.05	4.21
G0W36	WG	2.43	2.51	2.66	2.84	3.00	3.17	3.31	3.45	3.62	3.82
G0W37	WG	1.95	1.99	2.17	2.35	2.52	2.69	2.82	2.94	3.11	3.45
G0W38	WG	1.97	2.10	2.28	2.46	2.62	2.78	2.93	3.10	3.40	3.84
G0W39	WG	4.03	4.10	4.24	4.42	4.62	4.83	5.02	5.19	5.34	5.47
G0W40	WG	2.39	2.47	2.64	2.83	3.01	3.18	3.33	3.47	3.60	3.75
G0W41	WG	2.04	2.09	2.23	2.40	2.58	2.74	2.88	3.00	3.14	3.37
G0W42	WG	2.09	2.16	2.32	2.49	2.66	2.81	2.96	3.08	3.23	3.49
G0W63	WG	4.67	4.81	4.96	4.97	4.87	4.81	4.80	4.84	4.91	5.05

Specimen ID's in bold red text broke before dimensional inspection could be performed. The cut piece was used for CTE measurements, which corresponds to the cut specimen ID in B.3.3.

B.4 TD-D6

B.4.1 Pre-Irradiation Dimensions

ID	Mater.	Orient.	Mass (g)	X (mm)	Y (mm)	Z (mm)	Volume (mm ³)	Bulk Density [g/cm ³]
43W09	G458S	WG	0.2492	5.9880	5.9910	4.7780	134.62	1.8513
43W11	G458S	WG	0.2482	5.9820	5.9900	4.7618	134.01	1.8524
G3A11	G347S	AG	0.2486	4.7680	5.9905	5.9880	134.33	1.8509
G3A12	G347S	AG	0.2475	4.7690	5.9910	5.9785	134.16	1.8445
G3W03	G347S	WG	0.2475	5.9780	5.9720	4.7860	134.52	1.8397
G3W04	G347S	WG	0.2482	5.9910	5.9900	4.7855	134.91	1.8393
43W00	G458S	WG	0.2493	5.9970	5.9905	4.8073	135.64	1.8380
43W01	G458S	WG	0.2490	5.9895	5.9950	4.8053	135.51	1.8373
43W02	G458S	WG	0.2500	5.9935	5.9980	4.8030	135.61	1.8437
43W03	G458S	WG	0.2478	5.9945	5.9925	4.7798	134.85	1.8377
43W04	G458S	WG	0.2487	5.9920	5.9920	4.7825	134.86	1.8443
43W05	G458S	WG	0.2498	5.9975	5.9930	4.7763	134.83	1.8530
G3A06	G347S	AG	0.2488	4.7715	5.9875	5.9925	134.46	1.8503
G3A07	G347S	AG	0.2470	4.7580	5.9880	5.9840	133.90	1.8449
G3A08	G347S	AG	0.2481	4.7725	5.9930	5.9905	134.57	1.8436
G3A09	G347S	AG	0.2478	4.7755	5.9875	5.9860	134.43	1.8436
G3A10	G347S	AG	0.2480	4.7800	5.9905	5.9950	134.82	1.8391
G3A13	G347S	AG	0.2488	4.7750	5.9950	5.9905	134.68	1.8471
G3A14	G347S	AG	0.2483	4.7645	5.9920	5.9880	134.26	1.8492
G3A15	G347S	AG	0.2480	4.7755	5.9810	5.9895	134.36	1.8454
G3A16	G347S	AG	0.2478	4.7620	5.9850	5.9875	134.03	1.8486
G3A17	G347S	AG	0.2485	4.7705	5.9925	5.9850	134.38	1.8492
G3A18	G347S	AG	0.2484	4.7730	5.9935	5.9985	134.77	1.8427
G3A19	G347S	AG	0.2485	4.7735	5.9925	5.9940	134.66	1.8450
G3A20	G347S	AG	0.2487	4.7640	5.9935	5.9915	134.36	1.8508
G3A21	G347S	AG	0.2476	4.7835	5.9825	5.9840	134.50	1.8406
G3A22	G347S	AG	0.2473	4.7665	5.9870	5.9800	134.03	1.8448
G3A23	G347S	AG	0.2484	4.7800	5.9975	5.9920	134.91	1.8412
G3A24	G347S	AG	0.2480	4.7665	5.9885	5.9940	134.38	1.8454
G3A25	G347S	AG	0.2483	4.7740	5.9985	5.9885	134.69	1.8432
G3A26	G347S	AG	0.2478	4.7695	5.9960	5.9935	134.62	1.8408
G3A27	G347S	AG	0.2477	4.7715	5.9870	5.9900	134.39	1.8428
G3A28	G347S	AG	0.2486	4.7835	5.9990	5.9905	135.01	1.8413

ID	Mater.	Orient.	Mass (g)	X (mm)	Y (mm)	Z (mm)	Volume (mm ³)	Bulk Density [g/cm ³]
G3A29	G347S	AG	0.2479	4.7765	5.9865	5.9900	134.52	1.8427
G3A30	G347S	AG	0.2480	4.7690	5.9910	5.9900	134.41	1.8448
G3A31	G347S	AG	0.2479	4.7755	5.9855	5.9915	134.51	1.8429
G3A32	G347S	AG	0.2477	4.7635	5.9920	5.9945	134.38	1.8433
G3A33	G347S	AG	0.2465	4.7800	5.9775	5.9775	134.14	1.8375
G3A34	G347S	AG	0.2478	4.7805	5.9900	5.9875	134.66	1.8398
G3A35	G347S	AG	0.2474	4.7715	5.9835	5.9910	134.34	1.8415
G3A36	G347S	AG	0.2483	4.7925	5.9860	5.9940	135.05	1.8382
G3A37	G347S	AG	0.2478	4.7880	5.9880	5.9905	134.89	1.8367
G3A43	G347S	AG	0.2464	4.7735	5.9820	5.9805	134.13	1.8372
G3W05	G347S	WG	0.2475	5.9875	5.9850	4.7805	134.54	1.8394
G3W06	G347S	WG	0.2490	5.9940	5.9930	4.7940	135.25	1.8410
G3W07	G347S	WG	0.2478	5.9890	5.9900	4.7875	134.77	1.8388
G3W08	G347S	WG	0.2457	5.9855	5.9800	4.7700	134.24	1.8304
G3W09	G347S	WG	0.2485	5.9930	5.9970	4.7795	134.87	1.8424
G3W10	G347S	WG	0.2492	5.9945	5.9940	4.7845	135.08	1.8450
G3W11	G347S	WG	0.2482	6.0040	6.0030	4.7840	135.22	1.8353
G3W13	G347S	WG	0.2493	5.9820	5.9820	4.7745	134.27	1.8565
G3W14	G347S	WG	0.2472	5.9910	5.9850	4.7870	134.68	1.8353
G3W15	G347S	WG	0.2477	5.9735	5.9730	4.7590	133.59	1.8540
G3W16	G347S	WG	0.2486	5.9855	5.9900	4.7740	134.41	1.8494
G3W17	G347S	WG	0.2484	5.9870	5.9830	4.7810	134.54	1.8460
G3W18	G347S	WG	0.2484	5.9865	5.9860	4.7765	134.34	1.8487
G3W19	G347S	WG	0.2481	5.9815	5.9750	4.7740	134.13	1.8496
G3W20	G347S	WG	0.2459	5.9805	5.9800	4.7545	133.57	1.8411
G3W21	G347S	WG	0.2481	5.9840	5.9860	4.7630	133.90	1.8527
G3W22	G347S	WG	0.2476	5.9825	5.9840	4.7630	133.94	1.8485
G3W23	G347S	WG	0.2472	5.9835	5.9830	4.7645	134.05	1.8439
G3W24	G347S	WG	0.2493	5.9875	5.9910	4.7700	134.28	1.8563
G3W25	G347S	WG	0.2480	5.9890	5.9960	4.7725	134.36	1.8461
G3W26	G347S	WG	0.2491	5.9855	5.9830	4.7690	134.27	1.8554
G3W27	G347S	WG	0.2493	5.9850	5.9840	4.7640	134.10	1.8590
G3W28	G347S	WG	0.2488	5.9915	5.9910	4.7570	134.16	1.8544
G3W29	G347S	WG	0.2485	5.9840	5.9830	4.7830	134.70	1.8449
G3W30	G347S	WG	0.2468	5.9880	5.9850	4.7710	134.19	1.8393
G3W31	G347S	WG	0.2485	5.9795	5.9850	4.7825	134.33	1.8497
G3W32	G347S	WG	0.2451	5.9765	5.9800	4.7600	133.61	1.8343

ID	Mater.	Orient.	Mass (g)	X (mm)	Y (mm)	Z (mm)	Volume (mm ³)	Bulk Density [g/cm ³]
G3W33	G347S	WG	0.2483	5.9835	5.9840	4.7785	134.33	1.8482
G3W34	G347S	WG	0.2486	5.9835	5.9860	4.7670	134.10	1.8535
G3W35	G347S	WG	0.2487	5.9755	5.9760	4.7805	134.23	1.8528
G3W36	G347S	WG	0.2485	5.9875	5.9830	4.7695	134.10	1.8528
G3W37	G347S	WG	0.2482	5.9755	5.9760	4.7785	134.24	1.8486
G3W38	G347S	WG	0.2477	5.9805	5.9800	4.7630	133.71	1.8528
G3W39	G347S	WG	0.2464	5.9815	5.9820	4.7820	134.42	1.8333
G3W40	G347S	WG	0.2492	5.9860	5.9840	4.7785	134.63	1.8511
G3W41	G347S	WG	0.2465	5.9830	5.9820	4.7565	133.80	1.8419
G3W42	G347S	WG	0.2462	5.9830	5.9820	4.7565	133.80	1.8403
G3W43	G347S	WG	0.2462	5.9785	5.9790	4.7660	133.68	1.8420
G3W44	G347S	WG	0.2488	5.9790	5.9800	4.7720	133.85	1.8590
G3W45	G347S	WG	0.2487	5.9865	5.9890	4.7800	134.57	1.8478
G3W46	G347S	WG	0.2473	5.9850	5.9870	4.7755	134.24	1.8421
G3W47	G347S	WG	0.2473	5.9830	5.9820	4.7740	134.23	1.8421
G3W48	G347S	WG	0.2468	5.9795	5.9820	4.7735	134.04	1.8415
G3W49	G347S	WG	0.2478	5.9895	5.9880	4.7695	134.30	1.8454
G3W50	G347S	WG	0.2471	5.9850	5.9870	4.7770	134.35	1.8390
G3W51	G347S	WG	0.2472	5.9870	5.9850	4.7625	133.89	1.8461
G3W52	G347S	WG	0.2474	5.9850	5.9860	4.7630	133.95	1.8468
G3W53	G347S	WG	0.2487	5.9920	5.9880	4.7645	134.21	1.8528
G3W54	G347S	WG	0.2480	5.9780	5.9800	4.7760	134.24	1.8477
G3W55	G347S	WG	0.2484	5.9855	5.9820	4.7635	134.14	1.8517
G3W56	G347S	WG	0.2470	5.9805	5.9780	4.7710	134.12	1.8413
G3W57	G347S	WG	0.2471	5.9785	5.9750	4.7665	133.85	1.8462
G3W58	G347S	WG	0.2469	5.9740	5.9710	4.7595	133.59	1.8480
G3W59	G347S	WG	0.2479	5.9895	5.9860	4.7715	134.20	1.8470
G3W60	G347S	WG	0.2486	5.9930	5.9920	4.7770	134.49	1.8486
G3W61	G347S	WG	0.2478	5.9820	5.9780	4.7670	134.21	1.8462
G3W62	G347S	WG	0.2482	5.9845	5.9850	4.7730	134.34	1.8476
G3W63	G347S	WG	0.2473	5.9805	5.9810	4.7630	133.92	1.8465
G3W64	G347S	WG	0.2476	5.9835	5.9820	4.7520	132.71	1.8654
G3W65	G347S	WG	0.2466	5.9755	5.9780	4.7655	133.62	1.8457
G3W66	G347S	WG	0.2477	5.9825	5.9840	4.7715	134.21	1.8453
G3W67	G347S	WG	0.2485	5.9855	5.9820	4.7665	134.05	1.8535

B.4.2 Pre-Irradiation Thermal Conductivity

ID	Mater.	Orient.	Thermal Conductivity (W/m/K)										
			25°C	100°C	200°C	300°C	400°C	500°C	600°C	700°C	800°C	900°C	1000°C
43W09	G458S	WG	124.96	115.96	103.36	92.18	83.56	76.51	70.65	65.63	61.14	57.62	55.36
43W11	G458S	WG	128.97	121.88	108.77	97.19	88.56	81.30	74.46	69.28	64.24	60.10	57.17
G3A11	G347S	AG	158.64	137.26	118.84	103.02	93.38	85.41	77.28	72.38	67.63	63.71	60.21
G3A12	G347S	AG	159.58	137.23	119.31	104.45	94.06	85.69	78.34	73.28	68.57	64.98	60.87
G3W03	G347S	WG	141.57	131.15	115.68	103.17	93.14	85.46	78.63	73.04	67.85	63.85	60.33
G3W04	G347S	WG	145.59	134.04	118.42	104.88	95.04	87.51	80.18	74.00	68.51	64.19	61.03

B.4.3 Post-Irradiation Dimensions

ID	Mater.	Orient.	Fluence ($\times 10^{25}$ n/m ² [E>0.1MeV])	Irradiation Temperature (°C)	Mass (g)	X (mm)	Y (mm)	Z (mm)	Volume (mm ³)	Bulk Density [g/cm ³]
43W00	G458S	WG	9.50	490	0.2497	5.8825	5.8880	4.7365	128.85	1.9379
43W01	G458S	WG	30.42	478	0.2498	5.8710	5.9777	4.9848	137.40	1.8181
43W02	G458S	WG	36.95	497	0.2498	5.9773	5.8917	5.0043	138.41	1.8048
43W03	G458S	WG	4.40	697	0.2482	5.9540	5.9410	4.7703	132.53	1.8730
43W04	G458S	WG	20.29	675	0.2494	5.8935	5.8910	4.9165	134.06	1.8603
43W05	G458S	WG	27.02	689	0.2495	6.0145	6.0100	5.0795	144.21	1.7302
G3A06	G347S	AG	32.33	446	0.2490	4.7420	5.9357	5.9853	132.32	1.8819
G3A07	G347S	AG	40.80	364	0.2472	4.7873	6.1067	6.0927	139.89	1.7671
G3A08	G347S	AG	9.73	341	0.2484	4.7023	5.9245	5.9250	129.64	1.9159
G3A09	G347S	AG	22.80	348	0.2463	4.6304	5.8760	5.8880	125.82	1.9571
G3A10	G347S	AG	28.54	460	0.2484	4.7093	6.0000	5.9163	131.29	1.8919
G3A13	G347S	AG	12.64	436	0.2494	4.6745	5.8780	5.9045	127.42	1.9569
G3A14	G347S	AG	21.00	473	0.2487	4.6472	5.8801	5.8709	126.00	1.9738
G3A15	G347S	AG	27.78	517	0.2484	4.6825	5.8697	5.9623	128.71	1.9300
G3A16	G347S	AG	36.06	467	0.2482	4.7868	6.1913	6.1560	143.29	1.7322
G3A17	G347S	AG	40.80	435	0.2492	4.8398	6.2450	6.2637	148.69	1.6760
G3A18	G347S	AG	11.87	592	0.2486	4.6830	5.9307	5.8933	128.55	1.9338
G3A19	G347S	AG	17.77	575	0.2489	4.6648	5.9145	5.8840	127.50	1.9518
G3A20	G347S	AG	23.76	492	0.2493	4.7193	6.0700	5.9740	134.41	1.8545
G3A21	G347S	AG	29.72	544	0.2476	4.7658	5.9953	6.0113	134.90	1.8355
G3A22	G347S	AG	35.99	538	0.2477	4.8918	6.2977	6.1123	147.89	1.6749
G3A23	G347S	AG	7.87	706	0.2489	4.7248	5.9645	5.9565	131.84	1.8883
G3A24	G347S	AG	13.84	657	0.2484	4.6785	5.9065	5.9420	128.96	1.9262
G3A25	G347S	AG	17.77	696	0.2488	4.6900	5.9395	5.9525	130.23	1.9101
G3A26	G347S	AG	23.76	751	0.2478	4.7918	6.1830	6.0995	141.93	1.7456
G3A27	G347S	AG	29.21	679	0.2478	4.8445	6.1660	6.2577	146.81	1.6879
G3A28	G347S	AG	4.68	710	0.2489	4.7465	5.9610	5.9735	132.74	1.8753
G3A29	G347S	AG	9.54	785	0.2482	4.7093	5.9515	5.9615	131.23	1.8914
G3A30	G347S	AG	14.14	812	0.2485	4.7270	6.0665	5.9470	133.94	1.8553
G3A31	G347S	AG	16.50	719	0.2484	4.6850	5.9070	5.9955	130.31	1.9058
G3A32	G347S	AG	9.50	436	0.2479	4.6763	5.8845	5.9045	127.61	1.9429
G3A33	G347S	AG	30.42	424	0.2468	4.7530	6.1050	6.0583	138.07	1.7875
G3A34	G347S	AG	36.95	443	0.2477	4.7368	6.0860	6.0053	135.97	1.8217
G3A35	G347S	AG	4.40	640	0.2478	4.7383	5.9545	5.9705	132.30	1.8731
G3A36	G347S	AG	20.29	618	0.2489	4.7140	5.9220	6.0145	131.87	1.8875

ID	Mater.	Orient.	Fluence ($\times 10^{25}$ n/m ² [E>0.1MeV])	Irradiation Temperature (°C)	Mass (g)	X (mm)	Y (mm)	Z (mm)	Volume (mm ³)	Bulk Density [g/cm ³]
G3A37	G347S	AG	27.02	632	0.2223	4.8565	6.2030	6.1495	145.50	1.5275
G3A43	G347S	AG	13.30	299	0.2463	4.6815	5.8700	5.8850	127.02	1.9387
G3W05	G347S	WG	9.50	478	0.2479	5.8830	5.8840	4.7005	127.79	1.9401
G3W06	G347S	WG	28.54	480	0.2497	5.8907	5.9477	4.8068	132.27	1.8878
G3W07	G347S	WG	32.33	466	0.2473	5.9297	5.9253	4.8013	132.49	1.8665
G3W08	G347S	WG	27.02	685	0.2478	6.1380	6.2160	5.0028	149.91	1.6530
G3W09	G347S	WG	9.73	361	0.2460	5.8950	5.8940	4.7090	128.50	1.9146
G3W10	G347S	WG	22.80	368	0.2483	5.8579	5.8395	4.6987	126.23	1.9670
G3W11	G347S	WG	13.30	319	0.2494	5.8910	5.8925	4.7075	128.34	1.9429
G3W13	G347S	WG	40.80	384	0.2511	6.0327	6.0897	4.9135	141.77	1.7712
G3W14	G347S	WG	12.64	457	0.2498	5.8825	5.8710	4.7000	127.49	1.9594
G3W15	G347S	WG	21.00	494	0.2470	5.8366	5.8591	4.7149	126.64	1.9505
G3W16	G347S	WG	27.78	538	0.2479	5.8753	5.8823	4.7393	128.64	1.9271
G3W17	G347S	WG	36.06	488	0.2487	6.0200	6.0170	4.9213	140.00	1.7764
G3W18	G347S	WG	40.80	456	0.2489	6.0853	6.1063	5.0255	146.67	1.6970
G3W19	G347S	WG	11.87	578	0.2485	5.8823	5.8807	4.7338	128.61	1.9322
G3W20	G347S	WG	17.77	561	0.2483	5.8595	5.8770	4.7103	127.39	1.9491
G3W21	G347S	WG	23.76	478	0.2463	5.9835	5.9230	4.7960	133.50	1.8450
G3W22	G347S	WG	29.72	530	0.2481	5.9690	5.9720	4.8405	135.52	1.8307
G3W23	G347S	WG	35.99	524	0.2478	6.1313	6.1480	4.9738	147.25	1.6828
G3W24	G347S	WG	7.87	739	0.2476	5.9390	5.9405	4.7490	131.59	1.8818
G3W25	G347S	WG	13.84	690	0.2494	5.8970	5.8905	4.7510	129.62	1.9238
G3W26	G347S	WG	17.77	729	0.2484	5.8850	5.8935	4.7908	130.50	1.9034
G3W27	G347S	WG	23.76	784	0.2497	6.0420	6.0475	4.9753	142.78	1.7485
G3W28	G347S	WG	29.21	712	0.2494	6.1310	6.1120	5.0510	148.66	1.6777
G3W29	G347S	WG	4.68	688	0.2493	5.9615	5.9660	4.7458	132.57	1.8807
G3W30	G347S	WG	9.54	763	0.2491	5.9085	5.9575	4.7593	131.57	1.8932
G3W31	G347S	WG	14.14	790	0.2476	5.9790	5.9165	4.8093	133.62	1.8531
G3W32	G347S	WG	16.50	697	0.2491	5.9435	5.9135	4.7773	131.87	1.8889
G3W33	G347S	WG	9.73	365	0.2456	5.9035	5.9000	4.7010	128.60	1.9098
G3W34	G347S	WG	22.80	372	0.2472	5.8503	5.8420	4.7181	126.65	1.9515
G3W35	G347S	WG	28.54	484	0.2492	5.8917	5.8923	4.8113	131.18	1.8997
G3W36	G347S	WG	32.33	470	0.2494	5.9233	5.9073	4.8668	133.75	1.8647
G3W37	G347S	WG	40.80	388	0.2486	6.0103	6.0160	4.9443	140.41	1.7705
G3W38	G347S	WG	12.64	454	0.2488	5.8685	5.8760	4.7165	127.74	1.9474
G3W39	G347S	WG	21.00	491	0.2482	5.8385	5.8461	4.7123	126.33	1.9643
G3W40	G347S	WG	27.78	535	0.2472	5.8653	5.8843	4.7738	129.40	1.9103

ID	Mater.	Orient.	Fluence ($\times 10^{25}$ n/m ² [E>0.1MeV])	Irradiation Temperature (°C)	Mass (g)	X (mm)	Y (mm)	Z (mm)	Volume (mm ³)	Bulk Density [g/cm ³]
G3W41	G347S	WG	36.06	485	0.2499	6.1090	6.0587	4.9203	143.03	1.7472
G3W42	G347S	WG	40.80	453	0.2471	6.1507	6.1020	4.9833	146.89	1.6822
G3W43	G347S	WG	11.87	552	0.2466	5.8720	5.8753	4.7098	127.62	1.9324
G3W44	G347S	WG	17.77	535	0.2493	5.8690	5.8530	4.7398	127.88	1.9492
G3W45	G347S	WG	23.76	452	0.2493	5.9350	5.9265	4.8500	133.98	1.8607
G3W46	G347S	WG	29.72	504	0.2478	5.9627	5.9403	4.9050	136.45	1.8160
G3W47	G347S	WG	35.99	498	0.2476	6.1567	6.1563	5.0458	150.20	1.6484
G3W48	G347S	WG	7.87	741	0.2474	5.9280	5.9290	4.7465	131.02	1.8884
G3W49	G347S	WG	13.84	692	0.2481	5.8910	5.8875	4.7285	128.81	1.9262
G3W50	G347S	WG	17.77	731	0.2475	5.9050	5.9010	4.7445	129.85	1.9061
G3W51	G347S	WG	23.76	786	0.2477	6.0200	6.0050	4.8780	138.50	1.7885
G3W52	G347S	WG	29.21	714	0.2475	6.1947	6.0833	5.0125	148.36	1.6683
G3W53	G347S	WG	4.68	644	0.2494	5.9635	5.9665	4.7505	132.75	1.8785
G3W54	G347S	WG	9.54	719	0.2488	5.9125	5.9110	4.7813	131.24	1.8959
G3W55	G347S	WG	14.14	746	0.2491	5.9535	5.9360	4.8323	134.12	1.8572
G3W56	G347S	WG	16.50	653	0.2479	5.9200	5.9145	4.8313	132.86	1.8655
G3W57	G347S	WG	9.50	494	0.2479	5.8725	5.8910	4.6995	127.69	1.9417
G3W58	G347S	WG	30.42	466	0.2473	5.9973	5.9640	4.8643	136.65	1.8098
G3W59	G347S	WG	36.95	485	0.2483	6.0153	6.0543	4.9425	141.37	1.7564
G3W60	G347S	WG	4.40	693	0.2493	5.9525	5.9685	4.7675	133.03	1.8743
G3W61	G347S	WG	20.29	671	0.2489	5.9855	5.9580	4.8738	136.51	1.8234
G3W62	G347S	WG	27.02	701	0.2483	6.1540	6.1050	5.0730	149.69	1.6584
G3W63	G347S	WG	13.30	323	0.2475	5.8865	5.8795	4.7003	127.76	1.9372
G3W64	G347S	WG	30.42	482	0.2478	5.9820	5.9857	4.8295	135.82	1.8245
G3W65	G347S	WG	36.95	501	0.2471	6.0660	5.9857	4.8763	139.06	1.7770
G3W66	G347S	WG	4.40	709	0.2484	5.9640	5.9650	4.7670	133.19	1.8652
G3W67	G347S	WG	20.29	687	0.2492	5.9540	5.9515	4.8588	135.22	1.8425

B.4.4 Post-Irradiation Thermal Conductivity

ID	Mater.	Orient.	Thermal Conductivity (W/m/K)									
			50°C	100°C	150°C	200°C	250°C	300°C	350°C	400°C	450°C	500°C
43W00	G458S	WG	25.25	26.59		28.66		29.45	29.62	29.56	29.05	29.01
43W01	G458S	WG	11.00	11.82	12.65	13.15	13.57	13.94	14.15	14.42	14.53	14.69
43W02	G458S	WG	10.47	11.66	12.29	12.83	13.31	13.73	13.96	14.30	14.32	14.55
43W03	G458S	WG	29.49	30.92		32.70		33.31	32.97	33.00	32.89	32.14
43W04	G458S	WG	15.71	17.01	18.21	19.00	19.55	19.99	20.32	20.55	20.43	
43W05	G458S	WG	12.59	13.63	14.48	15.17	15.59	15.95	16.22	16.40	16.44	
G3A06	G347S	AG	15.14	17.01	17.91	18.80	19.20	19.77	20.07	20.29	20.45	20.72
G3A07	G347S	AG	10.16	11.13	11.57	12.18	12.59	13.01	13.31	13.56	13.72	14.05
G3A08	G347S	AG	17.11	18.65		20.06		20.85	21.14	21.25	21.47	21.44
G3A09	G347S	AG	19.02	20.53	21.64	22.44	23.07	23.46	23.84	24.06	23.87	
G3A10	G347S	AG	10.68	12.24	13.09	13.58	14.16	14.52	14.86	15.25	15.64	16.06
G3A13	G347S	AG	21.78	23.44	24.42	25.34	25.92	26.36	26.56	26.96	26.64	
G3A14	G347S	AG	24.76	27.03	28.10	28.99	29.64	30.00	30.14	30.32	29.84	
G3A15	G347S	AG	15.01	16.21	16.89	17.68	18.10	18.79	19.08	19.33	19.68	20.00
G3A16	G347S	AG	10.05	10.90	11.63	12.13	12.58	12.92	13.12	13.49	13.60	13.85
G3A17	G347S	AG	7.27	7.98	8.31	8.90	9.32	9.60	9.81	10.04	10.22	10.51
G3A18	G347S	AG	29.39	31.70	33.00	34.01	34.63	34.94	34.76	34.99	34.83	34.66
G3A19	G347S	AG	26.55	28.57	29.60	30.75	31.24	31.55	31.74	32.02	31.42	
G3A20	G347S	AG	17.77	19.22	20.52	21.29	21.82	22.23	22.53	22.79	22.51	
G3A21	G347S	AG	16.18	17.48	18.34	19.21	19.87	20.16	20.55	20.82	20.88	21.08
G3A22	G347S	AG	7.41	8.24	8.50	9.08	9.46	9.75	9.91	10.09	10.10	10.25
G3A23	G347S	AG	29.16	31.45		33.36		33.77	33.74	33.69	33.50	32.90
G3A24	G347S	AG	25.91	27.73	29.01	30.02	30.66	30.91	31.04	31.24		30.66
G3A25	G347S	AG	21.65	23.35	24.95	25.69	26.34	26.81	27.08	27.36		26.99
G3A26	G347S	AG	13.99	15.24	16.14	16.91	17.45	17.81	18.13	18.11		18.35
G3A27	G347S	AG	9.79	10.97	11.63	12.14	12.64	13.00	13.27	13.50	13.61	13.74
G3A28	G347S	AG	29.97	32.67		34.53		35.12		34.73		33.92
G3A29	G347S	AG	28.00	29.93		31.87		32.68		32.72		31.85
G3A30	G347S	AG	20.49	22.30	23.56	24.48	25.15	25.60	25.80	26.13		25.83
G3A31	G347S	AG	23.76	25.81	26.78	27.93	28.55	28.87	29.05	29.31		28.95
G3A32	G347S	AG	24.83	26.30		28.05		28.89	28.88	28.94	28.93	28.57
G3A33	G347S	AG	12.37	13.72	14.33	14.95	15.38	15.80	16.17	16.41	16.45	16.69
G3A34	G347S	AG	11.52	12.80	13.42	13.91	14.33	14.78	15.12	15.33	15.46	15.76
G3A35	G347S	AG	34.07	36.15		37.88		37.99		37.31		36.08
G3A36	G347S	AG	19.85	21.56	22.88	23.60	24.21	24.62	24.98	25.03		24.96

ID	Motor	Orient	Thermal Conductivity (W/m/K)									
			10.03	10.92	11.55	12.03	12.44	12.78	13.02	13.22		13.50
G3A37	G347S	AG	10.03	10.92	11.55	12.03	12.44	12.78	13.02	13.22		13.50
G3A43	G347S	AG	12.91	14.00	14.70	15.28	15.70	16.04	16.46	16.36	17.15	
G3W05	G347S	WG	26.39	28.02		29.69		30.23		30.35		29.75
G3W06	G347S	WG	14.74	15.97	16.78	17.41	17.97	18.39	18.76	19.01	19.18	19.48
G3W07	G347S	WG	14.01	15.19	16.08	16.68	17.35	17.73	17.99	18.24	18.55	18.88
G3W08	G347S	WG	12.15	13.31	14.08	14.79	15.29	15.64	15.90	16.11	16.01	
G3W09	G347S	WG	14.95	16.04		17.41		17.97		18.41		18.74
G3W10	G347S	WG	17.60	19.16	20.29	21.03	21.73	22.23	22.44	22.75	22.58	
G3W11	G347S	WG	13.38	14.48	15.28	15.76	15.86	16.03	16.26	15.86	17.71	
G3W13	G347S	WG	10.22	11.22	11.97	12.40	12.89	13.21	13.54	13.71	13.89	14.23
G3W14	G347S	WG	22.07	23.72	24.68	25.59	26.09	26.48	26.65	26.94	26.97	
G3W15	G347S	WG	22.61	24.32	25.29	26.32	26.80	27.15	27.41	27.69	27.71	
G3W16	G347S	WG	14.73	16.08	16.94	17.54	18.14	18.73	18.92	19.31	19.49	19.93
G3W17	G347S	WG	10.49	11.34	12.01	12.42	12.87	13.23	13.48	13.74	14.00	14.27
G3W18	G347S	WG	7.36	8.01	8.56	8.92	9.23	9.39	9.50	9.76	9.95	10.23
G3W19	G347S	WG	27.68	30.23	30.95	31.85	32.63	32.90	32.82	32.80	32.77	32.74
G3W20	G347S	WG	17.84	19.31	20.46	21.20	21.79	22.15	22.39	22.66	22.78	
G3W21	G347S	WG	25.85	27.69	28.97	29.74	30.38	30.63	30.75	30.96	30.91	
G3W22	G347S	WG	16.02	17.37	18.22	18.87	19.47	19.92	20.19	20.42	20.61	20.67
G3W23	G347S	WG	8.16	9.10	9.49	9.88	10.33	10.58	10.89	11.12	11.22	11.44
G3W24	G347S	WG	26.54	28.25		30.31		30.85		30.84		30.18
G3W25	G347S	WG	25.69	27.69	28.93	29.80	30.31	30.73	30.86	31.00	30.45	
G3W26	G347S	WG	20.51	22.47	23.64	24.56	25.19	25.57	25.80	26.08		25.81
G3W27	G347S	WG	13.81	15.12	16.04	16.74	17.22	17.70	17.99	17.76		18.23
G3W28	G347S	WG	9.79	10.42	11.26	11.76	12.13	12.48	12.75	13.03	13.10	13.37
G3W29	G347S	WG	30.23	32.53		34.07		34.68		34.28		33.30
G3W30	G347S	WG	29.02	31.48		33.11		34.16		34.34		33.70
G3W31	G347S	WG	20.05	22.08	23.22	24.02	24.68	25.11	25.39	25.56		25.28
G3W32	G347S	WG	22.78	24.47	25.93	26.86	27.55	27.85	28.08	28.34		27.96
G3W33	G347S	WG	15.14	16.54		17.97		18.84	19.10	19.42	19.77	19.85
G3W34	G347S	WG	18.50	20.16	21.12	21.82	22.44	22.81	23.08	23.39	23.61	
G3W35	G347S	WG	12.71	13.96	14.71	15.32	15.74	16.36	16.67	16.96	17.16	17.48
G3W36	G347S	WG	13.69	14.83	15.64	16.31	16.93	17.24	17.52	17.87	17.95	18.13
G3W37	G347S	WG	9.58	10.78	11.46	12.02	12.42	12.78	13.11	13.34	13.46	13.80
G3W38	G347S	WG	21.38	22.76	23.87	24.53	25.07	25.36	25.55	25.74	25.46	
G3W39	G347S	WG	23.54	25.25	26.65	27.52	28.07	28.47	28.71	28.92		28.58
G3W40	G347S	WG	16.20	17.65	18.43	19.28	19.72	20.30	20.54	20.73	20.85	21.31
G3W41	G347S	WG	10.52	11.27	11.94	12.52	12.97	13.33	13.63	13.88	13.97	14.29
G3W42	G347S	WG	7.17	8.05	8.50	9.09	9.42	9.61	9.75	9.90	10.02	10.37

ID	Mater.	Orient.	Thermal Conductivity (W/m/K)									
			550°C	600°C	650°C	700°C	750°C	800°C	850°C	900°C	950°C	1000°C
G3W43	G347S	WG	27.22	29.21	31.02	31.90	32.48	32.69	32.82	32.88	32.91	32.80
G3W44	G347S	WG	25.08	26.98	28.04	29.03	29.74	30.07	30.22	30.53		30.04
G3W45	G347S	WG	17.75	19.22	20.41	21.10	21.71	22.05	22.34	22.56		22.37
G3W46	G347S	WG	15.64	16.98	17.93	18.60	19.09	19.56	19.85	20.16	20.35	20.50
G3W47	G347S	WG	7.23	7.71	7.99	8.39	8.67	8.81	8.91	9.09	9.17	9.43
G3W48	G347S	WG	28.67	30.28		32.27		32.94		32.88		32.07
G3W49	G347S	WG	25.35	27.41	28.44	29.40	29.99	30.25	30.38	30.59		30.19
G3W50	G347S	WG	21.52	23.38	24.71	25.58	26.14	26.61	26.82	27.02		26.75
G3W51	G347S	WG	16.02	17.56	18.64	19.26	19.83	20.25	20.54	20.79		20.72
G3W52	G347S	WG	8.91	9.77	10.36	10.94	11.31	11.58	11.93	12.14	12.31	12.39
G3W53	G347S	WG	31.30	33.00		34.96		35.48		35.25		34.20
G3W54	G347S	WG	28.14	30.02		32.12		33.19		33.22		32.55
G3W55	G347S	WG	20.07	21.94	23.01	23.91	24.50	24.87	25.10	25.36		25.24
G3W56	G347S	WG	20.49	22.17	23.45	24.32	24.94	25.26	25.54	25.79		25.46
G3W57	G347S	WG	26.68	28.55		30.21		30.93		31.17	30.47	30.45
G3W58	G347S	WG	13.14	14.00	14.91	15.48	15.96	16.36	16.69	16.92	16.95	17.11
G3W59	G347S	WG	11.40	12.69	13.26	13.85	14.15	14.68	14.91	15.19	15.20	15.45
G3W60	G347S	WG	30.14	31.93		33.37		33.54		33.23		32.20
G3W61	G347S	WG	15.05	16.54	17.46	18.40	18.91	19.41	19.70	19.98	19.86	
G3W62	G347S	WG	11.74	12.92	13.77	14.44	14.91	15.26	15.58	15.79		15.78
G3W63	G347S	WG	12.00	13.02	13.75	14.26	14.73	15.08	15.38	15.82	16.26	
G3W64	G347S	WG	12.58	13.91	14.58	15.15	15.57	16.01	16.35	16.54	16.63	16.85
G3W65	G347S	WG	11.82	12.83	13.58	14.03	14.62	15.03	15.33	15.56	15.65	15.95
G3W66	G347S	WG	33.55	35.41		37.48		37.51		36.29	35.70	35.85
G3W67	G347S	WG	15.99	17.40	18.52	19.21	19.84	20.20	20.52	20.78		20.87

ID	Mater.	Orient.	Thermal Conductivity (W/m/K)									
			550°C	600°C	650°C	700°C	750°C	800°C	850°C	900°C	950°C	1000°C
43W00	G458S	WG	28.90	28.92		29.07	29.32	29.60				
43W01	G458S	WG	14.98	15.30	15.62	15.72	16.12	16.30	16.85	17.34		18.97
43W02	G458S	WG	14.77	15.05	15.26	15.42	15.64	16.01	16.45	16.91		17.36
43W03	G458S	WG	31.89	31.58		30.76	30.55	30.65				
43W04	G458S	WG	20.58		20.65		20.85		20.97		21.35	
43W05	G458S	WG	16.60		16.55		16.46		16.43		16.61	
G3A06	G347S	AG	20.93	21.34	21.70	21.83	22.00	22.74	22.90	23.56	23.25	24.77
G3A07	G347S	AG	14.39	14.76	15.00	15.24	15.84	16.15	16.80	16.75	17.50	16.97

ID	Motor	Orient	Thermal Conductivity (W/m/K)									
			21.68	21.95		22.48	22.97	23.66				
G3A08	G347S	AG	24.46		24.91							
G3A09	G347S	AG	16.55	17.09	17.50	17.81	18.56	18.70	19.05	20.04	21.27	20.86
G3A10	G347S	AG	27.36		27.85							
G3A13	G347S	AG	29.83		29.94		30.15					
G3A14	G347S	AG	20.56	20.90	21.21	21.60	21.59	21.80	22.96	22.98		24.31
G3A15	G347S	AG	14.19	14.49	14.80	15.31	15.45	15.98	16.26	16.59		17.27
G3A16	G347S	AG	10.89	11.14	11.47	11.89	12.14	12.73	12.98	13.46	13.79	13.95
G3A17	G347S	AG	34.53	34.38	33.92	33.73	34.30	34.24	34.60	35.07		37.31
G3A18	G347S	AG	31.46		31.42		31.58					
G3A19	G347S	AG	22.60		22.65		22.75					
G3A20	G347S	AG	21.16	21.28	21.38	21.40	21.65	21.74	22.23	22.46		23.62
G3A21	G347S	AG	10.55	10.74	10.84	11.06	11.40	11.68	11.71	12.65		13.66
G3A22	G347S	AG	32.72	32.20		31.49	31.01	31.38				
G3A23	G347S	AG		30.56		30.09		30.20		30.97		
G3A24	G347S	AG		26.93		26.71		26.78		27.38		28.30
G3A25	G347S	AG		18.46		18.41		18.56		18.56		18.83
G3A26	G347S	AG	13.93	14.13	14.26	14.49	14.51	14.76	14.59	14.99		15.50
G3A27	G347S	AG		33.16	32.98	32.47	32.10	32.29	33.30	33.50		
G3A28	G347S	AG		31.45	31.34	30.98	30.69	30.89	31.41	31.04		
G3A29	G347S	AG		25.86		25.59		25.49		25.46		25.93
G3A30	G347S	AG		28.84		28.62		28.71		29.31		30.64
G3A31	G347S	AG	28.55	28.60		28.88	29.20	29.85				
G3A32	G347S	AG	16.99	17.34	17.40	17.70	18.18	18.37	19.01	19.48	19.89	20.45
G3A33	G347S	AG	16.00	16.34	16.77	17.08	17.52	17.95	18.08	18.99	19.36	20.01
G3A34	G347S	AG		35.17	34.82	34.12	33.78	33.82	33.77	33.42		
G3A35	G347S	AG		24.94		24.73		24.91		25.66		
G3A36	G347S	AG		13.80		13.98		14.11		14.02		
G3A37	G347S	AG	17.94		18.71							
G3A43	G347S	AG		29.66		29.79		30.48				
G3W05	G347S	WG	19.68	20.27	20.63	20.59	21.36	21.67	21.74	21.92		23.38
G3W06	G347S	WG	19.27	19.86	19.92	20.34	20.58	20.95	21.71	21.73		23.31
G3W07	G347S	WG	16.19		16.16		16.18		16.19		15.96	
G3W08	G347S	WG		19.24		19.80		20.60				
G3W09	G347S	WG	23.15		23.67							
G3W10	G347S	WG	18.27		19.08							
G3W11	G347S	WG	14.47	14.89	15.23	15.46	15.76	15.81	16.50	16.75	17.36	17.84
G3W13	G347S	WG	26.96		27.42							
G3W14	G347S	WG	27.70		28.19		28.52					
G3W15	G347S	WG										

ID	Motor	Orient	Thermal Conductivity (W/m/K)								
G3W16	G347S	WG	20.30	20.70	21.10	21.46	21.79	22.07	22.49	22.57	24.16
G3W17	G347S	WG	14.55	14.99	15.33	15.46	15.75	16.03	16.98	17.44	17.46
G3W18	G347S	WG	10.62	10.83	11.17	11.38	11.82	12.14	12.63	12.95	14.00
G3W19	G347S	WG	32.59	32.53	32.26	31.75	31.84	32.35	32.88	33.47	35.65
G3W20	G347S	WG	22.73		22.71		22.99				
G3W21	G347S	WG	30.54		30.43		30.70				
G3W22	G347S	WG	20.81	20.87	20.88	21.00	21.44	21.50	21.74	22.60	23.44
G3W23	G347S	WG	11.57	11.88	11.96	12.27	12.37	12.71	12.96	13.38	14.24
G3W24	G347S	WG		29.82		29.24		29.26			
G3W25	G347S	WG	30.48		30.25		30.14		30.40		30.98
G3W26	G347S	WG		25.76		25.60		25.55		25.78	26.75
G3W27	G347S	WG		18.30		18.34		18.28		18.31	18.82
G3W28	G347S	WG	13.43	13.52	13.73	13.99	14.03	13.73	14.17	14.04	15.05
G3W29	G347S	WG		32.57	32.15	31.33		30.76		31.67	
G3W30	G347S	WG		32.69	32.47	31.78		30.71		31.14	
G3W31	G347S	WG		25.17		25.15		24.91		24.74	25.71
G3W32	G347S	WG		27.86		27.51		27.69		28.37	29.07
G3W33	G347S	WG	20.02	20.51		20.94	21.32	21.70			
G3W34	G347S	WG	24.06		24.77						
G3W35	G347S	WG	17.96	18.28	18.61	19.19	19.54	19.73	20.89	21.47	22.18
G3W36	G347S	WG	18.50	18.87	19.21	19.52	19.77	19.55	19.92	19.71	21.79
G3W37	G347S	WG	14.13	14.37	14.76	14.95	15.47	15.88	16.06	16.69	16.76
G3W38	G347S	WG	25.93		26.42						
G3W39	G347S	WG		28.86		29.12					
G3W40	G347S	WG	21.59	21.77	22.16	22.92	22.84	23.34	23.76	24.18	26.29
G3W41	G347S	WG	14.57	14.94	15.26	15.50	16.01	16.14	16.69	16.68	17.38
G3W42	G347S	WG	10.55	10.87	11.11	11.32	11.61	12.06	12.40	12.23	13.55
G3W43	G347S	WG	32.61	32.60	32.54	32.22	31.97	32.90	33.25	33.45	37.30
G3W44	G347S	WG		30.04		29.90					
G3W45	G347S	WG		22.35		22.57					
G3W46	G347S	WG	20.54	20.58	20.83	20.94	20.97	21.22	21.63	21.70	23.05
G3W47	G347S	WG	9.61	9.89	10.12	10.45	10.55	10.70	11.23	10.90	11.42
G3W48	G347S	WG		31.50		30.97	30.87	30.59	30.82	31.10	
G3W49	G347S	WG		29.91		29.66		30.08		30.99	32.55
G3W50	G347S	WG		26.70		26.64		26.87		27.65	29.06
G3W51	G347S	WG		20.82		20.74		20.69		20.83	21.48
G3W52	G347S	WG	12.64	12.87	13.06	13.18	13.26	13.35	13.35	13.85	14.59
G3W53	G347S	WG		33.68		32.76	32.30	32.27	32.51	32.90	
G3W54	G347S	WG		32.19		31.59	31.54	31.26	31.35	31.49	

ID	Motor	Orient	Thermal Conductivity (W/m/K)								
G3W55	G347S	WG		25.26		25.13		25.13		25.32	25.85
G3W56	G347S	WG		25.33		25.19		25.21		25.68	26.37
G3W57	G347S	WG	30.35	30.36		30.32	30.62	30.87	31.18	31.51	
G3W58	G347S	WG	17.36	17.68	17.74	18.21	18.44	18.83	19.18	20.18	20.88
G3W59	G347S	WG	15.70	15.93	15.96	16.30	16.73	17.42	18.19	18.11	19.55
G3W60	G347S	WG		31.43	31.04	31.01		30.14		30.96	
G3W61	G347S	WG	20.15		20.18		20.24		20.44		20.69
G3W62	G347S	WG		15.90		16.00		16.03		16.04	16.18
G3W63	G347S	WG	16.90		17.77						
G3W64	G347S	WG	17.07	17.43	17.75	17.93	18.37	18.32	18.62	19.47	20.91
G3W65	G347S	WG	16.05	16.34	16.49	16.84	17.01	17.41	18.02	18.44	19.22
G3W66	G347S	WG	35.32	34.76		34.12	33.38	32.90	33.01	33.53	
G3W67	G347S	WG		20.98		21.03		21.16		21.88	22.17

B.5 SQ6 STRENGTH COUPONS

Due to the irregular shape of the coupons for irradiation, the density and dimension values were not used in the volume and length change analyses, therefore the values are also not listed here.

B.5.1 Pre-Irradiation (G347A only, AG only)

ID	Strength (MPa)	ID	Strength (MPa)
G4021	60.28	G4051	56.35
G4022	62.18	G4052	58.91
G4023	60.45	G4053	55.40
G4024	60.47	G4054	53.06
G4025	59.13	G4055	56.18
G4031	61.84	G4061	60.16
G4032	63.06	G4062	63.18
G4033	62.08	G4063	63.98
G4034	61.69	G4064	63.57
G4035	53.48	G4065	58.52
G4041	57.72	G4071	54.75
G4042	62.81	G4072	59.43
G4043	62.13	G4073	65.76
G4044	61.33	G4074	57.87
G4045	60.18	G4075	60.25

B.5.2 Post-Irradiation (G347A only)

ID	Fluence ($\times 10^{25}$ n/m ² [E>0.1MeV])	Irradiation Temperature (°C)	Strength (MPa)
G4081	9.73	336	92.45
G4082	9.73	336	113.76
G4083	9.73	336	114.63
G4084	9.73	336	117.66
G4085	9.73	336	112.65
G4091	22.80	343	missing
G4092	22.80	343	115.04
G4093	22.80	343	112.06
G4094	22.80	343	110.75
G4095	22.80	343	77.20
G4101	28.54	455	Missing
G4102	28.54	455	Missing
G4103	28.54	455	Missing
G4104	28.54	455	Missing
G4105	28.54	455	Missing
G4111	32.33	441	72.04
G4112	32.33	441	79.19
G4113	32.33	441	82.09
G4114	32.33	441	70.69
G4115	32.33	441	75.24
G4121	40.80	359	74.09
G4122	40.80	359	66.66
G4123	40.80	359	68.76
G4124	40.80	359	81.93
G4125	40.80	359	72.95
G4131	12.64	389	98.14
G4132	12.64	389	100.21
G4133	12.64	389	107.57
G4134	12.64	389	98.04
G4135	12.64	389	106.85
G4141	21.00	426	107.67
G4142	21.00	426	102.15
G4143	21.00	426	113.25
G4144	21.00	426	103.54
G4145	21.00	426	106.03

ID	Fluence ($\times 10^{25}$ n/m ² [E>0.1MeV])	Irradiation Temperature (°C)	Strength (MPa)
G4181	27.78	470	79.71
G4182	27.78	470	88.04
G4183	27.78	470	86.39
G4184	27.78	470	88.03
G4185	27.78	470	85.01
G4191	36.06	420	63.81
G4192	36.06	420	66.30
G4193	36.06	420	66.06
G4194	36.06	420	68.92
G4195	36.06	420	77.30
G4201	40.80	388	62.32
G4202	40.80	388	61.46
G4203	40.80	388	64.84
G4204	40.80	388	59.10
G4205	40.80	388	66.70
G4211	11.87	586	79.15
G4212	11.87	586	93.45
G4213	11.87	586	97.36
G4214	11.87	586	92.71
G4215	11.87	586	99.05
G4221	17.77	569	105.62
G4222	17.77	569	106.08
G4223	17.77	569	102.29
G4224	17.77	569	103.77
G4225	17.77	569	100.23
G4231	23.76	486	98.55
G4232	23.76	486	94.36
G4233	23.76	486	91.29
G4234	23.76	486	89.18
G4235	23.76	486	83.54
G4251	29.72	538	77.00
G4252	29.72	538	61.42
G4253	29.72	538	66.77
G4254	29.72	538	56.99
G4255	29.72	538	75.94

ID	Fluence ($\times 10^{25}$ n/m ² [E>0.1MeV])	Irradiation Temperature (°C)	Strength (MPa)
G4261	35.99	532	56.21
G4262	35.99	532	54.08
G4263	35.99	532	54.28
G4264	35.99	532	48.44
G4265	35.99	532	53.30
G4271	7.87	662	90.61
G4272	7.87	662	88.07
G4273	7.87	662	83.04
G4274	7.87	662	90.88
G4275	7.87	662	84.47
G4281	13.84	613	89.80
G4282	13.84	613	95.39
G4283	13.84	613	85.00
G4284	13.84	613	88.60
G4285	13.84	613	97.09
G4291	17.77	652	98.52
G4292	17.77	652	99.62
G4293	17.77	652	100.32
G4294	17.77	652	95.27
G4295	17.77	652	90.94
G4301	23.76	707	broken
G4302	23.76	707	broken
G4303	23.76	707	59.29
G4304	23.76	707	67.96
G4305	23.76	707	82.44
G4311	29.21	635	55.48
G4312	29.21	635	59.56
G4313	29.21	635	63.22
G4314	29.21	635	68.68
G4315	29.21	635	74.55
G4321	4.68	700	81.82
G4322	4.68	700	87.28
G4323	4.68	700	86.59
G4324	4.68	700	89.26
G4325	4.68	700	83.27
G4331	9.54	775	83.44
G4332	9.54	775	77.38

ID	Fluence ($\times 10^{25}$ n/m ² [E>0.1MeV])	Irradiation Temperature (°C)	Strength (MPa)
G4333	9.54	775	90.58
G4334	9.54	775	91.91
G4335	9.54	775	97.57
G4341	14.14	802	83.42
G4342	14.14	802	100.54
G4343	14.14	802	87.76
G4344	14.14	802	65.18
G4345	14.14	802	84.28
G4351	16.50	709	96.91
G4352	16.50	709	89.94
G4353	16.50	709	92.88
G4354	16.50	709	87.77
G4355	16.50	709	90.14
G4371	9.73	344	98.20
G4372	9.73	344	111.97
G4373	9.73	344	114.23
G4374	9.73	344	102.85
G4375	9.73	344	100.31
G4381	22.80	351	107.40
G4382	22.80	351	117.40
G4383	22.80	351	110.67
G4384	22.80	351	110.96
G4385	22.80	351	93.31
G4391	28.54	463	76.76
G4392	28.54	463	76.07
G4393	28.54	463	80.45
G4394	28.54	463	82.52
G4395	28.54	463	85.39
G4401	32.33	449	50.53
G4402	32.33	449	64.47
G4403	32.33	449	72.16
G4404	32.33	449	76.68
G4405	32.33	449	73.69
G4411	40.80	367	69.52
G4412	40.80	367	79.88
G4413	40.80	367	80.18
G4414	40.80	367	73.69

ID	Fluence ($\times 10^{25}$ n/m ² [E>0.1MeV])	Irradiation Temperature (°C)	Strength (MPa)
G4415	40.80	367	35.91
G4421	12.64	398	105.58
G4422	12.64	398	97.29
G4423	12.64	398	missing
G4424	12.64	398	broken
G4425	12.64	398	107.06
G4431	21.00	435	108.26
G4432	21.00	435	94.00
G4433	21.00	435	117.98
G4434	21.00	435	112.33
G4435	21.00	435	104.77
G4451	27.78	479	88.19
G4452	27.78	479	79.86
G4453	27.78	479	78.74
G4454	27.78	479	89.28
G4455	27.78	479	69.08
G4461	36.06	429	52.89
G4462	36.06	429	56.49
G4463	36.06	429	60.74
G4464	36.06	429	64.03
G4465	36.06	429	67.96
G4471	40.80	397	46.21
G4472	40.80	397	53.28
G4473	40.80	397	45.65
G4474	40.80	397	48.34
G4475	40.80	397	50.86
G4481	11.87	586	91.76
G4482	11.87	586	94.65
G4483	11.87	586	92.21
G4484	11.87	586	88.86
G4485	11.87	586	94.05
G4491	17.77	569	98.15
G4492	17.77	569	102.43
G4493	17.77	569	99.84
G4494	17.77	569	103.60
G4495	17.77	569	102.54
G4501	23.76	486	87.51

ID	Fluence ($\times 10^{25}$ n/m ² [E>0.1MeV])	Irradiation Temperature (°C)	Strength (MPa)
G4502	23.76	486	87.75
G4503	23.76	486	92.94
G4504	23.76	486	98.40
G4505	23.76	486	92.61
G4511	29.72	538	51.25
G4512	29.72	538	broken
G4513	29.72	538	56.93
G4514	29.72	538	broken
G4515	29.72	538	54.57
G4521	35.99	532	48.39
G4522	35.99	532	61.47
G4523	35.99	532	53.58
G4524	35.99	532	53.76
G4525	35.99	532	58.03
G4531	7.87	676	87.37
G4532	7.87	676	89.57
G4533	7.87	676	80.32
G4534	7.87	676	82.02
G4535	7.87	676	78.48
G4541	13.84	627	93.61
G4542	13.84	627	93.14
G4543	13.84	627	97.96
G4544	13.84	627	95.95
G4545	13.84	627	96.55
G4551	17.77	666	95.75
G4552	17.77	666	92.49
G4553	17.77	666	97.83
G4554	17.77	666	94.66
G4555	17.77	666	89.98
G4571	29.21	649	59.15
G4572	29.21	649	68.48
G4573	29.21	649	57.74
G4574	29.21	649	68.23
G4575	29.21	649	66.93
G4581	4.68	700	88.02
G4582	4.68	700	90.84
G4583	4.68	700	86.58

ID	Fluence ($\times 10^{25}$ n/m ² [E>0.1MeV])	Irradiation Temperature (°C)	Strength (MPa)
G4584	4.68	700	91.14
G4585	4.68	700	89.01
G4591	9.54	775	84.93
G4592	9.54	775	90.47
G4593	9.54	775	98.26
G4594	9.54	775	95.44
G4595	9.54	775	93.20
G4601	14.14	802	89.19
G4602	14.14	802	95.41
G4603	14.14	802	141.87
G4604	14.14	802	95.67
G4605	14.14	802	93.68
G4611	16.50	709	94.81
G4612	16.50	709	92.36
G4613	16.50	709	92.64
G4614	16.50	709	91.30
G4615	16.50	709	86.02
G4631	23.76	649	57.78
G4632	23.76	649	61.51
G4633	23.76	649	broken
G4634	23.76	649	broken
G4635	23.76	649	broken
G4641	13.30	294	104.17
G4642	13.30	294	103.96
G4643	13.30	294	105.18
G4644	13.30	294	106.09
G4645	13.30	294	74.63
G4651	13.30	302	88.83
G4652	13.30	302	84.18
G4653	13.30	302	87.27
G4654	13.30	302	89.59
G4655	13.30	302	92.78
G5711	9.50	406	99.33
G5712	9.50	406	106.74
G5713	9.50	406	100.99
G5714	9.50	406	106.25
G4584	4.68	700	91.14

ID	Fluence ($\times 10^{25}$ n/m ² [E>0.1MeV])	Irradiation Temperature (°C)	Strength (MPa)
G5721	30.42	394	57.94
G5722	30.42	394	71.73
G5723	30.42	394	61.71
G5724	30.42	394	56.50
G5731	36.95	413	missing
G5732	36.95	413	61.14
G5733	36.95	413	66.57
G5734	36.95	413	missing
G5741	4.40	582	92.31
G5742	4.40	582	87.40
G5743	4.40	582	94.97
G5744	4.40	582	98.96
G5751	20.29	560	96.80
G5752	20.29	560	88.83
G5753	20.29	560	90.70
G5754	20.29	560	89.33
G5761	27.02	574	85.65
G5762	27.02	574	69.74
G5763	27.02	574	80.39
G5764	27.02	574	74.96
G5771	9.50	412	100.40
G5772	9.50	412	105.03
G5773	9.50	412	104.15
G5774	9.50	412	102.01
G5781	30.42	400	67.73
G5782	30.42	400	71.04
G5783	30.42	400	75.17
G5784	30.42	400	83.65
G5791	36.95	419	broken
G5792	36.95	419	51.07
G5793	36.95	419	66.01
G5794	36.95	419	missing
G5801	4.40	590	84.48
G5802	4.40	590	84.40
G5803	4.40	590	90.73
G5804	4.40	590	89.79
G5811	20.29	568	85.96

ID	Fluence ($\times 10^{25}$ n/m² [E>0.1MeV])	Irradiation Temperature (°C)	Strength (MPa)
G5812	20.29	568	82.21
G5813	20.29	568	89.14
G5814	20.29	568	100.51
G5821	27.02	582	66.72

ID	Fluence ($\times 10^{25}$ n/m² [E>0.1MeV])	Irradiation Temperature (°C)	Strength (MPa)
G5822	27.02	582	79.62
G5823	27.02	582	63.90
G5824	27.02	582	65.95

INTERNAL DISTRIBUTION

1. Y. Katoh
2. A.A. Campbell
3. M.A. Snead
4. T.D. Burchell
5. M. Vance
6. L.K. Laymance-RC

EXTERNAL DISTRIBUTION

7. Mr. Toshiaki Fukuda, Tokai Carbon Co., Ltd.
8. Mr. Kentaro Takizawa, Tokai Carbon Co., Ltd.
9. Mr. Thomas J. O'Connor, DOE Office of Nuclear Energy, NE-20/GTN, Telephone: (301) 903-6781,
email: Tom.Oconnor@hq.doe.gov